To the Graduate Council:

I am submitting herewith a dissertation written by Jean Adamson Solomon entitled "Euglenoid Flagellar Root Systems: Ultrastructure and Phylogenetic Significance." I have examined the final copy of this dissertation for form and content and recommend that it be accepted in partial fulfillment of the requirements for the degree of Doctor of Philosophy, with a major in Botany.

Patricia L. Walne

Patricia L. Walne, Major Professor

We have read this dissertation
and recommend its acceptance:

R. Lee Hoffman

L. Evans Roth

Beth C. Mullin

Ruth S. Whaley

Accepted for the council:

Lee Minkel

Vice Provost
and Dean of the Graduate School

EUGLENOID FLAGELLAR ROOT SYSTEMS: ULTRASTRUCTURE AND PHYLOGENETIC SIGNIFICANCE

A Dissertation

Presented for the

Doctor of Philosophy

Degree

The University of Tennessee, Knoxville

Jean Adamson Solomon

June 1986

ACKNOWLEDGMENTS

There are a number of people I would like to thank for their contributions during the course of this research. My major professor, Dr. Patricia Walne, provided encouragement and advice; her flexibility and understanding during times of stress are much appreciated. The suggestions of my committee members, Dr. Jeffrey Becker, Dr. Beth Mullin, Dr. Raymond Holton, Dr. Evans Roth, and Dr. Ruth Willey, were very helpful.

Dr. John Dunlap provided technical advice cheerfully, and often at a moment's notice; Dr. Peter Kivic offered encouragement and intellectual challenge. Mr. Dick Williams and Ms. Nancy Dawson also contributed much to this work. Dr. David Patterson, Dr. Keith Roberts, and Dr. Lula Hilenski provided thoughtful reviews of parts of this dissertation.

This research was supported in part by National Science Foundation Grant No. DEB 82-08401 to Dr. P. L. Walne. My employer, Environmental Sciences Division, Oak Ridge National Laboratory, has offered much flexibility during this period, and I am grateful to them. I thank the University of Colorado Laboratory for High Voltage Electron Microscopy (HVEM) for training and for use of the microscope. The HVEM facility is supported by the Biotechnology Resources Program, Division of Research Resources, National Institutes of Health.

Finally, my husband, Allen, contributed daily to this work, through his love and encouragement; his unflagging confidence in me has been a great source of strength. Ms. Letitia Solomon cheerfully assumed an inordinate amount of the domestic duties at home. My children, Robert and Charles, were a continual reminder of the reasons for which I decided to study biology; their good humor has been most helpful. My parents, Bob and Helen Adamson, actively encouraged my early biological interest and have been supportive throughout.

ABSTRACT

The ultrastructure and arrangement of flagellar root systems have become increasingly important indicators of phylogenetic relatedness among the algae. In this ultrastructural study, the flagellar roots of two euglenoid organisms, Entosiphon sulcatum and Eutreptia pertyi, are examined in detail and are compared with fragmentary published information available on other euglenoid roots, and with the more intensively studied bodonid flagellar root systems. This is the first systematic investigation of euglenoid roots; names for the roots are applied on the basis of their location in the basal body complex where they originate. The euglenoid root pattern consists of three microtubular flagellar roots, one on either side of the two functional basal bodies and one between them, nearer to the basal body of the posterior flagellum. All three roots extend anteriorly along the reservoir margin. The dorsal root is associated with an electron-dense plate and a band of stigma-related microtubules, which are continuous with the canal and pellicle microtubules. The intermediate root originates between the two basal bodies and has a predictable spatial relationship with the posterior flagellum. The ventral root originates near the posterior flagellum and becomes incorporated into the supporting structure of the cytopharynx. The dorsal, intermediate, and ventral euglenoid roots correspond to the

dorsal connector, ventral fiber, and reinforced microtubules, respectively, of the bodonids. The similarity of euglenoid and bodonid flagellar root patterns lends strong support to the recently proposed euglenoid-kinetoplastid supergroup, the Euglenozoa.

TABLE OF CONTENTS

PART	PAGE
1. GENERAL INTRODUCTION	1
APPENDIX: PART 1	22
2. *ENTOSIPHON SULCATUM*: FLAGELLAR ROOTS OF THE BASAL BODY COMPLEX AND RESERVOIR REGION	25
APPENDIX: PART 2	54
3. *ENTOSIPHON SULCATUM*: FLAGELLAR ROOTS ANTERIOR TO THE RESERVOIR	69
APPENDIX: PART 3	92
4. *EUTREPTIA PERTYI* AND *EUTREPTIA VIRIDIS*: FLAGELLAR ROOT SYSTEMS	107
APPENDIX: PART 4	125
5. CONCLUSION	138
APPENDIX: PART 5	153
LIST OF REFERENCES	157
APPENDIX	170
VITA	180

LIST OF TABLES

TABLE PAGE

PART 1. GENERAL INTRODUCTION

1. A Partial Listing of Pertinent Literature Concerning Euglenoid Phylogeny 4

2. A Partial Listing of Pertinent Structural Studies on Flagellar Root Systems of Protistan Organisms 9

3. A Partial Listing of Pertinent Literature on Euglenoid Ultrastructure 13

4. Comparison of Flagellar Root Terminology 21

PART 2. ENTOSIPHON SULCATUM: FLAGELLAR ROOTS OF THE BASAL BODY COMPLEX AND RESERVOIR REGION

1. Interpretation of Microtubular Flagellar Roots and Related Structures in other Euglenoid Flagellates 39

LIST OF FIGURES

FIGURE PAGE

PART 1. GENERAL INTRODUCTION

1. Line drawings of Eutreptia, Entosiphon, and a representative bodonid, showing the relationship between the reservoir (R) and the cytopharynx (Cp) 23

PART 2. ENTOSIPHON SULCATUM: FLAGELLAR ROOTS OF THE BASAL BODY COMPLEX AND RESERVOIR REGION

1. SEM overview of Entosiphon sulcatum 55
2. TEM view of median longitudinal section of E. sulcatum 55
3. Flagellar basal region 55
4. Transverse section of E. sulcatum at base of reservoir 55
5. Three-dimensional diagrammatic reconstruction of the basal body complex of Entosiphon sulcatum as seen from the right dorsal side of the cell . . . 57
6. Diagram of a median transverse section through the basal body complex of Entosiphon sulcatum as seen from the posterior end of the cell 59
7. Transverse section through posterior end of basal body complex of Entosiphon sulcatum 61
8. Transverse section through basal body complex, anterior to Fig. 7 61
9. Transverse section through flagellar transition zone 61
10. Transverse section through base of reservoir . . . 61
11. Transverse section through reservoir, anterior to Fig. 10 61
12. Transverse section of Entosiphon sulcatum at anterior end of basal body complex 63

FIGURE PAGE

PART 2 (CONTINUED)

13. Transverse section posterior to Fig. 12 63

14. Transverse section including all four basal bodies, posterior to Fig. 13 63

15. The dorsal root (DR) extends away from the anterior functional basal body at an angle of about 30° . . 65

16. Transverse section at the anterior end of the reservoir 65

17. Fibrils connect the two flagella to one another (arrow) 65

18. Longitudinal section through the reservoir-canal transition zone 65

19. The IR lies opposite the PAR of F_2 on a ridge projecting into the reservoir 65

20. High voltage electron micrograph of thick section (0.4 μm) 65

21. Longitudinal section of the large connective fiber (LCF) 67

22. Nonstriated fibers (NSF, arrow) extend away from the basal body complex 67

23. A small connective fiber (arrow) extends from bb_1 toward bb_1'. 67

24. A small connective fiber (arrow) attaches to three microtubular triplets of bb_1' 67

25. Oblique view of basal body complex 67

PART 3. ENTOSIPHON SULCATUM: FLAGELLAR ROOTS ANTERIOR TO THE RESERVOIR

1. Transverse view of Entosiphon sulcatum 93

2. Higher magnification of the siphon 93

3. Higher magnification of a pharyngeal rod 93

FIGURE PAGE

PART 3 (CONTINUED)

4. Transverse section of the anterior tip of Entosiphon sulcatum, siphon retracted (cf. Fig. 7) 95

5. The asymmetrical dome and terminal appendages are covered with fine hairs of three different lengths 95

6. Tapered end of siphon reaches to posterior end of cell 95

7. Transverse section through anterior tip of cell, siphon extended (cf. Fig. 4) 95

8. Transverse section of vane complex 95

9. Longitudinal thick section at tip of siphon of Entosiphon sulcatum 97

10. Transverse section of tip of siphon 97

11. Electron-dense web covers most of siphon tip . . . 97

12. Terminal web is connected to dome at tip of siphon 97

13. Oblique section through anterior end of cell . . . 97

14. Serial section anterior to Fig. 13 97

15. Transverse section of reservoir of Entosiphon sulcatum showing intermediate root (IR, arrow) on ridge on left side of reservoir 99

16. Transverse section of reservoir showing IR (arrow) in trough adjacent to ridge 99

17. Transverse section of reservoir showing IR (arrow) on ventral side of reservoir 99

18. Transverse section of reservoir showing IR (arrow) on right side of reservoir 99

19. Transverse section of reservoir showing IR (arrow) lining invagination on right side of reservoir . . 99

FIGURE PAGE

PART 3 (CONTINUED)

20. A microtubular band, possibly the dorsal branch of the IR, extends dorsally between the reservoir and the siphon 99

21. Intermediate voltage micrograph of a thick section showing the ventral edge of the anterior depression 99

22. The band of microtubules (arrow) lining the ventral ridge may be an extension of the dorsal branch of the IR 99

23. Transverse section of anterior end of reservoir with IR on left side, opposite F_2 101

24. Transverse section of anterior end of reservoir with IR in a more ventral position (cf. Fig. 23) . 101

25. Transverse section of anterior end of reservoir with microtubular band (arrow) encircling ventral side of reservoir 101

26. Transverse section of anterior end of reservoir with microtubular band (arrow) extending ventrally from reservoir margin 101

27. Traced outlines of reservoir and associated structures (Figs. 25, 26) are overlain to reveal possible branching of the intermediate root (IR) . 103

28. Microtubules (arrow), probably from the ventral root (VR), extend into the cytoplasm 104

29. Microtubules (arrow), probably from the VR, encircle the reservoir and connect to the PRL extension 104

30. Fibers (large arrow) cross from top of reservoir into siphon, paralleling the reservoir-PRR connector 104

31. Thick section shows groove connectors (GC) 104

32. The reservoir-PRR connector (large arrow) consists of reinforced microtubules 104

FIGURE PAGE

PART 4 (CONTINUED)

33. The major, nonflagellar root, structural connections between the siphon and the remainder of the cell in Entosiphon sulcatum 106

34. Diagram summarizing paths of bodonid microtubular flagellar roots and cytoskeleton 106

PART 4. EUTREPTIA PERTYI AND EUTREPTIA VIRIDIS: FLAGELLAR ROOTS

1. Longitudinal view of reservoir-canal complex of Eutreptia pertyi 126

2. Transverse section of reservoir of E. pertyi . . . 126

3. Longitudinal view of striated structure (arrow) near the base of F_1 126

4. Longitudinal section near base of F_1 126

5. Longitudinal section of the base of F_1 126

6. Longitudinal section through reservoir-canal system of Eutreptia pertyi 128

7. The two functional basal bodies in oblique section 128

8. Oblique thick section (adjacent to Fig. 7) through the functional basal bodies 128

9. The basal body complex of Eutreptia viridis has an arrangement similar to other euglenoids 128

10. Transverse section through flagellar transition zone of E. viridis 128

11. Transverse section through base of the narrow reservoir 128

12. Transverse section of the middle region of the reservoir 130

13. The DR is attached to the anterior basal body (bb_1) by fine filaments (arrow) 130

14. Fine filaments within the IR and the DR connect individual microtubules to one another 130

FIGURE PAGE

PART 4 (CONTINUED)

15. Transverse section through the reservoir at stigma level 130

16. Transverse section through the reservoir-canal transition zone of Eutreptia pertyi 132

17. Transverse section anterior the Fig. 16 132

18. Transverse section of canal region, anterior to Fig. 17 132

19. Transverse section of E. pertyi at level of paraflagellar body (PFB) 132

20. Lower region of the reservoir has numerous membrane-lined invaginations 132

21. The microtubules of the VR are widely spaced and have small arms attached to them 134

22. Longitudinal view of the cytopharynx (Cp) in E. pertyi 134

23. Invagination of reservoir membrane forms the base of the cytopharynx (arrow) 134

24. Oblique section shows continuity of cytopharyngeal pocket (arrow) with reservoir-canal in the transition zone 134

25. Oblique thick section shows VR (arrow) connecting cytopharyngeal pocket (Cp) to canal of E. pertyi . 134

26. Longitudinal section through reservoir-canal transition zone of Eutreptia pertyi 136

27. Longitudinal section adjacent to Fig. 26 136

28. Longitudinal section shows canal collar of transversely oriented microtubules 136

29. Longitudinal section adjacent to canal 136

FIGURE PAGE

PART 5. CONCLUSION

1. Diagrammatic comparison of the paths of the three flagellar roots among Entosiphon, Eutreptia, and some bodonids 154

2. Hypothetical evolutionary sequence within the Euglenozoa, based primarily on relationships among the cytostome, flagellar pocket, and canal microtubules 156

APPENDIX

1. Transverse section through the reservoir of the contaminant, Euglena sp. 176

2. At canal level, the microtubules of the DMT are paired 176

3. Reservoir-canal (R) region of Euglena sp. 176

4. The ventral root of Euglena sp. is composed of two segments 176

5. The basal flagellar region of Euglena sp. 176

6. The dorsal margins of the reservoir of Euglena gracilis var. bacillaris are lined by the dorsal microtubules (DMT) 178

7. A transverse section of the anterior region of the reservoir of E. gracilis 178

8. An oblique section of the reservoir through the basal body complex and stigma 178

LIST OF ABBREVIATIONS

bb = basal body
bb_1 = anterior functional basal body
bb_1' = anterior accessory basal body
bb_2 = posterior functional basal body
bb_2' = posterior accessory basal body
Cp = cytopharynx, cytopharyngeal homologue
DMT = dorsal microtubules
DR = dorsal microtubular root
F = flagellum
FAS = cytopharynx-associated fiber
FD = dorsal fiber
FV = ventral fiber
F_1 = anterior flagellum
F_2 = posterior (recurrent) flagellum
GC = groove connectors
IR = intermediate microtubular root
kV = kilovolts
LCF = large connective fiber
min = minutes
MLS = multilayered structure
mM = millimolar
MTR = reinforced microtubules
N = nucleus
nm = nannometers
NSF = nonstriated fiber
P = plate
PAR = paraxial rod
PFB = paraflagellar body
PMT = parareservoir microtubules
PRL = left pharyngeal rod
PRR = right pharyngeal rod
PRV = ventral pharyngeal rod
PSF = perpendicular striated fiber
R = reservoir
S = siphon
SCF = small connective fiber
St = stigma, eyespot
SEM = scanning electron microscopy
TEM = transmission electron microscopy
tRNA = transfer ribonucleic acid
VR = ventral microtubular root
v/v = volume to volume
w/v = weight to volume
^{o}C = degrees centigrade
um = micrometers

PART 1. GENERAL INTRODUCTION

The Euglenophyceae have long been considered a phylogenetic enigma. With an unusual combination of plant and animal characteristics, they appear closely related to one another but, considering the available evidence, not to any of the other algae (e.g. Stewart and Mattox 1975, Leedale 1978, Ragan and Chapman 1978). In light of current knowledge, many of the traditional taxonomic criteria for algal classification (e.g. pigmentation; growth habit; cell shape; number, arrangement, and relative length of flagella in motile cells) are no longer considered useful for phylogenetic purposes (Stewart and Mattox 1975). New approaches are needed in order to understand phylogenetic affiliations among the various algal taxa.

Because the Euglenophyceae have chlorophylls a and b, they were historically classified, if not in the Chlorophyta, then at least in a closely allied taxon (e.g. Smith 1950, Christensen 1962). Pigmentation, however, represents practically the only similarity between the two taxa; in most other respects, the Euglenophyceae and the Chlorophyta are strikingly different (e.g. Ragan and Chapman 1978). It has been suggested (Stewart and Mattox 1975, Gibbs 1978, Whatley 1981) that euglenoid chloroplasts may have arisen from endosymbiotic green algae, thus explaining the similarities in pigmentation.

Over the years a number of workers have suggested that the closest ancestors of the Euglenophyceae are found, not

among the algae, but among the protozoa, specifically the Kinetoplastida, which includes the small free-living bodonids and the usually parasitic trypanosomes (e.g. Mignot 1964, 1966, Leedale 1978, Dodge 1980, Round 1980, Corliss 1984; see Table 1). Kivic and Walne (1984) recently summarized the evidence concerning a euglenoid-kinetoplastid relationship and concluded that euglenoids, kinetoplastids, and Isonema form a common phyletic supergroup. Such a group, the Euglenozoa, has recently been proposed by Corliss (1984). Kivic and Walne (1984) proposed an evolutionary direction within the supergroup: bodonid ancestors presumably gave rise to two lines, the trypanosomes and the euglenoid-Isonema line. Within the latter, the phagotrophic euglenoids were postulated as more primitive than the photosynthetic euglenoids. Definitive criteria are needed to evaluate these proposed relationships.

The conceptual foundation of phylogeny within the Chlorophyta has undergone a revolution within the past 20 years. As a result of the accumulation of ultrastructural information, particularly on mitotic and cytokinetic patterns and flagellar root systems, methodical examination of a variety of traits across green algal taxa is becoming possible (Pickett-Heaps and Marchant 1972, Stewart and Mattox 1975). The conservative nature of the flagellar apparatus, in particular, has been recognized, and

Table 1. A Partial Listing of Pertinent Literature Concerning Euglenoid Phylogeny.

Date	Author	Contribution
1883	Klebs	Described many euglenoid species. Recognized the families Euglenida, Astasiida, Peranemida primarily on nutritive mode.
1926	Calkins	Reclassified euglenoid flagellates by presence/absence of chloroplasts and number of flagella. Peranemida replaced by Heteronemidae.
1942	Hollande	Attempted to describe a more natural classification of euglenoids consisting of 5 families.
1946	Jahn	Reviewed knowledge of euglenoids, giving extensive bibliography. Discussed problems of classifying colorless euglenoids.
1947	Chu	Described 16 species of Euglena from China, emphasizing morphological variability under varying environmental conditions.
1948	Pringsheim	Discussed taxonomic problems of Euglenineae. Considered phagotrophic types to be distantly related to autotrophic and saprotrophic euglenoids. Considered Eutreptia primitive to Euglena.
1955	Huber-Pestalozzi	Produced a comprehensive, descriptive listing of over 800 species of Euglenophyceae.
1956	Pringsheim	Condensed the more than 100 described species of Euglena to approximately 50 valid ones in a monograph on the genus.
1962	Christensen	Wrote a definitive classification of the algae including the class Euglenophyceae with two orders: Euglenales and Peranematales.

Table 1 (Continued)

Date	Author	Contribution
1963	Christen	Summarized the taxonomy of colorless euglenoids.
1963	Pringsheim	Discussed evolution of the colorless algae.
1964	Honigberg et al.	Revised the system of protozoan classification listing Euglenida as an order with three suborders: Euglenina, Peranematina and Petalomonadina. Not widely used.
1967a	Leedale	Discussed taxonomy of euglenoids in relation to phylogeny.
1967b	Leedale	Divided Euglenophyceae into 6 orders, in an extensive and widely followed treatise on the group.
1967	Mignot	Discussed the evolution of the vestibular apparatus in several algal orders and concluded that the origin was different in each group.
1968	Buetow	Edited an extensive collection of chapters summarizing current knowledge of the genus Euglena.
1970	Leedale	Discussed phylogeny of the algae as reflected in nuclear cytology.
1970	Margulis	Described the serial endosymbiotic theory of evolution.
1972	Bovee	Discussed the possibility that the trypanosomes descended from the euglenoids.
1973	Sleigh	Discussed a common origin of the euglenoids and the trypanosomes.
1975	Stewart and Mattox	Discussed the possible origin of euglenoid chloroplasts from endosymbiotic green algae, accounting for the puzzling occurrence of chlorophyll b in euglenoids.

Table 1 (Continued)

Date	Author	Contribution
1976	Taylor	Discussed flagellate phylogeny emphasizing flagella, mitochondrial cristae, chloroplast lamellae and mitotic phenomena.
1978	Cavalier-Smith	Discussed non-symbiotic theory of microtubule and flagellar evolution.
1978	Gibbs	Suggested that the euglenophyte chloroplast was derived from a symbiotic event with a green alga.
1978	Leedale	Proposed colorless euglenoids as progenitors of green ones, reversing his earlier scheme.
1978	Moestrup	Discussed validity of flagellar apparatus as a phylogenetic indicator, emphasizing green algae, but mentioning euglenoids. Reports MLS in Eutreptiella.
1978	Taylor	Expanded on 1976 paper, discussing problems of determining phylogenetic relatedness based on only one set of criteria.
1980	Dodge	Discussed protist evolution; suggested origin of euglenoids from a kinetoplastid line.
1980	Round	Discouraged use of classification Protista as an "unnatural rag-bag" of organisms.
1981	Mignot	Suggested that because of their cytological complexity, euglenoids cannot be considered primitive.
1981	Whatley	Discussed euglenoids as being derived from a colorless ancestor and endosymbiotic green algal chloroplasts.

Table 1 (Continued)

Date	Author	Contribution
1983	McQuade	Discussed evolution of all eukaryotic organisms without reference to flagellar roots.
1984	Corliss	Proposed superphylum (Euglenozoa) to contain euglenoids, kinetoplastids, Isonema, and Stephanopogon.
1984	Kivic and Walne	Examined and summarized evidence for euglenoid kinetoplastid phylogenetic relationship.
1985a	Willey and Wibel	Discussed evolutionary implications of cytopharyngeal homologue.
1985b	Willey and Wibel	Discovered cytopharyngeal homologue in green euglenoids.

comparison of flagellar root systems across chlorophycean classes has led to a new understanding of relationships within the phylum and thus to extensive taxonomic revision (O'Kelley and Floyd 1984, Mattox and Stewart 1984).

The flagellar root system is not an easy system to study. It requires meticulous electron-microscopical examination and three-dimensional interpretation of serial sections, and is both tedious and time-consuming. As such, it will probably never be used for routine taxonomic determinations e.g. in ecological surveys of algal populations. For such uses we will undoubtedly continue to rely on the more traditional taxonomic criteria (e.g. pigmentation, cell shape, habitat, flagellar complement, nature of the cell wall, and storage products) for many years to come. However, as a means of determining the underlying relationships of the protistan and plant kingdoms, comparisons of flagellar root systems are providing information of unparalleled significance (see Table 2).

Euglenophycean flagellar root systems have not been systematically studied. The information available comes as incidental observations made during the course of ultrastructural studies carried out for other purposes (see Table 3). These studies have shown that there are usually three microtubular roots plus assorted striated fibers, all arising from the basal bodies. In addition, Moestrup

Table 2. A partial Listing of Pertinent Structural Studies on Flagellar Root Systems of Protistan Organisms.

Date	Author	Contribution
1926	Hall	Described a rhizoplast in Peranema.
1929	Lackey	Described basal body complex of Entosiphon.
1933	Lackey	Observed flagellar root system and ingestion apparatus in Peranema; reported no rhizoplast.
1934	Hall	Discussed flagellar apparatus in Peranema.
1958	Roth	Reported flagellar roots in Euglena, reservoir microtubules in Peranema.
1962	Hoffman and Manton	Described flagellar apparatus of Oedogonium zoospores.
1963	Hoffman and Manton	Described flagellar apparatus of Oedogonium spermatozoids.
1963	Mignot	Described ultrastructure of Entosiphon, including basal body complex.
1964	Mignot	Described basal body complex of Entosiphon in greater detail than in 1963.
1965	Manton	Suggested that flagellar roots could be used as phyletic indicators. Described flagellar roots in Chlorophyta and Chromophyta.
1966	Mignot	Described fibrils of the "vestibular system" in 6 colorless euglenoid genera.
1967	Ringo	Described cruciate flagellar root system in Chlamydomonas.
1969	Lembi and Walne	Reported interconnections between basal bodies and microtubular roots of green algae.

Table 2 (Continued)

Date	Author	Contribution
1969	Pitelka	Discussed three types of fibrillar systems in protozoa: microtubular roots, striated fibrils, and filaments.
1972	Moestrup	Described fine structure of Golenkinia spermatozoids; summarized flagellar root structure of 15 algal species.
1973	Swale	Described ultrastructure of Rhynchomonas, a bodonid.
1974	Hitchen	Described fine structure of Cephalothamnium, a bodonid.
1974	Moestrup	Described flagellar roots of Chaetosphaeridium and proposed it was on the line giving rise to higher plants.
1974	Pitelka	Summarized literature on basal bodies of protozoa, including associated structures.
1975	Burzell	Described fine structure of Bodo curvifilus.
1975	Graham and McBride	Described multilayered structures (MLS) of flagellar bases in Trentepohlia (Trentepohliales).
1975	Lembi	Reported striated fiber, a rhizoplast, extending from basal bodies toward nucleus in Carteria (Volvocales).
1975	Pickett-Heaps	Summarized bryophytan and chlamydomonad flagellar root patterns.
1977	Eyden	Described ultrastructure of Bodo designis.
1978	Goodenough and Weiss	Described association of compound flagellar root with gametic mating structure in Chlamydomonas.

Table 2 (Continued)

Date	Author	Contribution
1978	Moestrup	Summarized structural data on flagellar roots of green algae.
1978	Piccini and Mammi	Described basal portion of flagella in Euglena. Reported MLS in Eutreptiella.
1979	Brugerolle et al.	Described flagellar root system of five bodonid species; summarized the bodonid root pattern.
1980	Floyd et al.	Introduced concepts of 180° rotational symmetry, absolute configuration of green algal flagellar root patterns.
1980	Melkonian	Discussed potential usefulness of fibrous flagellar roots for determining phylogenetic relationships among the greens algae.
1981	Roberts et al.	Described a cryptomonad flagellar root system.
1982	Hoops and Floyd	Described Pyrobotrys flagellar roots as lacking 180° rotational symmetry, possibly due to colonial structure.
1982	Moestrup	Reviewed literature on algal flagellar structure.
1983	Gillott and Gibbs	Described roots of two Cryptomonas species.
1983	Hoops and Floyd	Described influence of colony formation on flagellar root pattern in Astrephomene (Volvocales).
1984	Nohynkova	Described ultrastructure of Cryptobia, a bodonid.
1984	Roberts et al.	Assessed flagellar roots of siphonaceous green algal motile cells.

Table 2 (Continued)

Date	Author	Contribution
1984	Solomon et al.	Described flagellar root system of Entosiphon.
1985	Andersen	Described four absolute orientations of flagellar roots in one species of Synura.
1985	Farmer and Triemer	Described roots of Distigma (euglenoid).
1985	Hilenski and Walne	Described flagellar roots of Peranema.
1985	Roberts	Described flagellar apparatus of Oxyrrhis, a dinoflagellate.
1985	Taylor et al.	Described developmental reorientation of basal body complex, roots and functional consequences in Platydorina colonies.
1985b	Willey and Wibel	Described cytostome and flagellar roots of Colacium in reservoir region.

Table 3. A Partial Listing of Pertinent Literature on Euglenoid Ultrastructure.

Date	Author	Contribution
1958	Roth	Described reservoir microtubules and flagellar roots of *Peranema*, *Euglena*.
1959	Roth	Described ultrastructure of *Peranema*.
1963	Mignot	Described ultrastructure of *Entosiphon sulcatum*.
1963	Pitelka	Summarized ultrastructural studies of many protozoans, including euglenoids.
1963	Ringo	Described ultrastructure of *Astasia longa*.
1964	Leedale	Described cytology and ultrastructure of *Euglena spirogyra*, emphasizing pellicle.
1964	Mignot	Described flagellar ultrastructure of *Entosiphon sulcatum*.
1964	Sommer and Blum	Studied *Astasia longa* pellicle during cell division.
1965	Leedale et al.	Studied many aspects of *Euglena spirogyra*, including ultrastructure of the anterior end.
1965	Mignot	Studied the pellicle of 10 euglenoid genera.
1965	Sommer	Described fine structure of *Euglena gracilis* pellicle.
1965	Sommer and Blum	Described fine structure of *Astasia* cell division.
1967	Arnott and Walne	Described ultrastructure of pellicle pores of *Euglena granulata*.
1967	Walne and Arnott	Studied fine structure of eyespots in *Euglena granulata*.

Table 3 (Continued)

Date	Author	Contribution
1968	Schuster et al.	Described Isonema nov. gen.
1971	Guttman	Studied the interior of Euglena gracilis using scanning electron microscopy.
1971	Walne	Compared eyespot ultrastructure in Euglena sanguinea, E. granulata, Lepocinclis and Trachelomonas.
1972	Fize and Michel	Described fine structure of Astasia fennica.
1972	Kivic and Vesk	Described eyespot ultrastructure Euglena gracilis strain Z.
1972	Palisano and Walne	Described ultrastructure of aging Euglena granulata cells.
1973	Dodge	Described ultrastructure of Trachelomonas emphasizing reservoir area.
1973	Porter	Described Isonema papillatum.
1973	Throndsen	Described Eutreptiella gymnastica.
1973	Willey et al.	Described the anterior end of Colacium.
1974	Gomez et al.	Described ultrastructure of aging Euglena gracilis cells.
1974	Guttman and Ziegler	Described ultrastructure of Euglena gracilis strain Z emphasizing cytoskeletal role of pellicular microtubules.
1974	Kivic and Vesk	Described stigma apparatus in bleached Euglena.
1974	Leedale and Hibberd	Described the fine structure of the colorless Rhabdomonas and Menoidium.
1974	Nisbet	Studied ultrastructure and function of Peranema ingestion apparatus.

Table 3 (Continued)

Date	Author	Contribution
1974	Schuster and Hershenov	Studied ultrastructure of Khawkinea quartana.
1975	Dynesius and Walne	Described MTS and hairs in reservoir of Phacus.
1976	Bourrelly et al.	Described ultrastructure of two Euglena species.
1976	Hoffman and Bouck	Described pellicle growth in Euglena using immunolabeling.
1977	Rosowski and Willey	Studied stalk development in Colacium.
1978	Miller and Miller	Found distinct membrane types in Euglena corresponding to pellicle, reservoir, and flagellar areas.
1978	Moestrup	Presented micrographs of Eutreptiella roots and putative MLS.
1978	Rosowski and Lee	Described ultrastructure of Cryptoglena.
1979	Donnelly	Described ultrastructure of Trachelomonas emphasizing envelope microarchitecture.
1980	Hilenski	Described ultrastructure of Peranema emphasizing feeding apparatus, mucocysts and mastigonemes.
1980	Osafune and Schiff	Presented many longitudinal and cross sectional views through the stigma region of Euglena.
1980	West et al.	Described ultrastructure of cytoskeleton and flagellar system of Trachelemonas.
1982	Leedale	Reviewed euglenoid ultrastructure literature.
1982	Moestrup	Reviewed literature on algal flagellar structure, including roots.

Table 3 (Continued)

Date	Author	Contribution
1984	Solomon et al.	Described flagellar roots of *Entosiphon*.
1985	Farmer and Triemer	Described flagellar roots of *Distigma*.
1985	Hilenski and Walne	Described *Peranema* flagellar roots.
1985b	Willey and Wibel	Described cytopharyngeal homologue and reservoir microtubules of *Colacium*.
1986	Walne et al.	Described *Eutreptiella eupharyngea* sp. nov.

(1978) reported a multilayered structure (MLS) associated with one of these roots, similar in appearance to the MLS of Charophyceae, bryophytes, and higher plants. If the structure described by Moestrup is determined to be homologous to the MLS of the higher plant line, the phylogenetic implications would be profound.

Some phagotrophic euglenoids possess an ingestion apparatus, an additional microtubular structure with potential phylogenetic significance. The ingestion apparatus consists of microtubular supporting rods, putative contractile elements, and connecting fibrils (Mignot 1966, Leedale 1967, Nisbet 1974). The bodonids also have an ingestion apparatus, the cytopharynx, consisting of similar elements (e.g. Hitchen 1974, Brugerolle et al. 1979). In the bodonids, the flagellar roots arise in the basal body region and extend anteriorly, one of them eventually becoming part of the structural support of the cytopharynx (Brugerolle et al. 1979).

This investigation was undertaken to determine

1. whether a common flagellar root pattern exists among the euglenoids;

2. what components of the system are most stable and which most variable, and thus which aspects may prove valuable for comparisons at different taxonomic levels;

3. how the euglenoid root pattern compares with that of the kinetoplastids.

In order to address these questions, detailed information on the flagellar root systems of two representative euglenoid species was obtained and compared with published information on other euglenoid and kinetoplastid species. Entosiphon, a colorless phagotroph (Fig. 1[1]), was selected because it has a prominent ingestion apparatus and hence might reveal suspected flagellar root-ingestion apparatus similarities with the bodonids (Fig. 1), which are also colorless phagotrophs. The second organism, the phototrophic Eutreptia (Fig. 1), was selected because it is usually considered more primitive than most other green euglenoids due to the presence of two emergent flagella (the second flagellum being reduced to nonemergence in the presumably more advanced greens, such as Euglena). If the evolutionary sequence proposed by Kivic and Walne (1984) for the Euglenophyta were correct, there might be a corresponding sequence detectable within the flagellar root apparatus of Entosiphon, Eutreptia, and the advanced euglenoids, e.g. Euglena.

Moreover, during the course of this study, an organelle believed to be a vestigial ingestion apparatus (cytopharynx) was discovered in a supposedly advanced green euglenoid, Colacium (Willey and Wibel 1985a, b). The

---

[1]All figures referenced in Part 1 are found in the appendix at the end of Part 1.

present investigation was then broadened to include a search for a cytopharyngeal homologue in Eutreptia and, eventually, to trace the linkage between its flagellar roots and the cytopharynx.

Terminology

The assignment of names to the individual roots was recognized as a problem early in this study. Flagellar roots are defined as "(fibrous) appendages internal to the cell, which radiate from the region of the flagellar bases" (Manton 1965). Consequently, in this study names were assigned to euglenoid flagellar roots based on configuration of the roots in the basal body complex, the point of their origin. Thus, the dorsal root (DR) lies on the left dorsal side of the basal body complex, the intermediate root (IR) is between the two functional basal bodies, and the ventral root (VR) is on the right ventral side of the complex. For clarity, all figures in this document and all descriptions in the text are presented as if one were viewing the organism from its posterior end or from its dorsal side, as appropriate, insofar as possible.

However, there is variation in the location of the roots as they extend anteriorly so that e.g., the ventral root does not necessarily retain a ventral position throughout its length. This is especially noticeable in Entosiphon.

The only euglenoid roots to which names have previously been assigned are those of Colacium (Willey and Wibel 1985b). In the bodonids, flagellar roots have been examined in a number of studies (see Table 2) and names have been assigned, for the most part, independently by each author. Willey and Wibel (1985a, b) partially follow the terminology of Brugerolle et al. (1979), who deal in depth with five species of bodonids. To reduce proliferation of terms and to provide consistency, it would have been desirable to adopt the terminology used in previous work. However, such a course of action was not indicated in this study, wherein the roots are named on the basis of their relative positions at the point of origin. Furthermore, because this study presents evidence for homology but does not prove such a relationship, it would be premature to apply identical names at this time. Thus, it is perhaps worthwhile to risk the introduction of new terminology now, since it may prove helpful to future workers in this area.

In an effort to clarify the terms used throughout this study, Table 4 summarizes my current interpretation of the correspondence between bodonid and euglenoid flagellar root terminology.

Table 4. Comparison of Flagellar Root Terminology

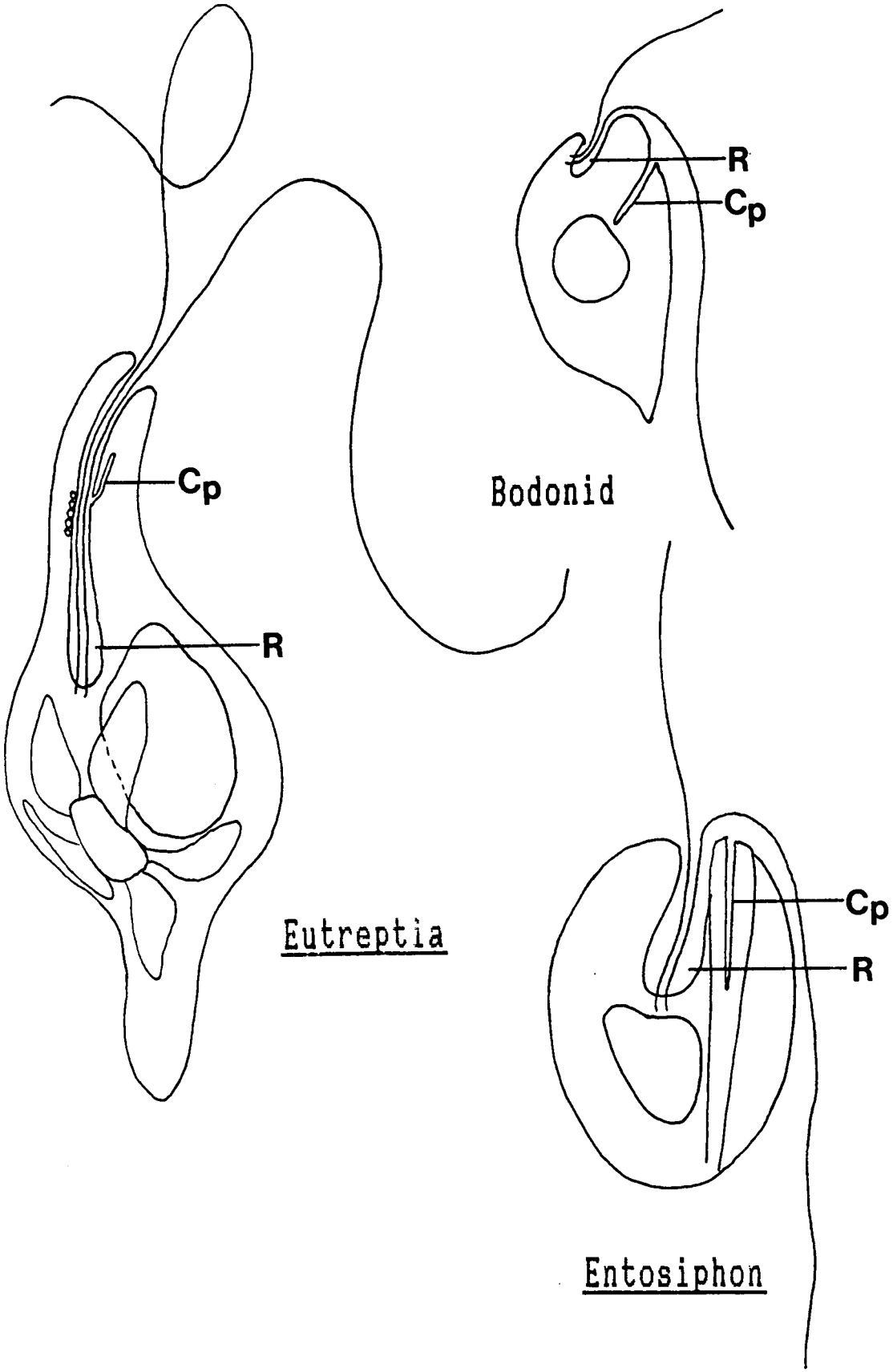
Euglenoids	Colacium[a]	Bodonids[b]
Dorsal root (DR)	-	Dorsal connector
Dorsal microtubules (DMT)	Dorsal microtubules (DMT)	Dorsal system "Fibre dorsale" (FD)
Intermediate root (IR)	Parareservoir microtubules (PMT)	Ventral fiber "Fibre ventrale" (FV)
Ventral root (VR)	Reinforcing microtubules (MTR)	Reinforced microtubules "Microtubules renforces de cytopharynx" (MTR)

[a]Willey and Wibel 1985b.

[b]Brugerolle et al. 1979.

APPENDIX: PART 1

Figure 1. Line drawings of Eutreptia, Entosiphon, and a representative bodonid, showing the relationship between the reservoir (R) and the cytopharynx (Cp). N = nucleus.


R
Cp
Bodonid
Cp
R
Eutreptia
Cp
R
Entosiphon

PART 2. *ENTOSIPHON SULCATUM*: FLAGELLAR ROOTS OF THE BASAL BODY COMPLEX AND RESERVOIR REGION

Abstract

The flagellar root system of Entosiphon sulcatum (Duj.) Stein (Euglenophyceae) is described and is compared with kinetoplastid and other euglenoid systems. An asymmetric pattern of three microtubular roots, one between the two functional basal bodies and one on either side (here called the intermediate, dorsal, and ventral roots), is consistent within the euglenoid flagellates studied thus far. The dorsal root is associated with the anterior functional basal body and lies on the left dorsal side of the basal body complex. Originating between the two functional basal bodies, and associated with the posterior functional one, the intermediate root is morphologically distinguished by fibrils interconnecting the individual microtubules to one another and to the overlying reservoir membrane; the root itself is often borne on a ridge projecting into the reservoir. The ventral root originates near the basal body of the posterior flagellum and lies on the right ventral side of the cell. Fibrillar connections link the membrane of the posterior flagellum with the reservoir membrane at the reservoir-canal transition level. A large cross-banded fiber joins the two functional basal bodies, and a series of smaller striated fibers links the anterior accessory basal body to the anterior functional one. The striations on these fibers do not have a periodically repeated

pattern. Large nonstriated fibers extend from the basal body complex laterally and posteriorly into the cytoplasm.

Introduction

The euglenoids have long been a phylogenetic enigma. A common ancestry with the green algae (Chlorophyta) is often assumed, based on chlorophyll and carotenoid types. Due to lack of other similarities, any divergence from the greens is thought to have occurred very early in the history of the euglenoids (e.g. Leedale 1978, Moestrup 1978, Ragan and Chapman 1978, Taylor 1978). It has been suggested that this similarity in pigmentation can be accounted for by an endosymbiotic event between a colorless euglenoid ancestor and a green alga (Stewart and Mattox 1975, Gibbs 1978, Whatley 1981). A close kinship with the kinetoplastid flagellates (bodonids and trypanosomes) has been repeatedly suggested (e.g. Mignot 1964, 1966, Leedale 1970, Bovee 1972, Burzell 1973, Dodge 1973, Round 1980, Walker 1985) and has recently been explored in depth Corliss (1984) and by Kivic and Walne (1984) who concluded that the euglenoids, bodonids, trypanosomatids, and Isonema form a common phyletic supergroup, with the euglenoids probably being descended from the kinetoplastids.

Primarily on the basis of flagellar root systems and mitotic and cytokinetic patterns, phylogenetic relationships within the Chlorophyta have undergone

considerable reevaluation within the past decade (Stewart and Mattox 1975, Moestrup 1978, Irvine and John 1984). The flagellar root systems of euglenoids, although poorly understood at present, could well provide information of comparable importance in the determination of euglenophycean relationships. So few details of the euglenoid root system are available, however, that any meaningful comparison among euglenoid taxa, between euglenoids and kinetoplastids, and among all of the chlorophyll a and b groups is currently impossible. The most complete information on euglenoid roots to date is available for Colacium spp. (Willey and Wibel 1985b), Euglena gracilis strain Z (Piccini and Mammi 1978), Peranema trichophorum (Hilenski and Walne 1985), and Rhabdomonas costata and Menoidium bibicillatum (Leedale and Hibberd 1974). Mignot (1963, 1964, 1966) has provided considerable morphological and ultrastructural information on a number of colorless euglenoids.

Entosiphon sulcatum was chosen for detailed study for several reasons. It is thought to have diverged from the euglenoid evolutionary pathway quite early (Leedale 1978) and might therefore demonstrate a little-modified flagellar root system. It has a well-developed ingestion apparatus, such as is found in the kinetoplastids, which permits investigation of possible linkages between this apparatus and the flagellar roots. Also, it was thought that

morphological interpretation would be simplified in the absence of pronounced metaboly, which would otherwise result in spatial displacement of cellular organelles. In fact, the movements of the siphon, even in the absence of traditional euglenoid metaboly, resulted in considerable spatial distortion.

In this paper, the absolute configuration of the flagellar root system of Entosiphon sulcatum, in the region of the cell from the basal body complex to the anterior portion of the reservoir, is described. This flagellar root pattern is compared with published micrographs of other euglenoid flagellar roots, and possible phylogenetic relationships between the euglenoids and the kinetoplastid flagellates, based on similarities in flagellar root patterns, are discussed.

Materials and Methods

Entosiphon sulcatum (Duj.) Stein was isolated from a mixed protozoan culture obtained from Carolina Biological Supply. The specific taxonomic designation was assigned based on comparison with Lackey (1929), Mignot (1963, 1964, 1966), and Leedale (1967), although future studies may show that E. sulcatum (Duj.) Stein and E. ovatus Stokes are conspecific. The organisms were grown at 21° C in a culture chamber in either a liquid medium (1.5% whole milk and 1.5% $CaSO_4$) or in a biphasic medium of 2% agar in petri

plates overlaid with an equal volume of the milk medium.

For transmission electron microscropy (TEM), cells grown in liquid culture were centrifuged gently (1500 x G) to a pellet and fixed in 2% glutaraldehyde and 2% OsO_4 (final concentration) in 0.1 M sodium cacodylate buffer (pH 7.2) for 10 min. The solutions used for fixation were at 4° C, but subsequent steps were carried out at room temperature. Afterward, the cells were rinsed three times with buffer, dehydrated through an acetone series, and embedded in Spurr's (1969) low viscosity resin.

Thin sections (80-100 nm thick) were obtained with a Sorvall MT-2 ultramicrotome, using a Dupont diamond knife. The sections were poststained with uranyl acetate followed by lead citrate and were examined with either a Zeiss EM 9S-2 or a Hitachi H-600 transmission electron microscope operated at an accelerating voltage of 60, 75, or 100 kV.

Serial thick sections (350 nm thick) were obtained in a similar manner but were poststained with ethanolic uranyl acetate for 30 min, followed by Sato's triple lead stain (Sato 1968) for 5 min at 50° C. Thick sections were examined with a Jeol JEM-1000 transmission electron microscope operated at an accelerating voltage of 1000 kV.

For scanning electron microscopy (SEM), cells were fixed for 30 min by flooding the plate culture with 2% aqueous OsO_4. The cells were then washed in distilled water, centrifuged, resuspended, and allowed to settle on a

glass cover slip coated with poly-d-lysine. Dehydration through a continuous acetone series was accomplished on the cover slip, followed by critical-point drying in a Bomar SPC-900 apparatus, and coating with gold-palladium. Cells were examined in an ETEC Autoscan scanning electron microscope operated at an accelerating voltage of 20 kV.

Results

The general morphology of the cell and the spatial relationships among the major organelles of Entosiphon sulcatum are shown in Figs. 1-4[1]. The ovoid cell body is striated with 12 longitudinally oriented grooves that scarcely show the helical pattern typical of euglenoids except at the extreme posterior end (Fig. 1). Two heterodynamic flagella emerge from the anterior end of the cell. The shorter anterior flagellum (F_1) beats actively, whereas the longer, posterior flagellum (F_2) usually trails on the ventral side of the cell adjacent to the substratum.

Protruding from the anterior right ventral side of the cell (as seen from a dorsal point of view) is the siphon (S; Fig. 1, arrow), which functions as an ingestion apparatus (Mignot 1966; D. J. Patterson, pers. comm.). It extends the length of the cell, tapering posteriorly, and can be retracted or extended (Fig. 2). Thoughout most of

[1]All figures referenced in Part 2 are found in the appendix at the end of Part 2.

its length, the siphon consists of three microtubular pharyngeal rods and four vane-like lamellae, which are in a pinwheel configuration (Fig. 4). Membranous elements, suggestive of endoplasmic reticulum, commonly surround the pharyngeal-rod portion of the siphon, and numerous cytoplasmic vesicles occur on its open side (Fig. 4). At the extreme anterior end of the siphon, a complex structure consisting of lamellar and other microtubular elements, links the pharyngeal rods, partially enclosing this three-sided tube (Fig. 2).

The two flagella extend from the base of the reservoir (Fig. 3), through the canal, and out of the anterior end of the cell through a cup-shaped depression (Fig. 2). Adjacent to the reservoir, and sometimes continuous with it, is a large contractile vacuole (CV, Fig. 2); posterior to the reservoir is the prominent nucleus containing an electron-dense nucleolus (endosome). The posterior half of the cell is dominated by food vacuoles containing densely staining bacteria and other particulate matter (Figs. 2, 4). Mitochondria are almost always peripheral (Fig. 4).

Basal Body Complex

The basal body complex is located beneath the reservoir membrane in a zone of exclusion (i.e. devoid of ribosomes and other structures; Figs. 3, 4), adjacent to the siphon and surrounded on the remaining sides by lobes of the nucleus (Figs. 2, 4). Spatial relationships among

the components of the basal body complex are presented diagrammatically in Figures 5 and 6. The complex consists of two functional basal bodies (bb_1 and bb_2), giving rise to flagella, in one plane and two accessory basal bodies (bb_1' and bb_2') in a second plane, at an angle of about 8^{o} to the first plane. Linking bb_1 and bb_2 to one another is a large striated connective fiber (LCF); smaller connective fibers (SCF) join bb_1 to bb_1'. Three microtubular roots extend anteriorly adjacent to the reservoir membrane, and a number of nonstriated fibers (NSF) emanate laterally and posteriorly from the basal body complex. In Figures 7-11, a nonadjacent series of transverse serial sections of the basal body complex are presented, extending from the posterior end of the basal body complex anteriorly to the lower region of the reservoir.

Microtubular Roots

Three microtubular roots originate in the basal body complex and extend anteriorly adjacent to the reservoir membrane. None of the three roots consists exclusively of microtubules. Rather, each contains additional distinctive elements and each changes morphologically as it progresses anteriorly.

Dorsal microtubular root (DR). The dorsal microtubular root, adjacent to bb_1, contains three microtubules at the level of the basal body complex (Figs.

12-14). In addition, there is an electron-dense layer on each side of the microtubular band, the proximal layer being somewhat narrower and more darkly staining than the distal layer. Anteriorly, the dorsal root angles away from bb_1, and linear elements are attached crosswise to it (Fig. 15, arrow). At the base of the reservoir, a band of singlet microtubules originates near the dorsal root (DMT, Fig. 16 shows it in the anterior reservoir region). An electron-dense plate overlies the DR and connects it to the DMT (Fig. 16). The three microtubules of the dorsal root which originate in the basal body complex can be distinguished from the DMT by their closer spacing, by their position relative to the other roots (i.e., they are on the side of the DMT near the IR; Fig. 16), and, in fortuitous sections, by their overlying plate.

Intermediate root (IR). The intermediate root, which originates between bb_1 and bb_2, contains five, or occasionally six, closely spaced microtubules forming a characteristic arc in the basal body complex (Figs. 13, 14). Within the basal body complex, the IR is adjacent to the large connective fiber (LCF) on the dorsal side, toward the accessory basal bodies (Figs. 7, 8, 12-14). The IR then crosses the LCF diagonally (Fig. 20) and, thus, is located on the ventral side of the LCF, away from the accessory basal bodies (cf. Figs. 7, 10).

The IR extends anteriorly along the reservoir membrane on a ridge projecting into the reservoir (Figs. 10, 11, 19). In the reservoir, the posterior flagellum (F_2) is always located opposite this ridge, the latticelike array of its paraxial rod (PAR) oriented toward the root (Figs. 11, 16, 17, 19). The spatial relationship between the two flagella is predictable, with the PARs being adjacent to one another and the two flagellar membranes linked by fine fibrils (Figs. 16, 17).

Anteriorly in the reservoir, the IR assumes a very distinctive appearance. The individual microtubules of the root (almost always numbering six) are interconnected by fine fibrils approximately 21 nm long (Fig. 19). Each of the component microtubules is also connected by another small link (approximately 7 to 14 nm long) to the overlying reservoir membrane (Fig. 19). There are also two sets of electron-dense fibers, one on either side of the root (Fig. 19). Between the IR and the DR, in the reservoir-canal transition zone, fine fibrils (100 to 150 nm long) join the flagellar membrane to the reservoir membrane (Figs. 16, 18). The fibrils are attached to F_2 adjacent to the paraxial rod and to a ridge on the reservoir margin located between the DR and the IR. Subtending the reservoir membrane of the ridge are some electron-dense granules (Fig. 16).

Ventral root (VR). The ventral root originates between the posterior functional basal body (bb_2) and the siphon (Figs. 7-9). In the basal body complex, the VR consists of six microtubules with attached fibrillar material. The spatial relationships among the VR, the siphon, and the basal body complex vary, both from cell to cell and from anterior to posterior within one cell (cf. Figs. 12, 14). As the VR extends anteriorly along the reservoir membrane, the microtubules of the root separate somewhat to form two segments (Figs. 10, 11). The segment consisting of two microtubules is set back slightly from the reservoir membrane, and a thin plate lies between the microtubules and the membrane.*

Other microtubular structures. A fourth type of microtubular structure consisted of two microtubules positioned dorsal to each of the four basal bodies (e.g. Fig. 24, arrow). These structures were of very limited extent, identified only occasionally in the posterior portion of the basal body complex and could not be traced anteriorly, nor were they identified posterior to the basal body complex. Due to their restricted occurrence, we hesitate to refer to them as roots.

Striated Fibers

There are several different striated connective fibers in the basal body complex. The most prominent is the large

connective fiber (LCF) linking the two functional basal bodies (bb_1 and bb_2). The LCF extends the length of the basal bodies (more than 1.5 μm; Fig. 21) and has a width of about 0.13 μm (Figs. 7, 8, 13, 14). It is symmetrically striated, having one electron-dense cross-band located centrally between the two basal bodies and less prominent cross-bands on either side of the central band (Figs. 12-14). The terminal fibrils are constricted into electron-dense bundles (Figs. 7, 8, 13, 21); each bundle is connected to one of the basal body triplets on either end of the fiber.

Adjacent to the IR, and parallel with the LCF, is a smaller striated fiber (Figs. 7, 13, 14). It extends from bb_2 toward bb_1, where it connects with at least one of the basal body triplets anchoring the LCF. The striations of the smaller fiber do not form the same pattern as those of the LCF.

Also adjacent to the IR, but perpendicular to it, is another very short, broad, striated fiber (PSF; Fig. 14). A series of small striated connective fibers (SCF), each only about 25 nm wide, joins bb_1 to bb_1' (Figs. 23, 24). As interpreted from serial sections, the structure includes several separate fibers, each with the same configuration, and each connected to one or two basal body triplets at either end (Fig. 6). The fibers are orthogonal to, and in contact with, the dorsal root (Fig. 24).

A second set of fibers (joining bb_2 to bb_2', similar to the set linking the anterior basal bodies) was not found. At the extreme posterior end of the complex is a structure that may serve this linking function (Fig. 22, arrow).

Nonstriated Fibrous Roots (NSF)

Several large nonstriated fibrous roots originate in the basal body complex and extend toward other cell organelles. A major NSF is attached to the VR in the basal body complex (Figs. 22, 25). This fibrous root extends posteriorly, approaching the siphon (Fig. 25), but the actual point of attachment was not identified. A second large NSF leads toward the cell surface, approaching the ventral groove (i.e. directly below the siphon; Figs. 24, 25).

Discussion

Comparison of this information with other published micrographs that include information on euglenoid flagellar roots confirms the validity of the typical euglenoid root pattern described by Moestrup (1982, p. 507): "one root opposite each basal body and a single root in between." To this general description, I would add that the root between the two basal bodies is near the basal body of the posterior flagellum. Table 1 summarizes my interpretation of published micrographs for a number of euglenoid species.

Table 1. Interpretation of Microtubular Flagellar Roots and Related Structures[a] in other Euglenoid Flagellates.

Species	Location: Basal Body	Location: Reservoir	Reference
Astasia fennica	VR(8)[b]		Fize and Michel 1972 (Fig. 9)
Astasia longa	2 SB		Sommer and Blum 1965 (Figs. 27, 28)
Colacium libellae	DR(4) IR(4) VR(5)	DMT DR IR(5) VR(7-9, cy)	Willey and Wibel 1985b (Figs. 3, 8, 9, 14, 17) and pers. comm.
Euglena acus		SB(12,cy) SB(15) DB	Leedale 1982 (Fig. 22)
Euglena gracilis var. bacillaris	DR8 IR(5) VR(9)	DMT SB IR(5) VR(9)	Solomon unpublished
Euglena gracilis strain Z	DR(4) IR(5) VR(7-9)	DMT DR(3-4,p) IR(5+4,f)	Piccini and Mammi 1978 (Figs. 1, 2, 3, 7, 9)
Eutreptiella cf. braarudii	DR(4)	DMT DR(4)	Moestrup 1978 (Figs. 17, 18, 22-25)
Eutreptiella eupharyngea		DMT SB(4) SB(10+10)	Walne et al. 1986
Khawkinea quartana	DR IR VR(6)	SB	Schuster and Hershenov 1974 (Figs. 4, 5, 7-11)
Menoidium bibicillatum	DR(5) IR(8) VR(5)	DR(5) IR(8,r) VR(5)	Leedale and Hibberd 1974 (Figs. 37, 41, 42)

Table 1 (Continued)

Species	Location: Basal Body	Location: Reservoir	Reference
Peranema trichophorum	DR(4) IR(6) VR(6)	DR(4,p) IR(10,f)	Hilenski and Walne 1985 (Figs. 9, 19, 20)
Phacus pleuronectes		SB (12,fpr)	Dynesius and Walne 1975 (Figs. 2-5)
Rhabdomonas costata		DR(6,p) IR(8,pr) VR(2+?)	Leedale and Hibberd 1974 (Fig. 38)
Trachelomonas hispida var. *coronata*	DR(4)	DMT SB(9) SB(24) SB	West et al. 1980 (Figs. 10, 11)

[a]Key to identity of structures:

DR = dorsal root
IR = intermediate root
VR = ventral root
SB = band of single microtubules
DB = band of doublet microtubules
DMT = dorsal microtubular band
cy = in cytoplasm, possibly related to cytopharynx
f = fibrils associated with microtubules
p = with associated plates
r = on ridge projecting into reservoir

[b]Numerals in parentheses refer to number of microtubules in that structure.

Because the number of microtubules and the appearance of the roots may vary depending on their anterior-posterior level within the cell, this level must be considered in any description of the roots. This listing is not exhaustive, and the root identifications presented are intended as tentative only, as an aid for future workers.

Microtubular Roots

Basal Body Level. Mignot (1966) reported a slightly different pattern of roots in Entosiphon sulcatum. He found six microtubules in the IR (Mignot 1966, fig. 40), which, as pictured, could also be described as a five-over-one arrangement. Similar configurations were occasionally seen in our study, but the five-membered pattern was seen more often in random sections and was traced consistently in several series. One series of sections from a single cell in our study (not shown), however, clearly had six microtubules throughout in the IR. Therefore, the number of microtubules in the IR, at least, cannot be considered a constant within this species.

Mignot identified a two-membered root (Mignot 1966, fig. 40) that corresponds, in both position and number of component microtubules, to one of the two-microtubule fragments found in this study. Further work may show that these fragments have a longer trajectory. Due to the sectioning angle, the DR was identifiable in Mignot's study

only as an electron-dense blur near the anterior flagellum (Mignot 1966, fig. 40).

There is a basic asymmetry to the euglenoid root pattern at basal body level because the intermediate root (IR) is located closer to bb_2 than to bb_1. This asymmetry was noted in Entosiphon sulcatum (e.g. Fig. 6) as well as in Euglena gracilis strain Z (Piccini and Mammi 1978), E. gracilis var. bacillaris (unpubl.), and Colacium libellae and C. mucronatum (Willey and Wibel 1985b). A similar pattern exists in Peranema trichophorum (Hilenski and Walne 1985), although the anterior and posterior functional basal bodies were labeled arbitrarily (L.L. Hilenski, pers. comm.). Based on further examination of euglenoid roots, I can identify Hilenski and Walne's F_1 as the posterior flagellum, F_2. An exception to this root pattern may be found in Menoidium bibicillatum, where the intermediate root appears to be more closely associated with bb_1 than with bb_2 (Leedale and Hibberd 1974, fig. 42).

The euglenoid ventral root (VR), at basal body level, usually contains more microtubules than does the DR. With one exception, all VRs identified in other published micrographs contained between five and nine microtubules, and the dorsal root had only three to six microtubules (Table 1). The apparent exception was Rhabdomonas costata (Leedale and Hibberd 1974), containing a two-membered ventral root and a six-membered dorsal one. The

micrograph of interest, however, was of a section through the reservoir, at which level the two-membered element may represent only one segment of the entire root. Such a bifurcation of the ventral root is described here in Entosiphon sulcatum.

At basal body level, the spatial orientation of euglenoid roots with respect to the four basal bodies is predictable. The dorsal root is almost perpendicular to the axis connecting the functional basal bodies (i.e. is tangential to bb_1), and the intermediate root is usually roughly parallel to this axis (Fig. 13). The orientation of the VR varies with respect to the siphon and the basal body complex, an arrangement suggesting that the ventral root serves as a link between these two structures. When the siphon changes position (extension or retraction), the orientation of the VR may also change. The VR, however, is often recognizable in cross-section as extending outward from the center of bb_2. Similar spatial orientations of the three flagellar roots were noted in Peranema (Hilenski and Walne 1985, fig. 9), Euglena (Piccini and Mammi 1978, figs. 3, 6), Menoidium (Leedale and Hibberd 1974, fig. 42), and Colacium (Willey and Wibel 1985b).

Upper reservoir level. The following distinct morphological features identify the IR in Entosiphon and can be used to trace its path anteriorly in the cell: (1) the IR microtubules are evenly spaced, with linkages to one

another and to the overlying reservoir membrane, (2) the root itself is often located on a ridge projecting into the reservoir, and (3) the IR is consistently positioned opposite the paraxial rod of the posterior flagellum. One or more of these features were also noted on a root of Euglena (Piccini and Mammi 1978, fig. 9), Menoidium (Leedale and Hibberd 1974, fig. 37), Rhabdomonas (Leedale and Hibberd 1974, fig. 38), and Peranema (Hilenski and Walne 1985, fig. 20).

Although it is more difficult to locate than the intermediate root in Entosiphon, the dorsal root (DR) also is recognizable in the upper reservoir level by the closer spacing of its component microtubules, by its association with an overlying electron-dense plate, and by its position adjacent to a long band of singlet microtubules, the DMT. These traits were also found in Euglena (Piccini and Mammi 1978, fig. 9) and Peranema (Hilenski and Walne 1985, fig. 19).

In the upper reservoir region of Entosiphon, a band of singlet microtubules, the DMT, was joined to the DR by an electron-dense plate. Peranema has a similar, but more highly differentiated, arrangement (DR, plate, microtubular band) with a large striated fibril running longitudinally behind the plate (Hilenski and Walne 1985, figs. 19, 20). In addition, an electron-dense plate between a four-stranded root and the stigma-associated microtubules was

reported by Moestrup (1978, fig. 18) in Eutreptiella eupharyngea nom. prov. (referred to as Eutreptiella cf. braarudii in Moestrup 1978). The stigma-related band of singlet microtubules in Trachelomonas, Euglena, and Colacium (Willey and Wibel 1985b), among others, are probably homologous with this structure.

The anterior fate of the ventral root remains to be determined. It may angle to run obliquely around the reservoir and would therefore be difficult to locate in transverse section. It may diverge into the cytoplasm, perhaps joining the microtubules of the siphon, or it may do both by splitting into two branches. There is evidence to support any of these possibilities. Changes in the position of the ventral root, (for example, with extension and retraction of the siphon) would explain much of the difficulty of locating this root.

Fibrous Roots

Cross-banded fibrous roots in Entosiphon are confined to the basal body complex and include the small and large connective fibers as well as an ill-defined linkage between the intermediate root and the large connective fiber. Very little comparative information is available on euglenoid connective fibers, possibly indicating the atypical nature of the LCF in Entosiphon. A structure of this size would probably have been observed in ultrastructural studies of other organisms if it existed. In Peranema, there is

extensive electron-dense material between the two functional basal bodies (Hilenski and Walne 1985, figs. 8, 9), but morphological details are obscure. In Euglena, a structure similar to one of the small connective fibers in Entosiphon extends from bb_1 toward bb_2 (Piccini and Mammi 1978, fig. 1).

Extending into the cytoplasm laterally and posteriorly, the nonstriated fibers in Entosiphon constitute a more extensive system than the striated ones. The largest fiber, referred to as a rhizoplast by Mignot (1966), extends more than 5 μm posteriorly toward the siphon. I am not aware of any comparable nonstriated fibrous roots in other euglenoids, but suspect that this is due more to difficulty in identifying these indistinct structures than to interspecific differences. In fact, the fibrillar layer attached to the ventral root of Euglena (Piccini and Mammi 1978, fig. 2) looks identical to a similar layer in Entosiphon (not shown).

In Peranema, Hilenski and Walne (1985) reported massive, darkly staining striated roots originating in the basal body complex and speculated on their phylogenetic implications. Interestingly, the nonstriated fibrous roots in Entosiphon arise in locations similar to the origins of the striated fibers in Peranema and are of similar diameter. They do not stain darkly nor in a striated pattern, however, suggesting differences in chemical

composition. Whereas, in Peranema, the fibrous roots connect directly to the rodorgan, in Entosiphon, these roots extend more than 5 μm toward the siphon but connect to it, if at all, far from the basal body complex. It may be functionally significant that Entosiphon lacks the membranous elements, probably endoplasmic reticulum, which surround both the striated roots and the basal body complex in Peranema (Hilenski and Walne 1985).

Fibrillar Connections

The fibrillar connections linking the flagellar and reservoir membranes between the DR and IR may explain the unvarying positional relationship between the intermediate root and the posterior flagellum. In addition, fibrous connections between the two flagella, previously noted in Menoidium (Leedale and Hibberd 1974), probably account for the close association and consistent orientation of the two flagella in Entosiphon. Beyond the maintenance of spatial relationships, the fibrils may serve other functions in the cell, e.g. sensory transduction. The platelike structures connected with these flagellar roots in Entosiphon and in Peranema (Hilenski and Walne 1985), Eutreptiella (Moestrup 1978), and Euglena (Piccini and Mammi 1978) may also be related to such functions, indicating a very intricate complex. A similar level of complexity was shown by West et al. (1980, fig. 13) in the paraxial rod and swelling complex of F_1 in Trachelomonas hispida var. coronata.

Phylogenetic Implications

In the few euglenoid species for which sufficient information is available, the pattern of microtubular flagellar roots is uniform. Although the number of microtubules in each root varies with location in the cell, from taxon to taxon, and to some extent within a given species, the arrangement of the roots is consistent. There is considerable variation in the fibrous roots, however. No generalizations can be made concerning the connective fibers, due to lack of information, but variability of the cytoplasmic roots (i.e., the nonstriated fibrous roots in Entosiphon and the striated fibers and fibril in Peranema) is great; it may prove useful in determining phylogenetic relationships within the Euglenophyceae.

Based on extensive morphological similarities and inferred homologies (Corliss 1984, Kivic and Walne 1984) and on comparisons of 5S RNA (Kumazaki et al. 1983, Walker 1985) and cytochrome c (Baba et al. 1981) sequences, a close phylogenetic relationship between the euglenoids and the kinetoplastid flagellates (the bodonids and trypanosomatids) has often been proposed. Areas of morphological similarity in the two groups include general cell shape, flagellar placement, possession of a paraxial rod, type of nuclear division, type of mitochondrial cristae, and the number of flagellar roots. In addition, as discussed by Kivic and Walne (1984), three structures

may be homologous in the two groups: (1) the peripheral microtubular cytoskeleton; (2) the structural support of the ingestion apparatus and its connection with the flagellar roots; and (3) the flagellar transition zone.

Flagellar root apparatus. A comparison of the flagellar root patterns of the euglenoids and bodonids shows many similarities. The bodonid flagellates have three microtubular roots originating in the basal body area and extending around the flagellar pocket, which is homologous with the euglenoid reservoir (Brugerolle et al. 1979). According to Brugerolle et al. (1979), in the bodonids a three-membered root is associated with the basal body of the anterior flagellum and lies near the dorsal side of the reservoir. The microtubules of this root are closely spaced, and adjacent to them is an electron-dense lamellar plate. This description is very similar to that for the euglenoid DR. A second bodonid root (the MTR) is morphologically distinguished by fibrils connecting the individual microtubules to one another and larger fibrils linking the microtubules to the overlying membrane. This root, which is often borne on a ridge projecting into the flagellar pocket, forms a loop anteriorly and then runs in a posterior direction adjacent to the wall of the cytostome-cytopharynx. A third bodonid root, the ventral fiber (FV), typically containing four microtubules, originates near bb_2

runs obliquely around the left side of the flagellar pocket, and then runs posteriorly lining the ventral groove. While correspondence between the latter two bodonid roots with the IR and/or VR of euglenoids is not yet clear, the resemblance is certainly suggestive of homology.

The picture is less clear with the trypanosomes because they are highly specialized for a parasitic existence, with a complicated life cycle and considerable morphological variation. Most have only one flagellum (which is usually recurrent and attached for most of its length to the cell body) and one accessory basal body (Vickerman and Preston 1976). Most species have one microtubular flagellar root, which originates near the functional basal body and extends anteriorly along the flagellar pocket membrane (e.g. Anderson and Ellis 1965, Lom et al. 1980). A second microtubular band originates near the opening of the flagellar pocket, extends anteriorly for a short distance, and then follows the border of the cytopharynx latero-posteriorly (Lom et al. 1980, Kivic and Walne 1984). Morphological and positional similarities indicate that this second band corresponds to the MTR in bodonids (Vickerman and Preston 1976, Brugerolle et al. 1979) and either the intermediate or ventral root in euglenoids. An aberrant representative, Trypanosoma lucknowi (Weinman et al. 1984), was recently found to have

two microtubular flagellar roots, one associated with each basal body. This could represent an intermediate evolutionary stage, in which only the functional and accessory basal bodies of the posterior flagellum were retained, with their associated roots. This would imply that the single flagellum of extant trypanosomes was derived from the posterior recurrent flagellum of a euglenoid or bodonid ancestor, as suggested by Kivic and Walne (1984).

Ingestion apparatus. A microtubular linkage between the flagellar roots and the ingestion apparatus, or cytopharynx, has been described in the kinetoplastids (Brugerolle et al. 1979, Lom et al. 1980). In addition, Willey and Wibel (1985b) have described a microtubular connection between the flagellar roots and a putative vestigial cytopharynx in Colacium, a green euglenoid. Because Entosiphon also has an ingestion apparatus (the siphon), a similar linkage between its flagellar roots and cytopharynx might be expected.

The ingestion apparatus of the bodonids and trypanosomes is structurally much simpler than the siphon in Entosiphon. The bodonid cytopharynx consists of a membrane-lined tube opening near the right ventral lip of the flagellar pocket, with associated microtubular supporting structures. One of these microtubular structures is continuous with a flagellar root (the MTR),

and the other originates near the cell surface adjacent to the cytostome (opening of the cytopharynx). Attached to the microtubules of the MTR are fibrous struts linking it to the overlying reservoir or cytopharyngeal membrane and to each other.

A similar membrane-lined tube arising inside the reservoir canal region was recently found in Colacium, a phototrophic euglenoid (Willey and Wibel 1985b). Here, too, this putative cytopharyngeal homologue is associated with a microtubular supporting structure which is continuous with a flagellar root. As described by Willey and Wibel (1985a), an evolutionary sequence involving the progressive displacement of the anterior cytopharyngeal opening into the flagellar pocket and then further down into the reservoir-canal transition zone is not difficult to envision. Such a sequence would correspond to the morphologies of present-day bodonids, trypanosomes, and Colacium, respectively.

A cytopharyngeal homologue similar to that of Colacium was not identified in Entosiphon. Here, the cytopharynx is probably represented by the siphon, and thus the ingestion apparatus is a dominant cellular feature. The presence and position of the cytopharyngeal homologue/remnant may well prove to be a valuable phylogenetic indicator among the various euglenoid taxa.

Summary

This study describes an asymmetric arrangement of three microtubular roots which extend anteriorly and subtend the reservoir membrane, confirming and refining previous fragmentary descriptions of the euglenoid flagellar root pattern. A number of other morphological details of these roots in Entosiphon are also described. The uniformity of these structural features in euglenoids as a whole, however, awaits detailed studies of the roots of additional euglenoid species.

APPENDIX: PART 2

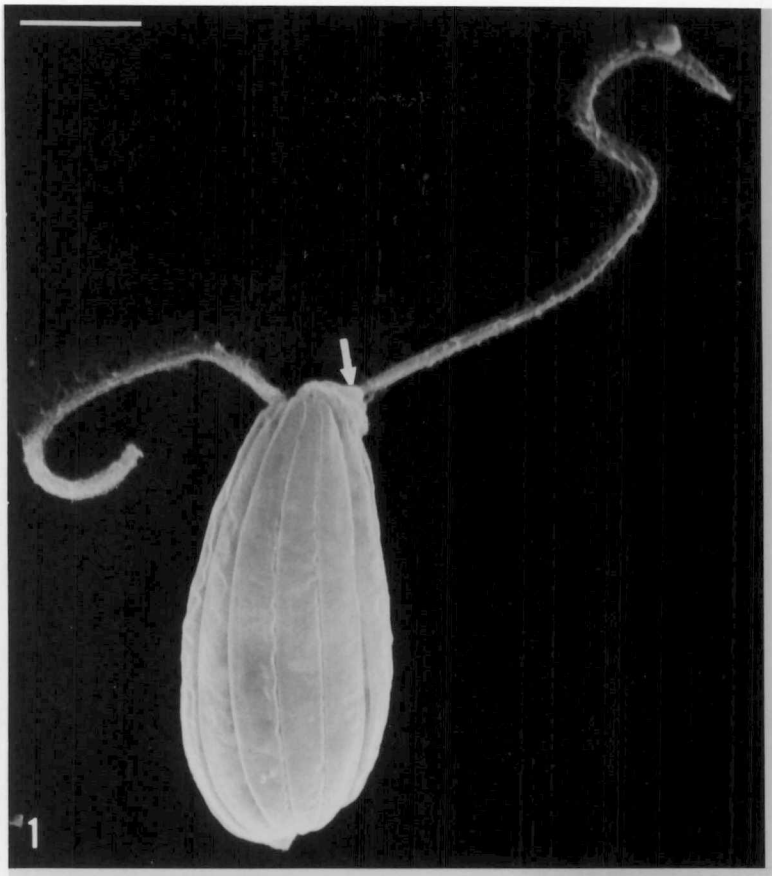
A complete list of abbreviations is provided on p. xv.

Figure 1. SEM overview of Entosiphon sulcatum. Long posterior recurrrent flagellum and shorter anterior flagellum project from anterior end of cell. Five of 12 longitudinal grooves are visible on dorsal surface of cell. Siphon (arrow) protrudes over proximal end of posterior flagellum. Scale bar = 5.0 μm.

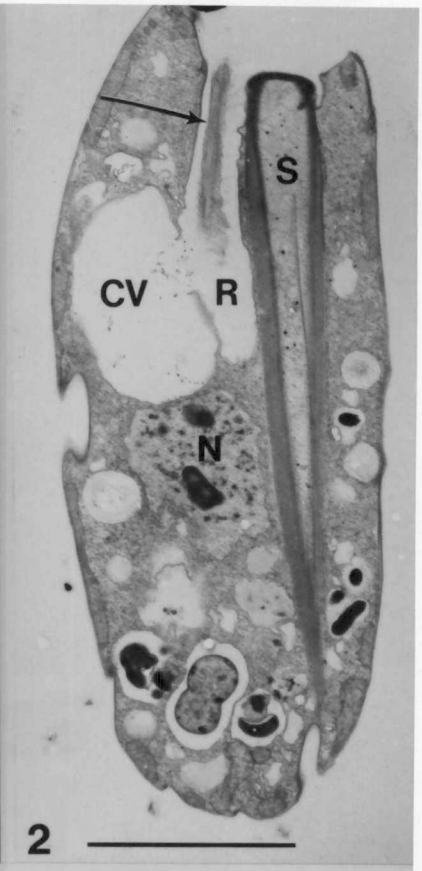
Figure 2. TEM view of median longitudinal section of E. sulcatum. Siphon (S) extends the length of the cell beside the reservoir (R) and nucleus (N). Flagella (arrow) extend through the canal and anterior depression. CV = contractile vacuole. Scale bar = 5.0 μm.

Figure 3. Flagellar basal region. Longitudinal section showing continuity between a flagellum (F) and its functional basal body (bb). A nonstriated (NSF) fiber extends posteriorly from the basal body complex. E. sulcatum. Scale bar = 1.0 μm.

Figure 4. Transverse section of E. sulcatum at base of reservoir. Basal body complex (arrow) is located to the left of the siphon (S) and is surrounded by lobes of the nucleus (N). Food vacuoles (FV) contain ingested bacteria. Scale bar = 1.0 μm.



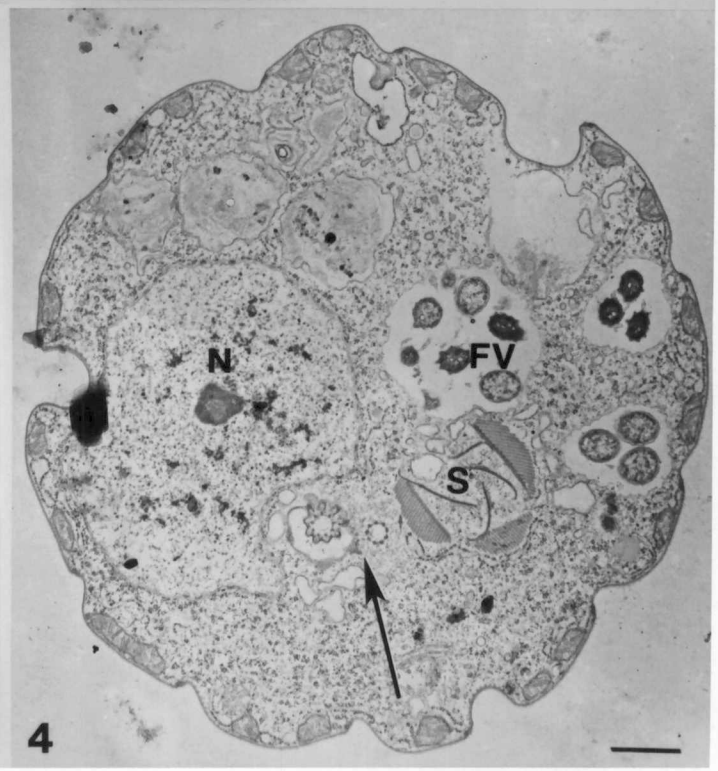
1



2



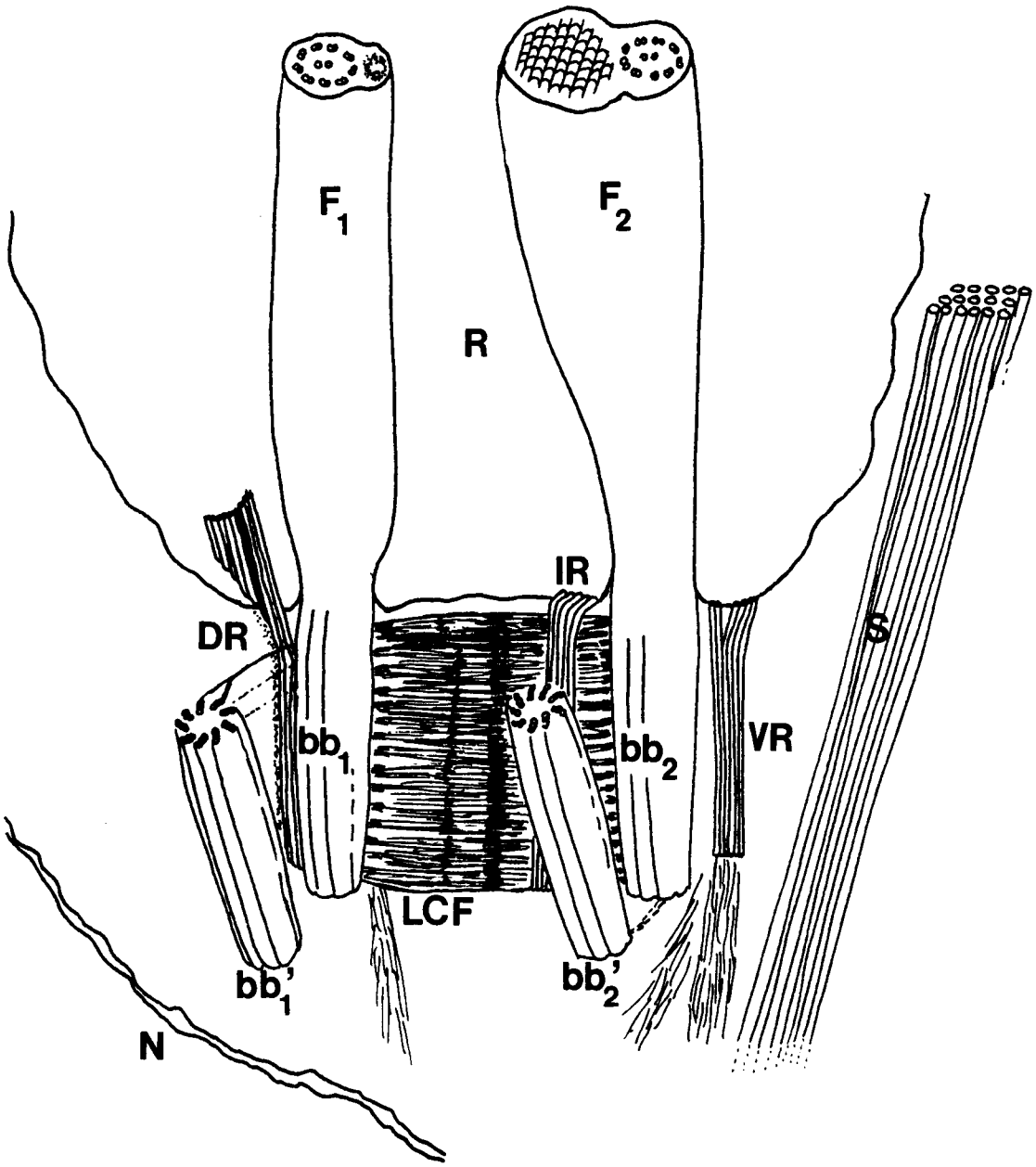
3



4

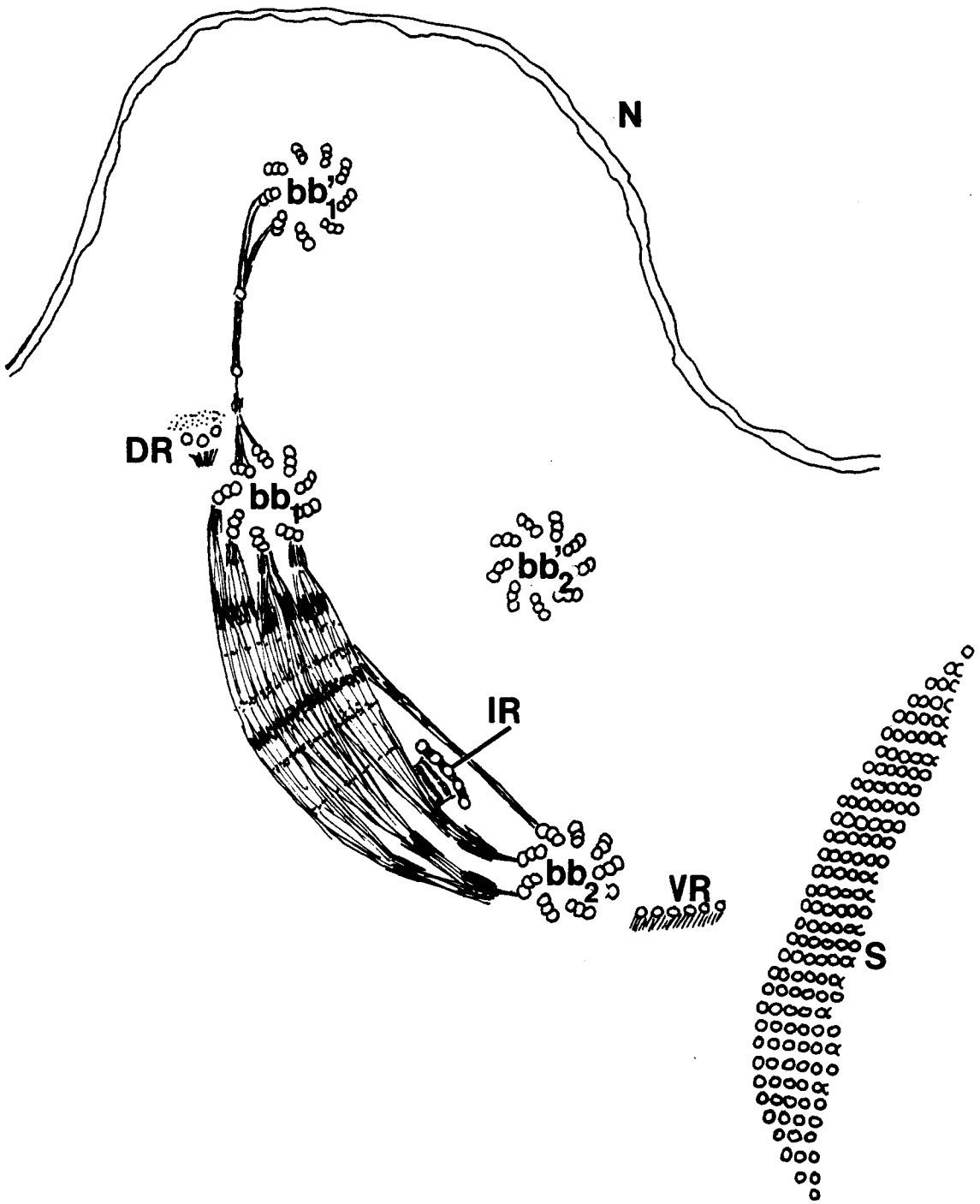
A complete list of abbreviations is provided on p. xv.

Figure 5. Three-dimensional diagrammatic reconstruction of the basal body complex of Entosiphon sulcatum as seen from the right dorsal side of the cell. Not to scale.


F1
F2
R
IR
DR
bb1
bb2
VR
S
LCF
bb'1
bb'2
N

A complete list of abbreviations is provided on p. xv.

Figure 6. Diagram of a median transverse section through the basal body complex of Entosiphon sulcatum as seen from the posterior end of the cell. Not to scale.


N
bb'1
DR
bb1
bb'2
IR
bb2
VR
S

A complete list of abbreviations is provided on p. xv.

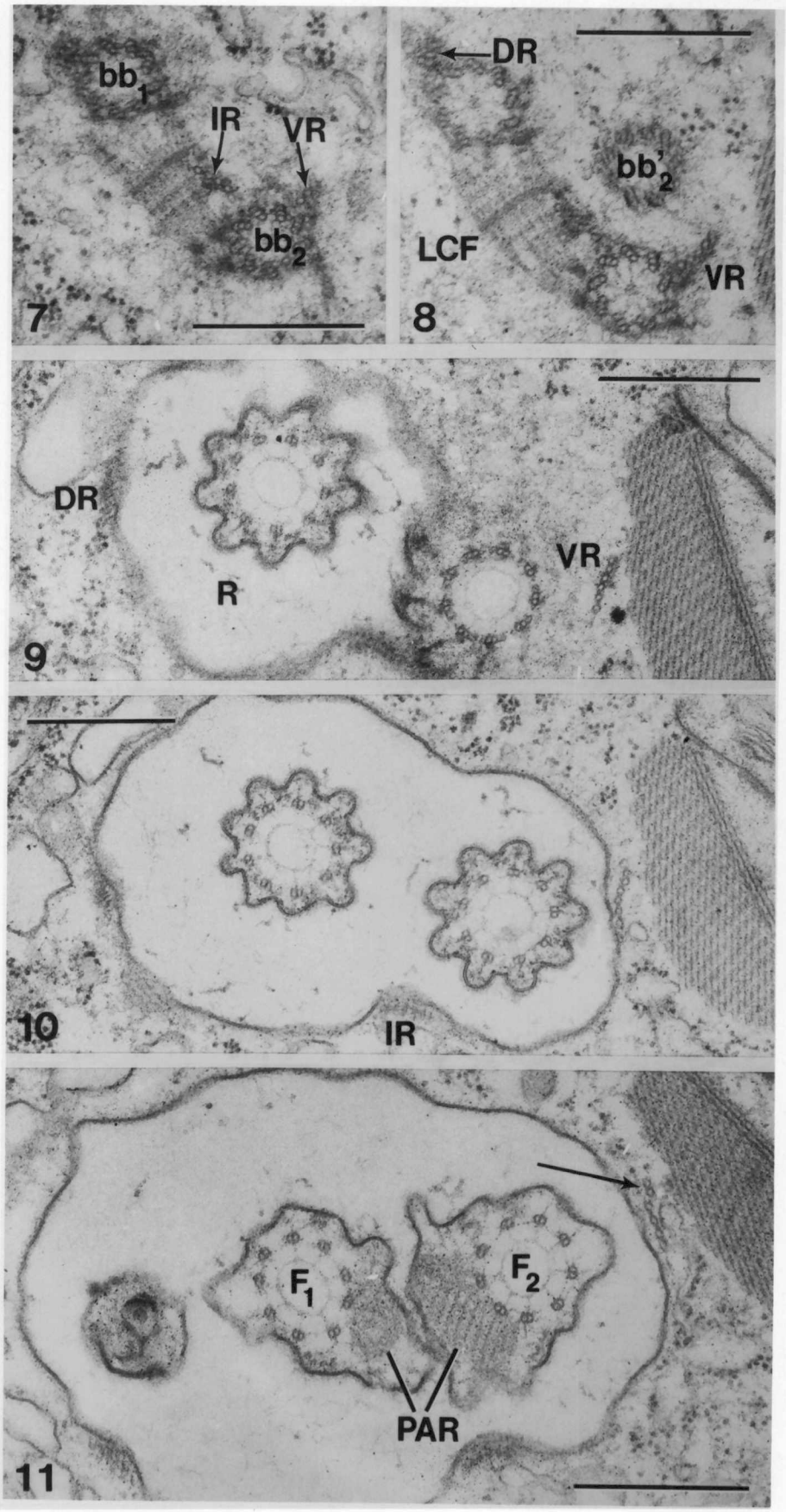
Figure 7. Transverse section through posterior end of basal body complex of Entosiphon sulcatum. At this level, only two of the four basal bodies are present (the two functional ones, bb_1 and bb_2). The ventral root (VR) consists of only two microtubules at this level and the intermediate root (IR) lies between bb_1 and bb_2. First in a series of five nonadjacent serial sections. Scale bar = 0.5 μm.

Figure 8. Transverse section through basal body complex, anterior to Fig. 7. The posterior accessory basal body (bb_2') is visible, the dorsal root (DR) is located near bb_1, and more microtubules are present in the VR. Second in a series of five nonadjacent serial sections. Scale bar = 0.5 μm.

Figure 9. Transverse section through flagellar transition zone. At the level where the flagella emerge into the reservoir (R), the DR and VR maintain their respective positions. Third in a series of five nonadjacent serial sections. Scale bar = 0.5 μm.

Figure 10. Transverse section through base of reservoir. The IR is located on the ventral side of the reservoir on a ridge projecting between the two flagella. Fourth in a series of five nonadjacent serial sections. Scale bar = 0.5 μm.

Figure 11. Transverse section through reservoir, anterior to Fig. 10. The VR consists of two segments, with two microtubules set back slightly from the reservoir membrane and overlain by a thin plate (arrow). The paraxial rods (PAR) are present in the two flagella and their different morphologies can be used to distinguish F_1 from F_2. Last in a series of five nonadjacent serial sections. Scale bar = 0.5 μm.

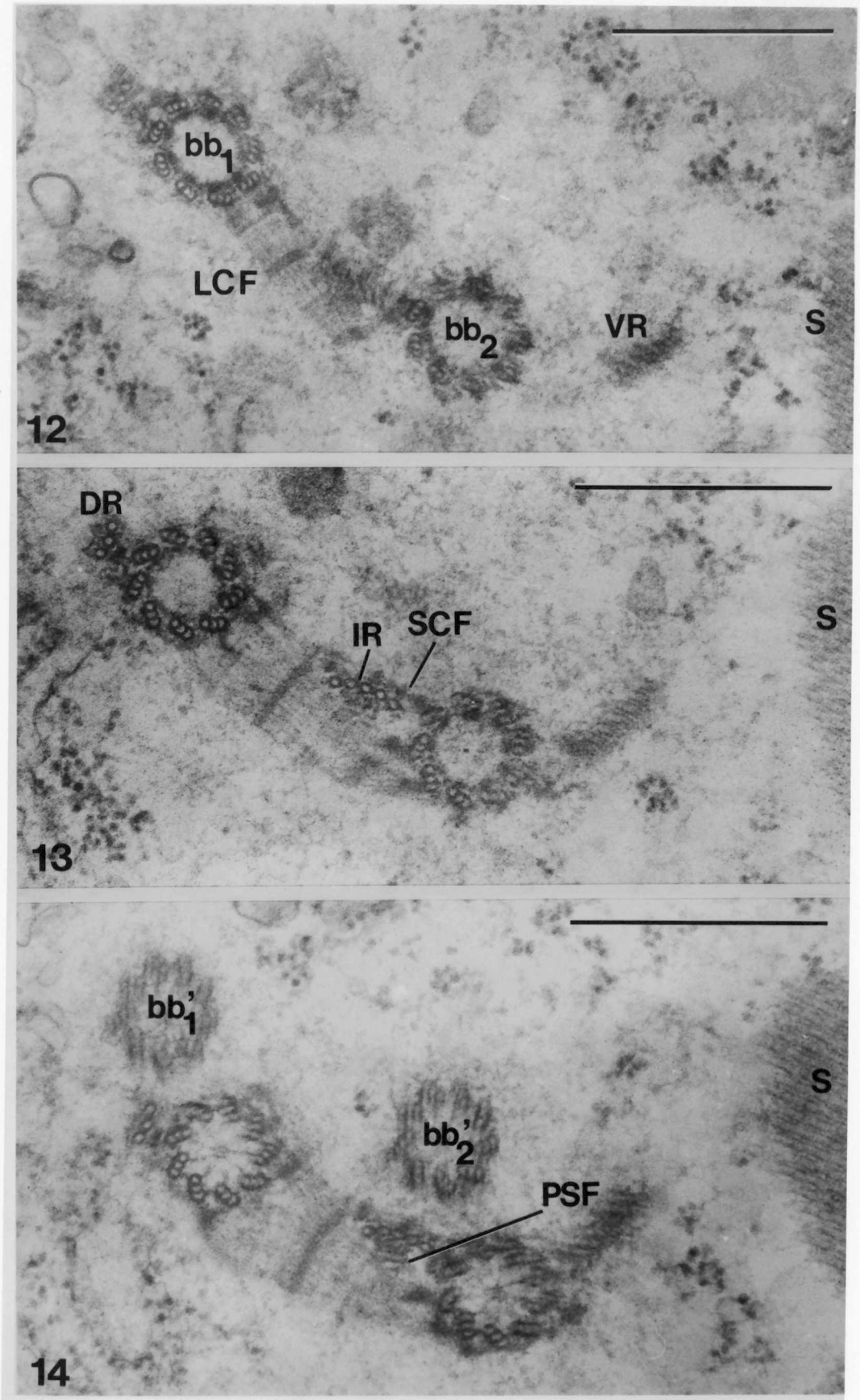

bb1
IR
VR
bb2
7
DR
bb'2
LCF
VR
8
DR
R
VR
9
IR
10
F1
F2
PAR
11

A complete list of abbreviations is provided on p. xv.

Figure 12. Transverse section of Entosiphon sulcatum at anterior end of basal body complex. The two functional basal bodies are linked by the large striated connective fiber (LCF); the VR extends toward the siphon (S). First in a series of three nonadjacent serial sections. Scale bar = 0.5 μm.

Figure 13. Transverse section posterior to Fig. 12. The DR has three microtubules and associated electron-dense layers. The IR lies adjacent to the LCF in a characteristic arc formation. Distal to the IR is a small connective fiber (SCF). Second in a series of three nonadjacent serial sections. Scale bar = 0.5 μm.

Figure 14. Transverse section including all four basal bodies, posterior to Fig. 13. The perpendicular striated fiber (PSF) extends from the IR toward the LCF. Scale bar = 0.5 μm.


bb1
LCF
bb2
VR
S
12
DR
IR
SCF
S
13
bb'1
S
bb'2
PSF
14

A complete list of abbreviations is provided on p. xv.

Figure 15. The dorsal root (DR) extends away from the anterior functional basal body at an angle of about 30°. Transverse elements are adjacent to the root near the reservoir membrane (arrows). Entosiphon sulcatum. Scale bar = 0.5 μm.

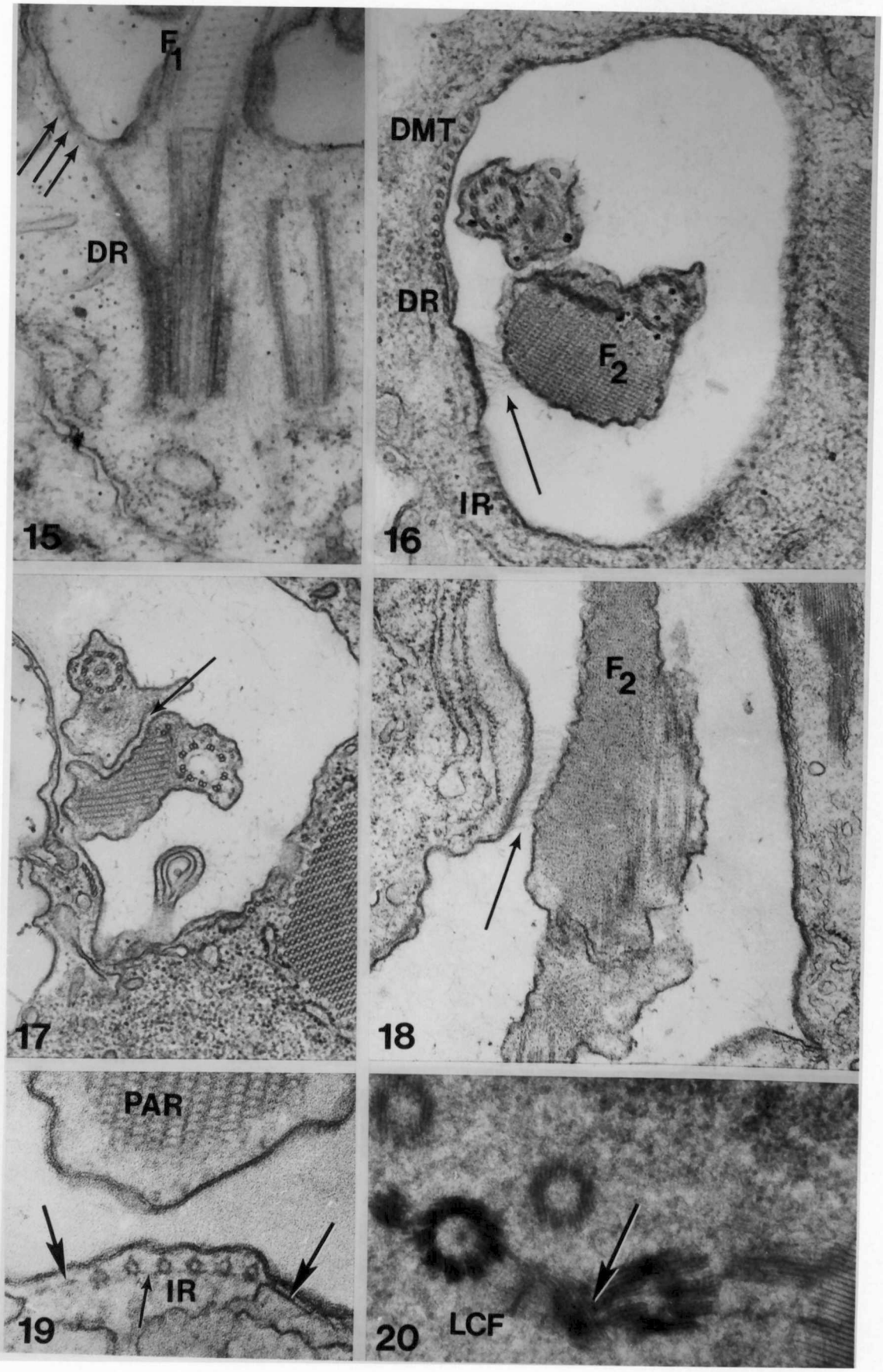
Figure 16. Transverse section at the anterior end of the reservoir. Fibrils connect the posterior flagellum (F_2) to a ridge between the DR and the intermediate root (IR). Overlying the three microtubules of the DR is an electron-dense plate which connects it to the dorsal microtubules (DMT). Scale bar = 0.5 μm.

Figure 17. Fibrils connect the two flagella to one another (arrow). Two additional microtubules lie adjacent to the PAR of F_2, outside of the axoneme. Scale bar = 0.5 μm.

Figure 18. Longitudinal section through the reservoir-canal transition zone. Fibrils (arrow) connect the paraxial rod portion of F_2 to the reservoir membrane (cf. Fig. 16). Scale bar = 0.5 μm.

Figure 19. The IR lies opposite the PAR of F_2 on a ridge projecting into the reservoir. The individual microtubules are interconnected by fine fibrils (small arrow); additional fibrils link each microtubule to the overlying reservoir membrane. On either side of the IR are electron-dense plates (large arrows). Posterior to Fig. 16. Scale bar = 0.1 μm.

Figure 20. High voltage electron micrograph of thick section (0.4 μm). The IR (arrow) crosses the large connective fiber (LCF) diagonally, in the basal body complex. Scale bar = 0.5 μm.


F1
DR
15
DMT
DR
F2
IR
16
17
F2
18
PAR
IR
19
LCF
20

A complete list of abbreviations is provided on p. xv.

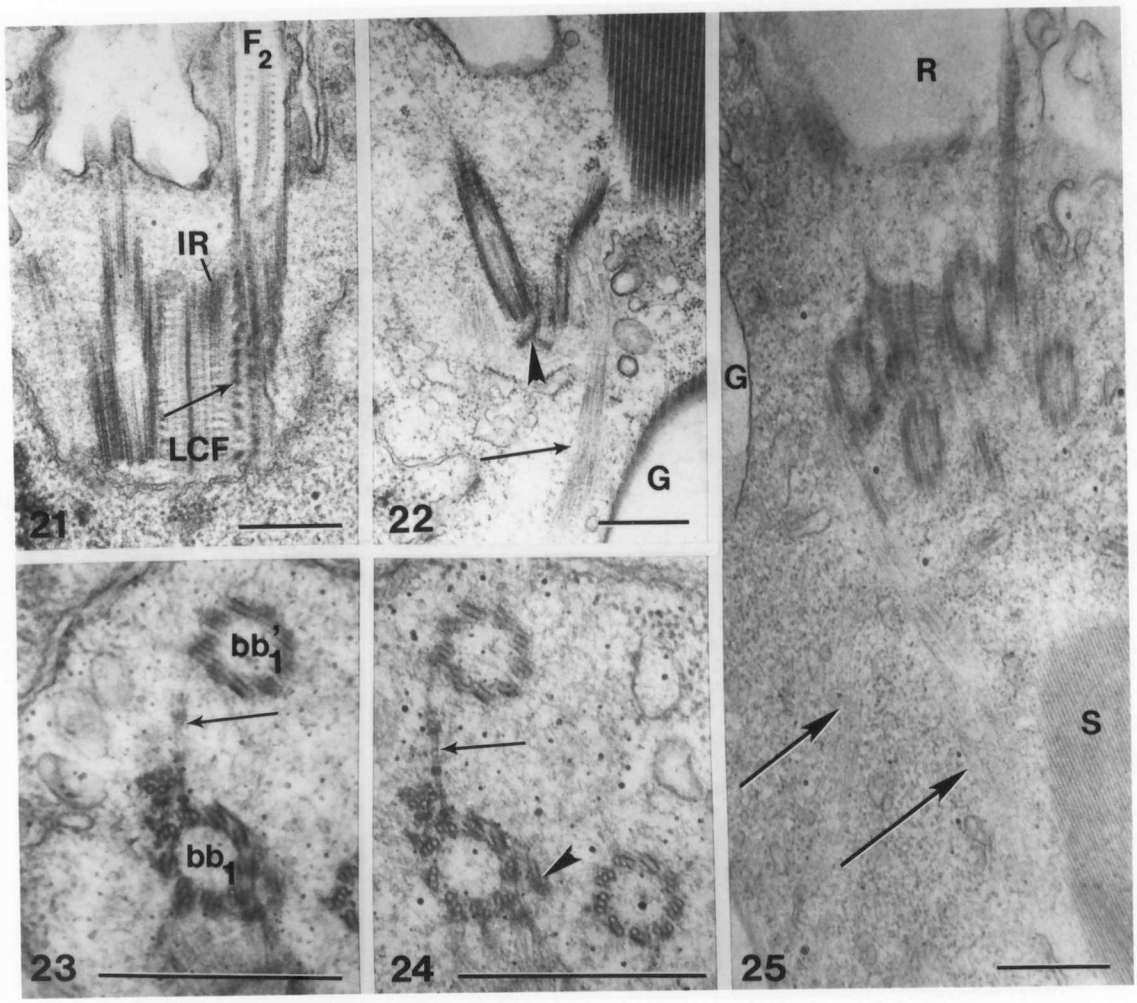
Figure 21. Longitudinal section of the large connective fiber (LCF). It is connected to the basal bodies by electron-dense terminal bundles of the component fibrils (arrow). The intermediate root (IR) is located near F_2. Entosiphon sulcatum. Scale bar = 0.5 μm.

Figure 22. Nonstriated fibers (NSF, arrow) extend away from the basal body complex. One NSF leads from the ventral root toward a groove (G). An unidentified structure (arrowhead) may link the two posterior basal bodies to one another. Scale bar = 0.5 μm.

Figure 23. A small connective fiber (arrow) extends from bb_1 toward bb_1'. First of two nonadjacent serial sections. Scale bar = 0.5 μm.

Figure 24. A small connective fiber (arrow) attaches to three microtubular triplets of bb_1'. A two-microtubular fragment (arrowhead) lies to the right dorsal side of bb_1. Second of two nonadjacent serial sections. Scale bar = 0.5 μm.

Figure 25. Oblique view of basal body complex. As seen from dorsal left side of cell, NSFs (arrows) extend away from basal body complex toward siphon (S). Scale bar = 0.5 μm.


F2
IR
LCF
21
22
G
G
R
S
25
bb'1
bb1
23
24

PART 3. ENTOSIPHON SULCATUM: FLAGELLAR ROOTS ANTERIOR TO THE RESERVOIR

Abstract

A close phylogenetic relationship between the euglenoid algae and the kinetoplastid protozoans is suggested by a number of morphological and biochemical similarities. This study examines the flagellar roots and microtubular cytoskeleton of Entosiphon sulcatum, a colorless, phagotrophic euglenoid, and finds a correspondence between the microtubular structures of this organism and those of the bodonids. Thus, on the basis of ultrastructural morphology, trajectory, and assumed function, the dorsal, intermediate, and ventral roots of Entosiphon strongly resemble the dorsal connector, ventral fiber (FV), and the reinforced microtubules (MTR), respectively, of the bodonids. In addition, the dorsal fiber (FD) of the bodonids seems to be represented in Entosiphon by the groove microtubules underlying the pellicle. The pharyngeal rods of Entosiphon may bear the same relationship to the cytopharyngeal homologue as does the cytopharynx-associated fiber (FAS) in the bodonids. This evidence provides strong support for a recently proposed superphylum containing both the Euglenophyta and the Kinetoplastida.

Introduction

The Euglenozoa is a recently proposed protistan taxon (Corliss 1984), composed of the previously separate algal

phylum, Euglenophyta, and the protozoan order, Kinetoplastida, plus several lesser-known organisms. The groups were united on the basis of morphological similarities which include metaboly, a peculiar form of closed nuclear division, flagellar paraxial rod, nucleus with a prominent nucleolus, and a peripheral microtubular cytoskeleton. Flagellar roots have been recognized as being evolutionarily conserved and hence may offer additional evidence to support this proposed phylogenetic linkage. In Part 2, much of the published information available on flagellar roots of the euglenoids was discussed and was compared with that of the bodonids. That detailed description of the roots of Entosiphon sulcatum, however, concerned only the posterior portions of the roots; much of the potential similarity between the euglenoids and bodonids may lie in the more anterior portions. This study addresses the anterior portion of the flagellar roots of Entosiphon and their interconnections with other cellular structures.

The bodonids and trypanosomes, constituting the Kinetoplastida, are colorless unicells that obtain their nutrition osmotrophically or phagotrophically (Vickerman and Preston 1976). The bodonids are free-living with an ingestion apparatus composed of a cytopharynx with associated microtubular structures. The trypanosomes are largely parasitic and osmotrophic with a cytostomal opening near the flagellar pocket opening. In both types of cells, the

flagellar pocket and the ingestion apparatus are linked by a microtubular flagellar root, termed the MTR or reinforced microtubules (see Table 4, Part 2).

While the Euglenophyceae contains many photosynthetic species, the class also includes many colorless representatives, including both osmotrophs and phagotrophs (Leedale 1967). The phagotrophic forms, comprising the Heteronematales, possess an ingestion apparatus; that found in Entosiphon is one of the most elaborate within the order: the siphon contains hundreds of microtubules and extends the length of the cell. If a flagellar root linkage between flagellar pocket and ingestion apparatus exists in the euglenoids as in the kinetoplastids, Entosiphon might be expected to have a prominent one.

In this study, the structure of the siphon of Entosiphon sulcatum, the ultrastructure of the anterior end of the reservoir-canal complex, and the relationships between the two regions are examined. The pattern of microtubular roots in Entosiphon is then related to that in the kinetoplastid flagellates. Finally, the probable homologies of the flagellar roots and cytopharynx between the euglenoids and the kinetoplastids, and the implications of these homologies for the postulated phylogenetic relationship among the members of the Euglenozoa, are discussed.

Materials and Methods

Entosiphon sulcatum (Duj.) Stein was isolated, cultured, fixed, and embedded as described previously (Part 2). Serial sections were obtained with a Dupont diamond knife mounted on a Sorval MT-2 ultramicrotome. Both moderately thin (90-120nm) and thick (0.25-0.40μm) series were utilized, as well as a number of random sections. All sections were poststained with saturated methanolic uranyl acetate and lead citrate. Thin sections were examined in a Hitachi H-600 transmission electron microscope operating at an accelerating voltage of 100 kV, and thick sections were viewed either with a Hitachi H-800 operating at 150 or 200 kV or with a Jeol JEM-1000 operating at 1000kV.

Results

Entosiphon sulcatum (Duj.) Stein is a colorless phagotrophic unicell approximately 25-30 μm long by 12-15 um wide (see Part 2, Figs. 1-4[1]). Usually circular in cross-section, the cell often undergoes a dorsiventral flattening. The twelve longitudinal pellicular grooves, whose cross-sectional size and shape may vary enormously within one organism (Fig. 1), extend the length of the cell. The typical subapical opening of the euglenoids is considerably expanded in this organism, forming a

[1]All figures referenced in Part 3 are found in the Appendix at the end of Part 3.

cup-shaped anterior depression in which the dorsal and lateral lips are somewhat longer than the ventral lip. From this anterior depression emerge the two flagella and the tip of the siphon (see Part 2, Figs. 1, 2).

Interpretation of the three-dimensional ultrastructure of the reservoir, siphon, and flagellar roots in Entosiphon poses a special difficulty. As noted by Lackey (1929), among others, the siphon can be both protruded from the cell body and retracted within it. This means that the spatial relationship between the siphon and the reservoir changes with the amount of extension of the siphon. The siphon is linked to the remainder of the cell by a number of different structures; thus, as the siphon changes its position, it follows that the structures linking the reservoir, for example, with the siphon must vary their orientation and position. For clarity, the structure of the siphon itself will first be described, then the structure of the reservoir-canal with associated flagellar roots, and finally both the clearly identified and hypothesized linkages between the two organelles. Results are presented, whenever possible, as if the cell were viewed from the posterior end or from the dorsal side.

Siphon Structure

The siphon, to the right (as viewed from the dorsal side of the cell) of the centrally located reservoir-canal complex, is composed for most of its length of three

microtubular pharyngeal rods that run parallel to one another (Figs. 1,2). Each rod is composed of between 200 and 300 microtubules in the anterior one-third of the cell and tapers, becoming smaller in the posterior region. The individual microtubules are linked to the six neighboring tubules by small filaments, probably microtubule-associated proteins or MAPs (Fig. 3), and an electron-dense substance forms a continuous layer adjacent to the innermost layer of microtubules (Figs. 3, 4). Toward the posterior end of the cell, each pharyngeal rod tapers, to consist of only a few microtubules which abut the cell membrane (Fig. 6). Anteriorly, the amount of electron-dense material increases as the number of microtubules decreases (Fig. 4).

Within the horseshoe arrangement formed by the rods in cross-section, and running the length of the siphon, are four electron-dense lamellae or "vanes" (Figs. 2, 7), each curved and extending from a centrally located microtubule, the four vanes resembling a pinwheel. An additional microtubule is located near these four, for a total of at least five pinwheel-associated microtubules (Fig. 8). At the center of the vane complex a vesicle is usually present; it varies considerably in size and is connected, in the reservoir and lower canal area, to cytoplasmic vesicles of variable shape (Figs. 2, 7, 8). The cytoplasmic vesicles are continuous, through the open side

of the horseshoe, with presumptive accessory contractile vacuoles (not shown).

Anterior to basal body level, the left and right pharyngeal rods (PRL and PRR, respectively) are joined to the ventral pharyngeal rod (PRV) by a band of microtubules linked to one another by an electron-dense matrix (Fig. 7). An accessory lamella parallels the PRR (Fig. 7) and connects anteriorly to an extensive electron-dense network (the "web") that covers the right and central portions of the anterior end of the siphon (Figs. 4, 11, 12). A set of fine fibrils connects the accessory lamella to the PRR (Fig. 7). On the left side of the siphon another accessory lamella appears only at the very tip of the siphon (Fig. 4). A much more extensive set of fibrils connects this lamella to a layer of microtubules adjacent to the PRL (Fig. 4). Posterior to this lamella and these fibrils is a large vesicle (Fig. 5), and atop the vesicle, attached to the PRL accessory lamella, is a sheet of electron-dense granules (Fig. 4) which is continuous with the web.

The anterior extensions of these accessory lamellae form a cap (the "dome") at the extreme anterior end of the siphon (Figs. 5, 9, 11, 12). The dome is asymmetrical and is attached to the remainder of the siphon only by linkages with the webbing (Fig. 12). At the anterior end of the linked pharyngeal rods is an electron-dense appendage (the "lips"; Mignot 1966) that overlaps the dome (Figs. 5, 12).

The anterior surfaces of the dome and lips are covered with a mat of fine hairs, one layer (80 nm long) on the dome and two layers (30 and 220 nm) on the appendages (Fig. 5).

The siphon opens to the environment anteriorly via the vane complex (consisting of much reduced vanes) in a channel formed between the dome and the terminal appendages (Fig. 9). Thus, the vesicle at the center of the pinwheel, while probably transitory, is continuous with the surrounding environment. The vesicle associated with the PRL, on the other hand, does not appear to be connected directly with the environment. The two systems, vane complex and vesicle, may be connected to one another, however, by means of the many small rounded vesicles which fill the siphon interior (Figs. 4, 5).

Reservoir-Canal Structure

The flagellar pocket consists of an expanded proximal bulbous portion, the reservoir, and a narrowed distal neck, the canal, which opens into the cup-shaped anterior depression (Part 2, Fig. 2). The reservoir is highly variable in shape due to deformation by contractile vacuole activity. The posterior margin of the reservoir lining is quite irregular in shape, with numerous indications of endo- and/or exocytosis (e.g., Fig. 1).

Beneath the base of the reservoir lies the basal body complex from which the two flagella originate and subsequently pass through the reservoir and canal. The

recurrent flagellum (F_2) can be identified by its large latticelike paraxial rod (PAR; Figs. 1, 15-19). The constant position of F_2 near the left side (as viewed from the posterior end) of the reservoir is maintained by connective fibers joining the reservoir membrane to the flagellar membrane (Figs. 15, 16; see also Part 2). The anterior flagellum, F_1, also has a relatively constant position, probably due to a fibrillar connection with F_2 (Figs. 15-19; also Part 2) and possibly to another linkage directly with the reservoir membrane (Figs. 16, 17).

Microtubular Roots

Three flagellar roots arise in the basal body region and extend anteriorly adjacent to the reservoir membrane, as described in Part 2.

Dorsal Root (DR). The dorsal root, consisting of three closely spaced microtubules and an associated electron-dense plate (see Part 2, Fig. 16), is located opposite the siphon and is joined near the base of the reservoir by a band of singlet microtubules (DMT) on the root's dorsal margin (Figs. 15, 28). At the base of the reservoir, the DR is located on the left dorsal side of the reservoir (Part 2). As it progresses anteriorly, it runs obliquely to lie adjacent to the IR, near the ridge (Fig. 15). Anterior to this level, the dorsal root could not be traced; it may terminate at the reservoir-canal transition

zone level. Progressing anteriorly, the DMT (associated with the DR), forms microtubule pairs, and the reservoir membrane assumes a scalloped outline (Figs. 4, 7); this band is continuous with the pellicular microtubules. On the left side of the reservoir, adjacent to these pellicle microtubules, an electron-dense mass is bifurcated (Figs. 13, 14) as some of the pellicle microtubules curve over the edge of the anterior depression.

Intermediate root. The intermediate root (IR) lies on the left side of the reservoir on a cytoplasmic ridge that projects into the reservoir (Fig. 15). As the root progresses anteriorly it is displaced from the crest of the ridge to a trough beside it (Figs. 16) and then circles the reservoir ventrally (Figs. 17, 23, 24). The connecting fibrils linking F_2 with the reservoir membrane, on the left side of the reservoir, are attached to this ridge, when the IR is no longer located there (Fig. 16).

The path of the IR after this point is less clear. Figures 23-26 show nonadjacent sections from a series in which the IR follows the path described, as far as the ventral side of the reservoir. Here, two bands can be seen (cf. Figs. 25 and 26, and the diagram, Fig. 27). One of these bands extends dorsally, toward the siphon, while the other extends from the reservoir membrane toward the ventral cell surface. This evidence suggests that the IR forms two separate branches, a dorsal and a ventral one.

Figures 18 and 19 show the putative dorsal branch of the IR further displaced toward the right side of the reservoir until it lies adjacent to the siphon. Microtubules extend from the location just described, between the PRL and the right side of the reservoir, to the opening on the dorsal side of the siphon (Fig. 20).

Figure 17 shows another set of microtubules, probably the putative ventral branch of the IR, extending from the ventral side of the reservoir. As pictured in Figure 21, a band of microtubules curves over the ventral lip of the reservoir, out of the anterior depression.

As in other euglenoids, the pellicle microtubules of Entosiphon bear a regular relationship to the grooves. Evenly spaced microtubules line the grooves, but are rarely found between them (Fig. 1), with one exception: at the anterior end of the cell only, on the ridge between the two ventral-most grooves, there is a single row of microtubules (Fig. 22). Although, the number of microtubules associated with a given groove varies considerably, apparently with the shape of the groove, no other ridge is regularly lined by a band of microtubules. It is reasonable to assume that this ventral microtubular band is continuous with the curving microtubular band shown in Figure 21 and, hence, possibly with the ventral branch of the IR. Therefore, the evidence suggests that the IR may split into two segments,

one extending toward the siphon opening and the other lining the ventral ridge.

Ventral root (VR). In the basal body complex, the ventral root (VR) lies between the siphon and the posterior functional basal body (bb_2), i.e., in a right ventral position relative to the complex (Part 2). As described in Part 2, the VR forms two segments, one set back slightly from the reservoir membrane and overlain by a small plate. The VR originates on the ventral side of the reservoir, then circles to lie on the dorsal side (not shown). Microtubules extend from the dorsal side of the reservoir into the cytoplasm (Fig. 28). At the same level, two microtubular bands attach to the PRL, forming the PRL extension. Figure 29 shows a microtubular band extending from the dorsal side of the reservoir (the location of the VR at this level) to join with the PRL. Evidence thus suggests that the VR becomes a structural part of the siphon by way of the PRL extension. However, further work is needed to establish this connection with certainty.

Interrelationship of Siphon and Cell

The siphon is structurally connected to other cytoplasmic components (Fig. 33). Three of these connections are quite straightforward, consisting of microtubular and/or lamellar features that are clearly identifiable whenever they are seen. Others, particularly

some of the smaller microtubular ones which may be the flagellar roots, are ill-defined and probably change their orientation and position with every movement of the siphon. Therefore, these could not be characterized with much accuracy.

The dominant connecting structure is a band of reinforced microtubules that extends from the left dorsal margin of the reservoir obliquely toward the siphon (Figs. 4, 13, 14, 32). This band joins with the PRR within the level of the webbing (Fig. 20). At the point of connection with the reservoir there is a pronounced hook at the end of the band on the side facing the siphon (Figs. 4, 13, 14, 32).

There is a somewhat similar extension from the PRL toward the right lateral groove (Fig. 32). It is noted above as the PRL extension, which formed from two separate microtubular segments (possibly the VR) in the cytoplasm. Near the siphon tip, the PRL extension reaches almost to the lateral cell surface (not shown).

In the region where the major reservoir-siphon connector links to the PRR is a group of electron-dense fibers, the groove connectors (GC). These fibers originate adjacent to a right lateral groove (Figs. 7, 32), where they are widely separated, and then taper toward one another as they approach and link to the web of the siphon (Fig. 31).

The final linkage identified between reservoir and siphon consists of two types of elements. On the dorsal side of the reservoir adjacent to the reservoir-siphon connector are five or six electron-dense fibers next to the reservoir membrane (Figs. 4, 13, 14, 32). Beside these is a set of microtubules, at least six in number, associated with an electron-dense matrix and forming a curved band (Fig. 32). The fibers, and possibly the microtubules, follow the path of the reservoir-siphon connector and enter the siphon at its extreme anterior end (Figs. 5, 30). These fibers join with a similar series of fibers that arise on the right side of the siphon in the channel formed between the dome and the lips of the pharyngeal rods (not shown). Both sets of fibers meet to form the pinwheel and continue posteriorly within the siphon (Figs. 9, 10). Thus, the vesicle in the center of the vane complex opens to the environment through this channel, the supports being formed by fibers connecting the reservoir with the siphon.

It is reasonable to assume that the curved microtubular band adjacent to these connecting fibers (Fig. 32) is continuous with the presumptive putative dorsal branch of the IR (Fig. 27). The path of the band after this point has not been determined. (It is tempting, however, to speculate that it enters the siphon and becomes

associated with the vane complex as the microtubules surrounding the lumen.)

Discussion

Mignot's (1963, 1964, 1966) studies of Entosiphon sulcatum laid a foundation for understanding the structure and function of the siphon and its interrelationship with other cellular organelles. The present study extends his description and includes much of the ultrastructural information necessary for a thorough understanding of flagellar root-siphon linkages and siphon function.

Tracing the flagellar roots of Entosiphon has proven to be far more difficult than initially envisioned. The problems are of two types. First, the movements of the siphon relative to the reservoir create considerable morphological variability. If, indeed, the two organelles are linked by microtubular roots, these would of necessity undergo deformation as the siphon is displaced.

The second type of difficulty involves visualization of the microtubules themselves. Unless the angle of sectioning with respect to the microtubules is close to true transverse or true longitudinal, the microtubules are often not visible, particularly in very thin sections. As described above, the roots probably assume highly distorted paths, which greatly accentuate this problem of visualization. Thus, positive evidence alone is convincing;

negative evidence (the absence of microtubules in a given location), while useful when seen repeatedly, is less than conclusive. It was found that thick sections increased the probability of locating a given microtubular root and thus were often used when appropriate.

Microtubular Flagellar Root Paths of Entosiphon

To summarize the results of Parts 2 and 3 of this study, the three flagellar roots of Entosiphon originate in the basal body complex. The DR is spatially associated with the anterior flagellum (F_1), and the other two roots, the IR and the VR, are closer to the posterior flagellum (F_2). All three roots extend anteriorly, with an additional microtubular band, the DMT, arising adjacent to the DR, near the base of the reservoir. While conclusive evidence (i.e., a definitive series of adjacent serial sections in the critical area) was not obtained, positional evidence suggests that (1) the DR extends part of the way up the canal and then ends, (2) the IR splits into two segments and is continuous both with the curved band of microtubules that probably enters the siphon and with a microtubular band lining the ventral ridge, and (3) the VR is identical with one or both segments of the PRL extension, and thereby becomes part of the structural support of the siphon. More research is needed to provide definitive information on points 2 and 3.

Bodonid Microtubular Cytoskeleton

As described by Brugerolle et al. (1979) and summarized by Kivic and Walne (1984, fig. 2), the bodonid microtubular cytoskeleton, including the flagellar roots, consists of the following components (Fig. 34):

1. The dorsal connector, a set of three microtubules arising in the basal body complex near the basal body of the anterior flagellum and extending partway up the flagellar pocket. Overlying the microtubules is an electron-dense lamina.

2. The dorsal fibril (FD), a sheet of microtubules running longitudinally along the dorsal and lateral surfaces of the cell, just beneath the plasma membrane.

3. A set of reinforced microtubules (MTR) beginning in the basal body region. It runs under the base of the flagellar pocket and then anteriorly along its right ventral margin, makes a U-turn and then borders the cytopharynx as it extends posteriorly. The S-shaped path of the MTR is strikingly uniform in the five bodonid species studied by Brugerolle et al. (1979). Electron-dense material is associated with these microtubules, the pattern being species-specific.

4. The ventral fiber (FV). This also begins as a flagellar root in the basal body complex, where it consists of five microtubules and is associated with the recurrent flagellum. It extends along the left side of the flagellar

pocket toward the ventral surface of the cell and then broadens to include additional microtubules as it runs longitudinally along the ventral cell surface. The recurrent flagellum is often associated with the plasma membrane overlying the FV. The FV is quite variable from species to species, consisting of two overlying microtubule layers in Cryptobia intestinalis and of two separate segments in Bodo sp. (Brugerolle et al. 1979, figs. 11, 37).

5. A fiber associated with the cytopharynx (FAS), present in three of the five bodonid species pictured by Brugerolle et al. (1979). It extends from the ridge surrounding the cytostome posteriorly into the cytoplasm, paralleling the cytopharyngeal lumen.

Comparison between Entosiphon and Bodonid Flagellar Roots and Microtubular Cytoskeletons

Dorsal root. The DR of Entosiphon and the dorsal connector of the bodonids are similar in several ways. Both arise near the basal body of F_1 (bb_1), extend part of the way up the dorsal side of the flagellar pocket, and then end. Both consist of three closely spaced microtubules (Brugerolle et al. 1979, fig. 11) overlain by an electron-dense lamina. As noted by Brugerolle et al. (1979), the dorsal connector could serve as a nucleating center (MTOC, microtubule organizing center) for the dorsal

fiber (FD): the FD originates at a region of amorphous electron-dense material, near the end of the dorsal connector. In Entosiphon, the DMT arises at the base of the reservoir, immediately adjacent to the DR, also suggesting a nucleating function for this root.

As just suggested, the DMT in Entosiphon corresponds in many respects to the FD of the bodonids. There are indications that both are nucleated by the F_1-associated flagellar root but are not, themselves, flagellar roots. In Entosiphon, the band is continuous with the pellicle microtubules which lie just beneath the plasma membrane-pellicle complex and run longitudinally the length of the cell. In bodonids, the FD consists of a continuous sheet of longitudinally oriented microtubules extending the length of the cell. The distinctive arms on the individual FD microtubules, noted by Brugerolle et al. (1979), were not found on the pellicle microtubules of Entosiphon.

Intermediate root. The ventral fiber (FV) of bodonids originates near the basal body of the recurrent flagellum. It follows the flagellar pocket surface briefly, then expands to assume a dominant position on the ventral surface of the cell. Here a series of fibrous connections link the overlying plasma membrane to the closely associated recurrent flagellum.

The IR in Entosiphon also arises near the basal body of F_2, extends along the left side of the reservoir, and

then probably gives rise to two separate branches. One branch curves over the anterior depression and presumably follows the ventral ridge posteriorly. The other follows the right side of the reservoir, possibly to enter the opening on the dorsal side of the siphon. Thus, there is evidence to suggest that the IR follows the same path as the FV in bodonids, and in addition, may also be associated with the siphon. Further research is needed to clarify this postulated structural arrangement in Entosiphon. The existence of two microtubular layers in the FV of Cryptobia intestinalis and of two segments in that of Bodo sp. (Brugerolle et al. 1979) is suggests a similar structural arrangement in the bodonids and warrants further examination.

Ventral root. The MTR is perhaps the most distinctive of the microtubular structures in the bodonids. Its tortuous pathway including a dual association with the flagellar pocket and the cytopharynx, the sometimes elaborate arrangement of the electron-dense associated structures, and the connections to the overlying membranes are found in all five species described by Brugerolle et al. (1979). In Entosiphon, the VR may have a similar path, though it has not been completely traced. It originates in the basal body complex, ascends along the reservoir and canal margins, and then probably becomes part of the structural support of the siphon. It is thus associated

with both the flagellar pocket and the cytopharygeal homologue, the siphon.

Pharyngeal rods (nemadesms). In some bodonids, an additional microtubular structure, the FAS, is associated with the cytopharynx and the MTR. While the FAS is present in only three of the five bodonids described by Brugerolle et al. (1979), and is a rather insignificant structure in them, in Cryptobia intestinalis it assumes a horseshoe shape surrounding the cytopharynx and opens toward the dorsal cell surface. The pharyngeal rods of the siphon of Entosiphon also fit this description. In other bodonid species, rods of parallel microtubules which have a linkage pattern similar to that of Entosiphon, parallel the cytopharynx (e.g. the rodorgan of Bodo designis, Eyden 1977 and the quintubular fiber of Cephalothamnium cyclopum, Hitchen 1974). Although these have not yet been equated with the FAS of Cryptobia intestinalis, (Brugerolle et al. 1979), Kivic and Walne (1984) point out their obvious similarity with the euglenoid pharyngeal rods.

Summary

This study demonstrates considerable similarity between the flagellar roots of the bodonids and Entosiphon sulcatum. There is good evidence that the dorsal connector corresponds to the DR, the FV to the IR, and the MTR to the VR. There is also great similarity between the bodonid FD

and Entosiphon's DMT. Furthermore, the relatively insignificant FAS has a similar position and morphology to the dominant pharyngeal rods of Entosiphon. This ultrastructural evidence, when coupled with the many other morphological and biochemical similarities between the euglenoids and the kinetoplastids, provides strong support for the Euglenozoa, a superphylum recently proposed by Corliss (1984).

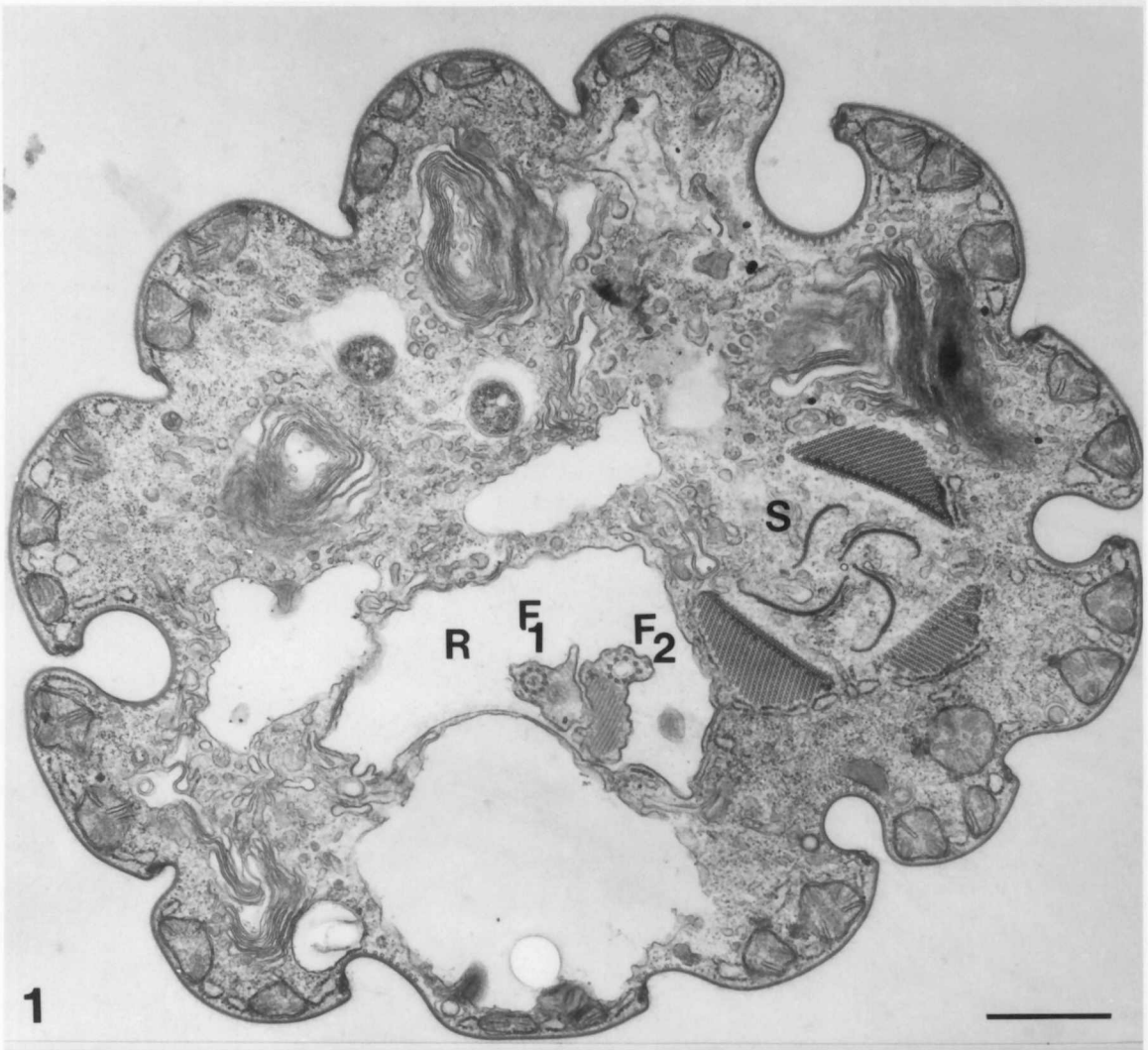
APPENDIX: PART 3

A complete list of abbreviations is provided on p. xv.

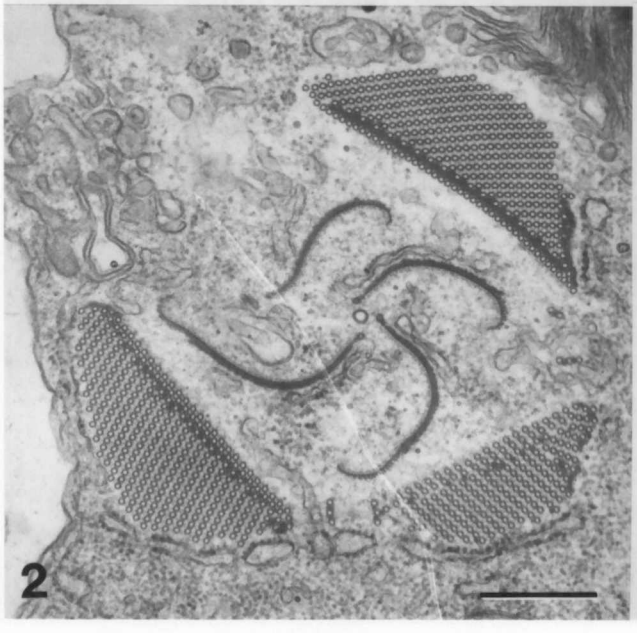
Figure 1. Transverse view of Entosiphon sulcatum. Twelve grooves of various sizes line the cell periphery. The siphon (S) and several cytoplasmic vacuoles surround the reservoir (R) in which both flagella (F_1 and F_2) are located. Scale bar = 1.0 μm.

Figure 2. Higher magnification of the siphon. Each of four vanes emanates from a proximal microtubule, the four surrounding a central lumen. Scale bar = 0.5 μm.

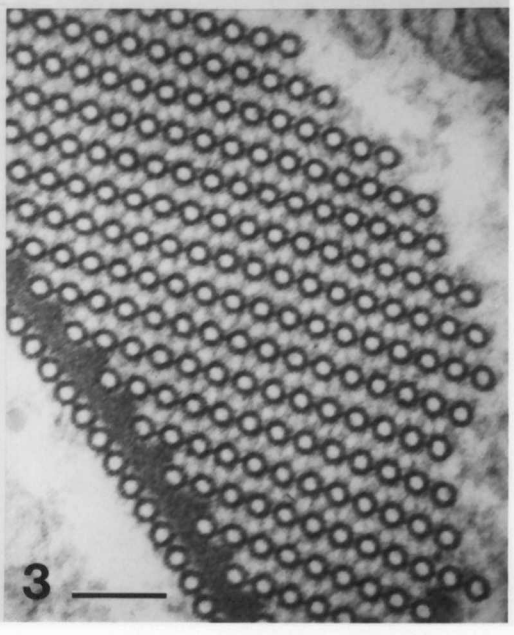
Figure 3. Higher magnification of a pharyngeal rod. Filaments, approximately 9 nm long, link adjacent microtubules, and longer filaments (approximately 22 nm) join each microtubule to two in the neighboring row. An electron-dense substance forms a matrix adjacent to the proximal microtubules. Scale bar = 0.1 μm.



1



2



3

A complete list of abbreviations is provided on p. xv.

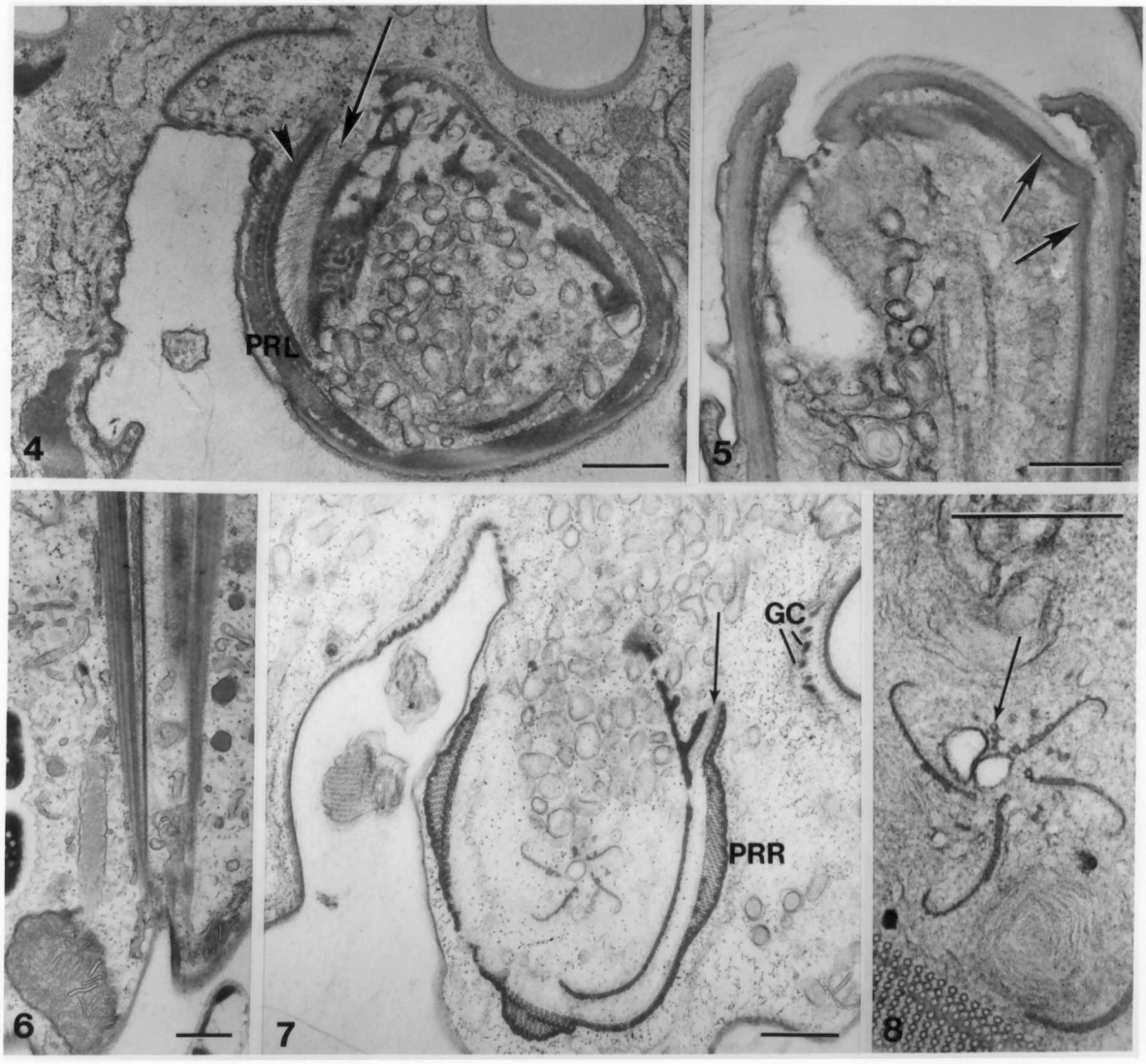
Figure 4. Transverse section of the anterior tip of Entosiphon sulcatum, siphon retracted (cf. Fig. 7). Fibrils (arrow) link accessory lamella to microtubular layer (arrowhead) paralleling PRL. Layer of electron-dense granules is continuous with web (seen here only as fragments). The pharygeal rods are composed of relatively few microtubules within an extensive electron-dense matrix. Scale bar = 0.5 μm.

Figure 5. The asymmetrical dome and terminal appendages are covered with fine hairs of three different lengths. Dome is attached to accessory lamella next to right pharyngeal rod (PRR, arrows). Scale bar = 0.5 μm.

Figure 6. Tapered end of siphon reaches to posterior end of cell. Scale bar = 0.5 μm.

Figure 7. Transverse section through anterior tip of cell, siphon extended (cf. Fig. 4). An accessory lamella is connected to the PRR by a series of fine fibrils (arrow). Electron-dense groove connectors (GC) near right lateral groove link to web at anterior end of siphon. Scale bar = 0.5 μm.

Figure 8. Transverse section of vane complex. Pinwheel arrangement within siphon contains at least five microtubules, four attached to vanes plus an unattached one (arrow). Scale bar = 0.5 μm.


PRL
4
5
6
GC
PRR
7
8

A complete list of abbreviations is provided on p. xv.

Figure 9. Longitudinal thick section at tip of siphon of Entosiphon sulcatum. Electron-dense fibers (arrows), originating at reservoir membrane, are continuous with elements of the vane complex (cf. Fig. 10). Scale bar = 0.5 μm.

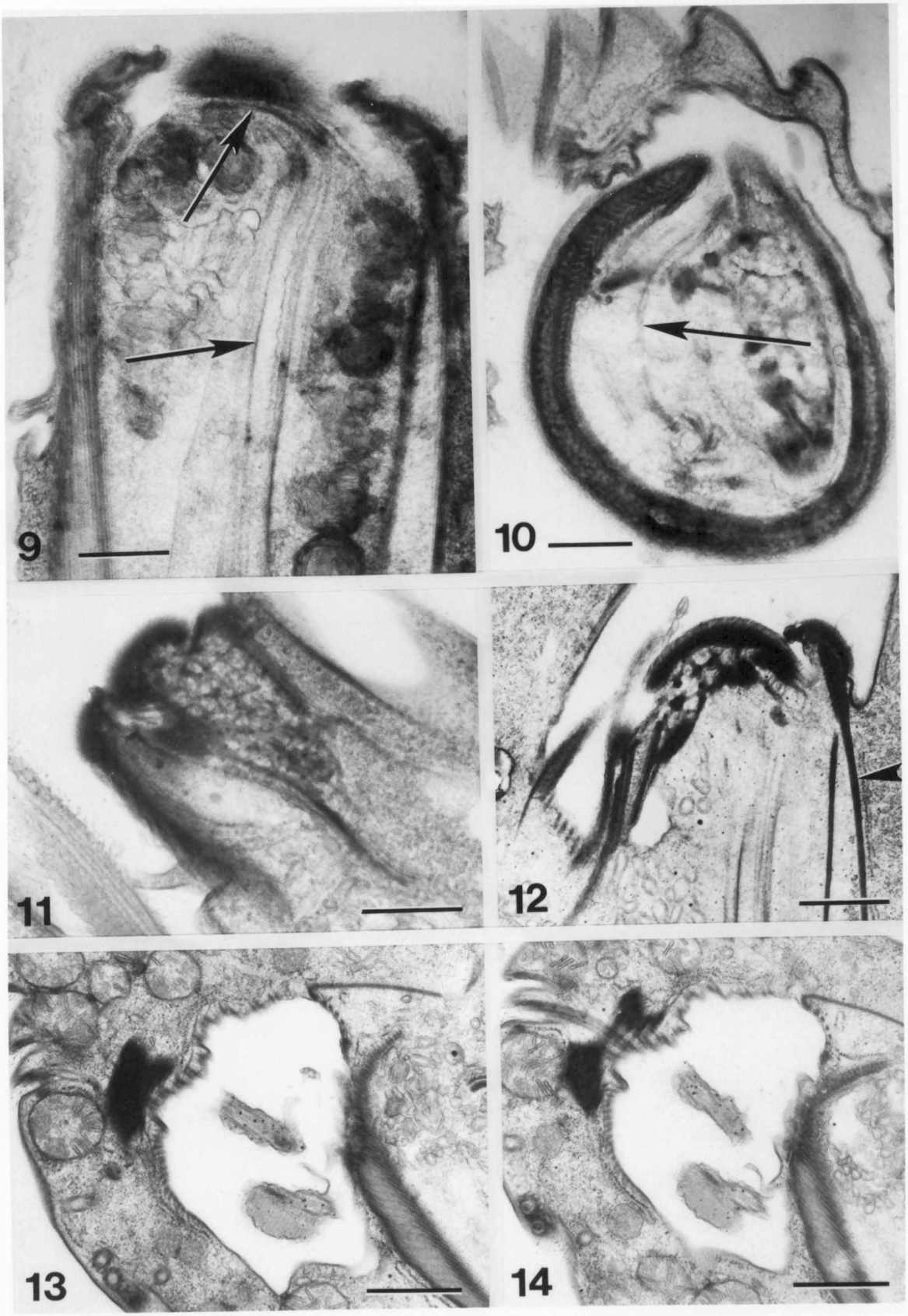
Figure 10. Transverse section of tip of siphon. Electron-dense fibers (arrow) are continuous with elements of the vane complex (cf. Fig. 9). Scale bar = 0.5 μm.

Figure 11. Electron-dense web covers most of siphon tip. High voltage micrograph of thick section (0.5 um). Scale bar = 1.0 um.

Figure 12. Terminal web is connected to dome at tip of siphon. Terminal appendage partially overlying the dome is attached to the right pharyngeal rod (PRR, arrowhead). Scale bar = 1.0 μm.

Figure 13. Oblique section through anterior end of cell. An electron-dense mass lies on the left side of the reservoir. Scale bar = 1.0 μm.

Figure 14. Serial section anterior to Fig. 13. The electron-dense mass on the left side of the reservoir is split into two separate segments as the paired DMT microtubules become the pellicle microtubules. Scale bar = 1.0 μm.


9
10
11
12
13
14

A complete list of abbreviations is provided on p. xv.

Figure 15. Transverse section of reservoir of Entosiphon sulcatum showing intermediate root (IR, arrow) on ridge on left side of reservoir. First of five nonadjacent serial sections. Scale bar = 1.0 μm.

Figure 16. Transverse section of reservoir showing IR (arrow) in trough adjacent to ridge. Second of five nonadjacent serial sections. Scale bar = 1.0 μm.

Figure 17. Transverse section of reservoir showing IR (arrow) on ventral side of reservoir. Microtubules (arrowhead), possibly the ventral branch of the IR, extend toward the ventral cell surface. Third of five nonadjacent serial sections. Scale bar = 1.0 μm.

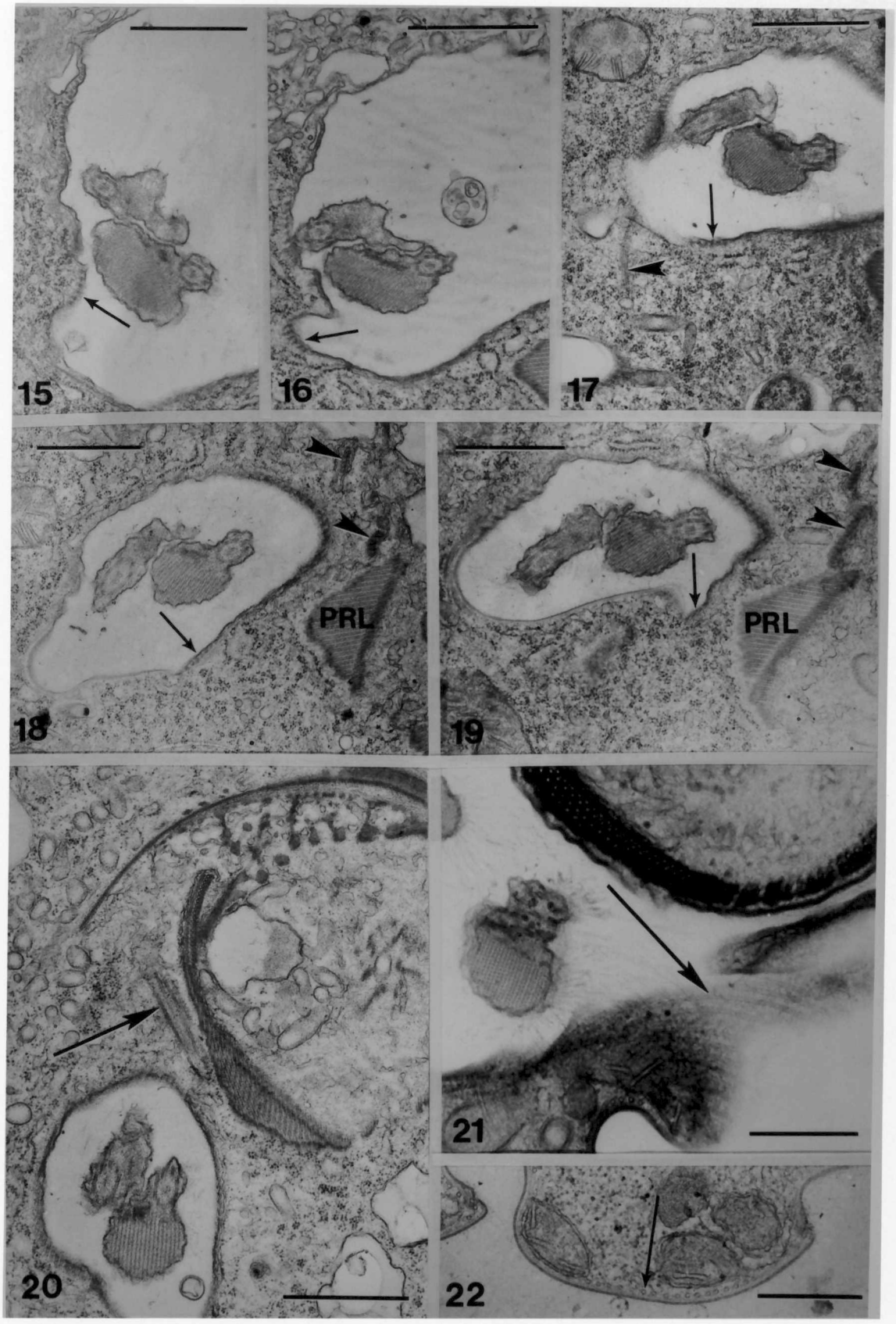
Figure 18. Transverse section of reservoir showing IR (arrow) on right side of reservoir. Microtubular bands (arrowheads) are located near left pharyngeal rod (PRL). Fourth of five nonadjacent serial sections. Scale bar = 1.0 μm.

Figure 19. Transverse section of reservoir showing IR (arrow) lining invagination on right side of reservoir. Microtubular bands (arrowheads) are located near PRL. Last, and most anterior, in a series of five nonadjacent serial sections. Scale bar = 1.0 μm.

Figure 20. A microtubular band, possibly the dorsal branch of the IR, extends dorsally between the reservoir and the siphon. Scale bar = 1.0 μm.

Figure 21. Intermediate voltage micrograph of a thick section showing the ventral edge of the anterior depression. Microtubular band (arrow), the putative dorsal branch of the IR, curves from the reservoir and over the ventral edge of the anterior depression. Scale bar = 0.5 μm.

Figure 22. The band of microtubules (arrow) lining the ventral ridge may be an extension of the dorsal branch of the IR. Scale bar = 0.5 μm.


15
16
17
PRL
18
PRL
19
20
21
22

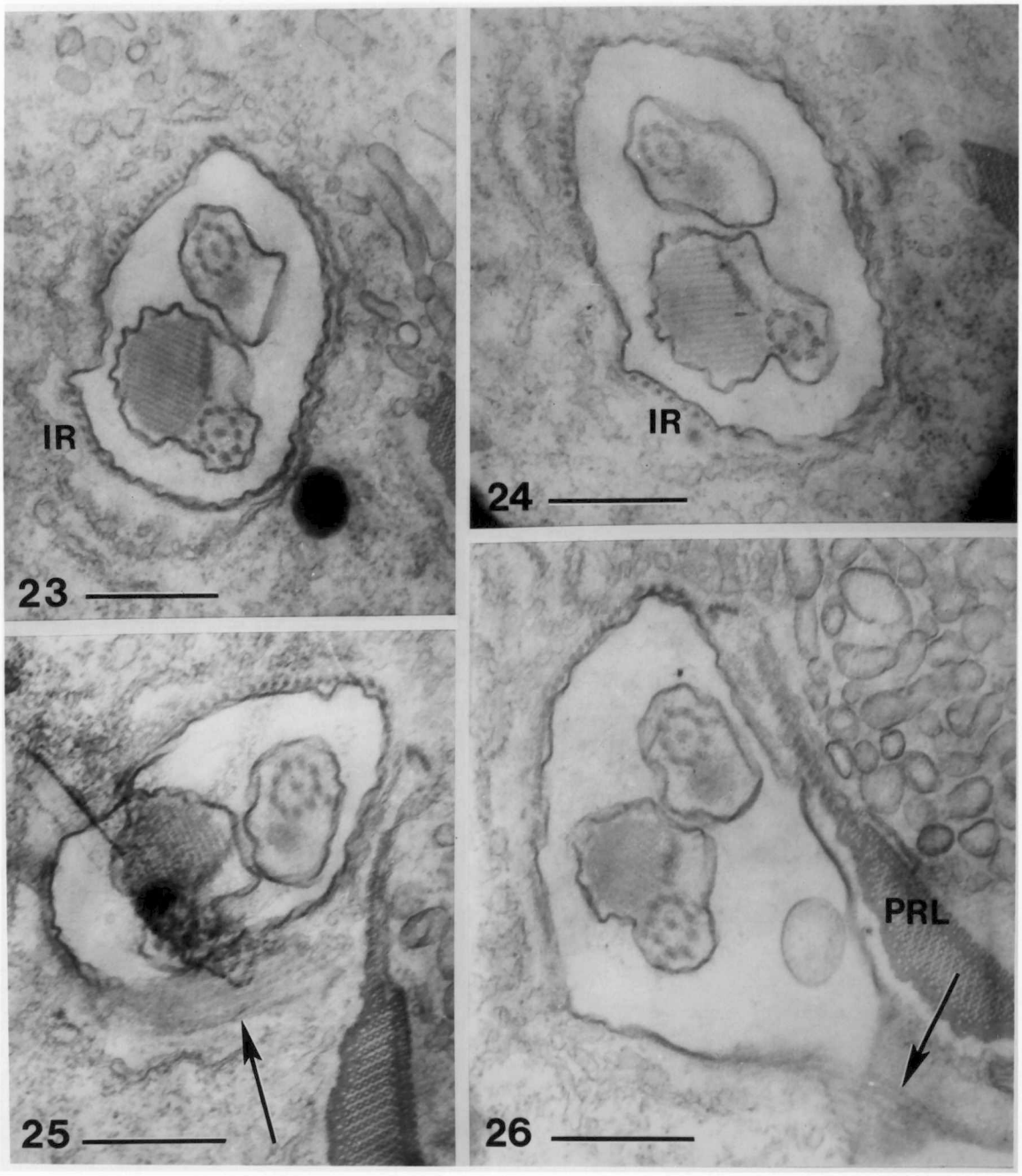
A complete list of abbreviations is provided on p. xv.

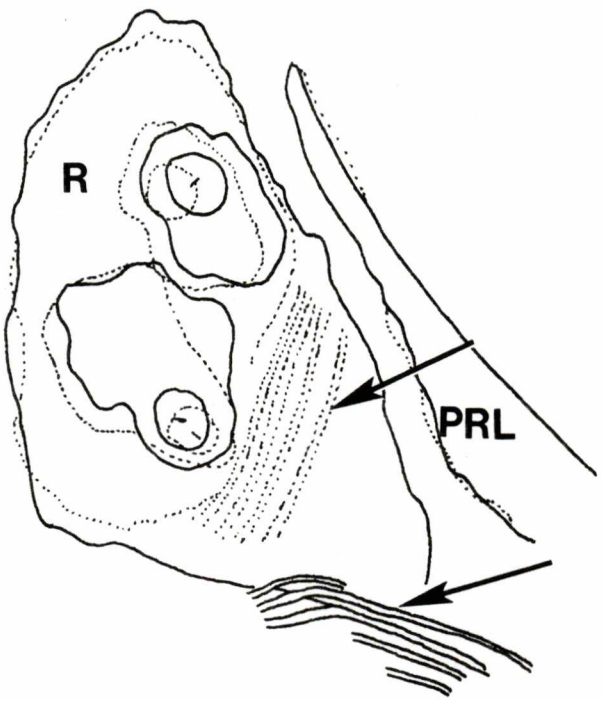
Figure 23. Transverse section of anterior end of reservoir with IR on left side, opposite F_2. First of four nonadjacent serial sections of Entosiphon sulcatum. Scale bar = 0.5 μm.

Figure 24. Transverse section of anterior end of reservoir with IR in a more ventral position (cf. Fig. 23). Second of four nonadjacent serial sections of E. sulcatum. Scale bar = 0.5 μm.

Figure 25. Transverse section of anterior end of reservoir with microtubular band (arrow) encircling ventral side of reservoir. Third of four nonadjacent serial sections of E. sulcatum. Scale bar = 0.5 μm.

Figure 26. Transverse section of anterior end of reservoir with microtubular band (arrow) extending ventrally from reservoir margin. Last in a series of four nonadjacent serial sections of E. sulcatum. Scale bar = 0.5 μm.


IR
23
IR
24
25
PRL
26



A complete list of abbreviations is provided on p. xv.

Figure 27. Traced outlines of reservoir and associated structures (Figs. 25, 26) are overlain to reveal possible branching of the intermediate root (IR). Entosiphon sulcatum.

A complete list of abbreviations is provided on p. xv.

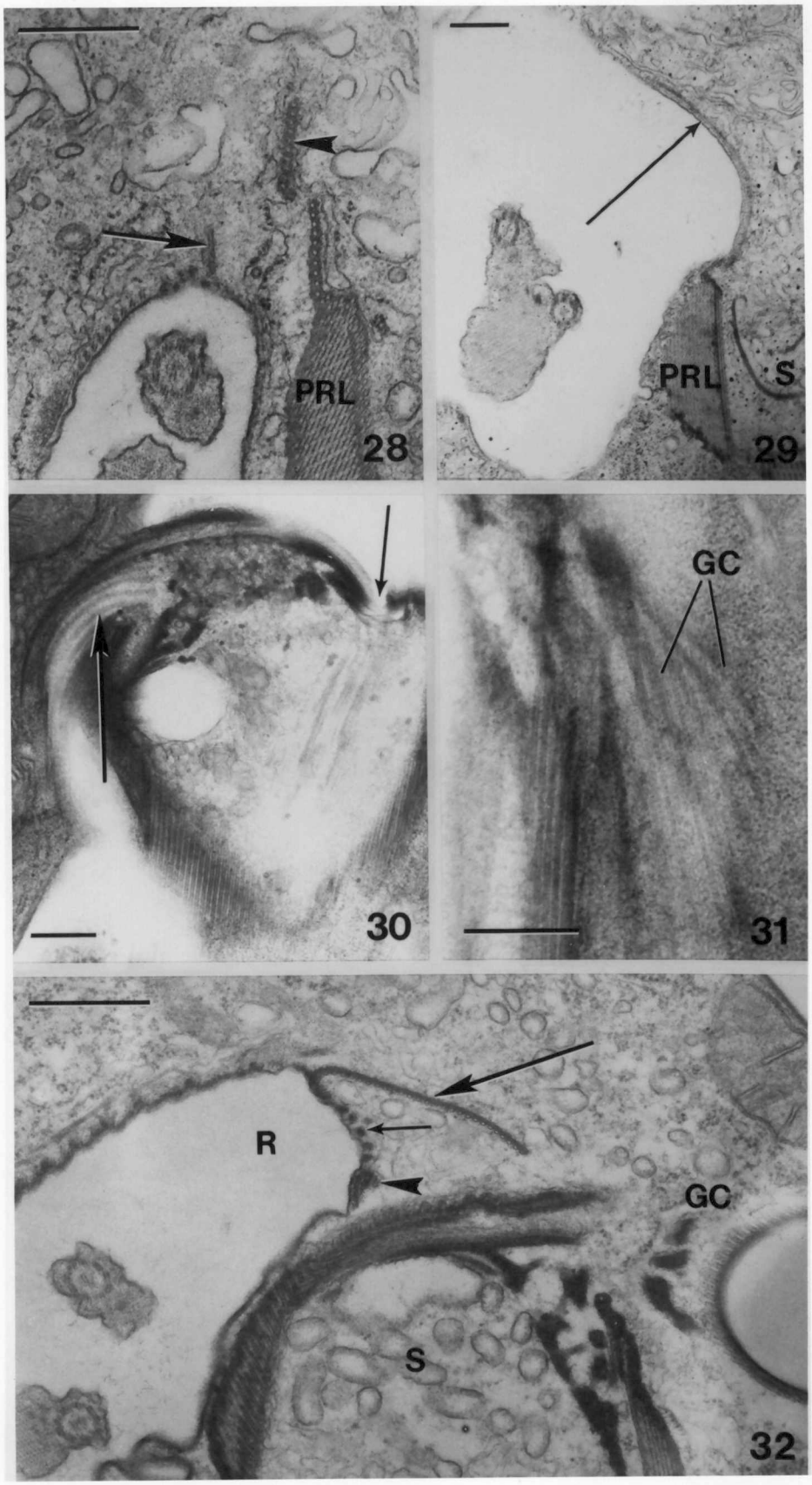
Figure 28. Microtubules (arrow), probably from the ventral root (VR), extend into the cytoplasm. One microtubular band is attached to the left pharyngeal rod (PRL) and a second (arrowhead) is nearby. Entosiphon sulcatum. Scale bar = 0.5 μm.

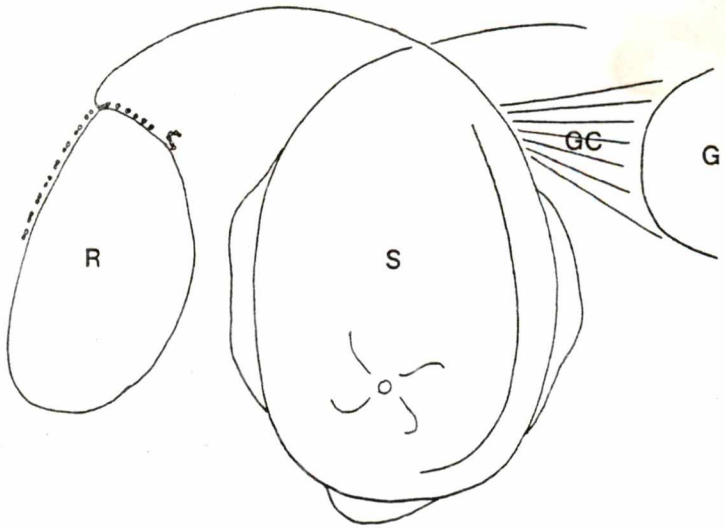
Figure 29. Microtubules (arrow), probably from the VR, encircle the reservoir and connect to the PRL extension. Scale bar = 0.5 μm.

Figure 30. Fibers (large arrow) cross from top of reservoir into siphon, paralleling the reservoir-PRR connector. Vane complex opens directly to the environment (small arrow). Scale bar = 0.5 μm.

Figure 31. Thick section shows groove connectors (GC). Extending from right lateral groove microtubules to web area of siphon, the GC are faintly visible in longitudinal section. Scale bar = 0.5 μm.

Figure 32. The reservoir-PRR connector (large arrow) consists of reinforced microtubules. Between it and the siphon are at least five electron-dense fibers (small arrow) and a curved band of microtubules (arrowhead). Scale bar = 0.5 μm.


PRL
28
PRL
S
29
30
GC
31
R
GC
S
32



A complete list of abbreviations is provided on p. xv.

Figure 33. The major, nonflagellar root, structural connections between the siphon and the remainder of the cell in Entosiphon sulcatum. Not to scale.

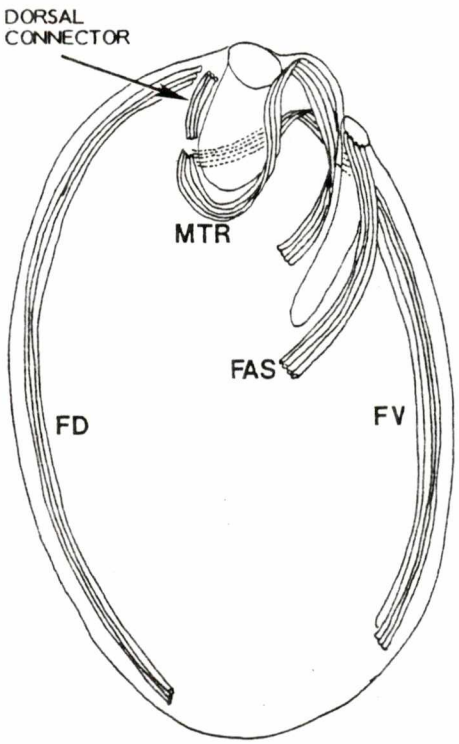


Figure 34. Diagram summarizing paths of bodonid microtubular flagellar roots and cytoskeleton. FD = dorsal fiber, FV = ventral fiber, FAS = cytopharynx-associated fiber, MTR = reinforced microtubules. After Kivic and Walne 1984.

PART 4. *EUTREPTIA PERTYI* AND *EUTREPTIA VIRIDIS*: FLAGELLAR ROOT SYSTEMS

Abstract

The structure and arrangement of flagellar root systems have become increasingly important indicators of phylogenetic relatedness among the algae. In this study, the flagellar roots of a presumably primitive photosynthetic euglenoid, Eutreptia, are described and compared with those of other euglenoid organisms. The arrangement of roots is similar to that of other euglenoids, with very little lateral displacement as the roots progress from the basal body complex to the anterior end of the cell. A vestigial cytopharynx is present at the reservoir-canal transition zone and is morphologically very much like that described in other green euglenoids. The ventral root of Eutreptia forms part of the structural support of the cytopharynx and is, on that basis, homologous with the MTR of bodonids and Colacium.

Introduction

A close phylogenetic relationship between the euglenoid and kinetoplastid flagellates has been proposed by a number of workers (e.g. Leedale 1967, Vickerman and Preston 1976, Round 1980, Corliss 1984, Kivic and Walne 1984), based largely on morphological similarities of the pellicle, mitochondria, mitotic pattern, flagella, and flagellar pocket. Other workers have reached the same conclusion independently, based on similarity of the amino

acid sequence of cytochrome c (Baba et al. 1981, Dayhoff and Schwartz 1981) and of the nucleic acid sequence of 5S ribosomal RNA (Kumazaki et al. 1983, Walker 1985). In view of the recognized phylogenetic importance associated with flagellar root systems in other algal groups (e.g. Mattox and Stewart 1984), investigation of the flagellar root systems of euglenoids may prove to be phylogenetically significant. For example, the flagellar roots of a colorless, phagotrophic euglenoid, Entosiphon sulcatum, were compared with those of the bodonids (Parts 2, 3), and the structural similarities of the root systems support the proposed euglenoid-kinetoplastid affiliation.

In the bodonids, the flagellar roots form well-defined connections with the ingestion apparatus; similar connections could have phylogenetic significance in euglenoids (Part 3). A putative cytopharynx and its involvement with the flagellar roots was demonstrated in the green euglenoid, Colacium (Willey and Wibel 1985b).

The flagellar roots of the euglenoids have not been extensively investigated. Evidence from published micrographs reveals a similar overall pattern in the basal body complex: three microtubular roots, one on either side of the functional basal bodies and a third between them, associated with the basal body of the recurrent flagellum (Part 2). However, the only euglenoid root system which has been examined in detail has been that of a colorless

organism (Parts 2, 3). To achieve a more complete understanding of euglenoid roots, it was necessary to examine a photosynthetic representative in some detail.

Eutreptia is a photosynthetic euglenoid with two emergent flagella. There have been no previous ultrastructural studies of Eutreptia, although several workers have described the closely related genus, Eutreptiella (Throndsen 1973, Moestrup 1978, Walne et al. 1986). The two genera are currently separated largely on the basis of flagellar length, with the flagella of Eutreptia being of approximately equal length and those of Eutreptiella unequal (Leedale 1967), although the validity of this separation is in question (Walne et al. 1986). The Eutreptiales are distinguished from the more numerous Euglenales by the fact that the latter have only one emergent flagellum, the second ending within the reservoir. It is thought that reduction of the second flagellum represents evolutionary advancement and, for this reason, the Eutreptiales are often considered more primitive than the Euglenales (Leedale 1967, 1978). This investigation presents results from an ultrastructural study of Eutreptia spp., a green unicell with two emergent flagella.

Materials and Methods

Eutreptia pertyi (Prings.) was obtained from the University of Texas Culture Collection of Algae (UTEX

LB1290). Cells were fixed for electron microscopy by adding glutaraldehyde in Sorenson's phosphate buffer (pH 7.0) to gently centrifuged cells, followed immediately by OsO_4 (final concentration 2.5% glutaraldehyde v/v, 1.3% OsO_4 w/v). After ten minutes at room temperature, the cells were washed in distilled water, dehydrated through a graded acetone series, and embedded in Spurr's resin (Spurr 1969). Sections were obtained with a Dupont diamond knife on a Sorval MT-2 ultramicrotome, were sequentially poststained with methanolic uranyl acetate and lead citrate, and were viewed on either a Hitachi H-600 or H-800 transmission electron microscope operated at an accelerating voltage of 100-200 kV, depending on the thickness of the section. Sections of various thickness (70 to 300 nm) were used to obtain information of different types.

A culture of Eutreptia viridis (Perty) was obtained from the University of Göttingen Algal Culture Collection (no. 1226-1C). Cells were fixed in 2% glutaraldehyde with 0.25 M sucrose and 0.1 M sodium cacodylate buffer (pH 7.3) on ice for one hour, rinsed three times in the same buffer and post-fixed for one hour in 0.5% OsO_4 on ice. They were then stained en bloc in 1% uranyl acetate in 12% acetone for 15 minutes. The remaining procedures were identical to those described above for E. pertyi.

Results

Eutreptia pertyi, a photosynthetic euglenoid with two emergent heterodynamic flagella, is approximately 80 μm long and circular in cross-section, the diameter varying due to a pronounced metaboly (see Part 1, Fig. 1).

Canal-Reservoir System

The canal-reservoir system consists of a narrow canal and an only slightly expanded reservoir with markedly dissected margins (Figs. 1, 2, 6[1]). The stigma, presumably a part of the photoreceptor system, is located along the anterior margin of the reservoir and can be used as a marker to designate the dorsal side of the cell (Leedale 1967). The canal is distinguished from the reservoir by its collar of transversely oriented microtubules (Fig. 1, arrowhead). The distinctively different morphologies of the flagellar paraxial rods (PAR; Figs. 2, 11), together with the electron-dense crystalline paraflagellar body (PFB; Fig. 1) of the anterior flagellum, were used to identify the anterior and posterior flagella throughout this study.

Basal Body Complex

The basal body complex lies at the posterior end of the reservoir, beneath the reservoir membrane (Fig. 6,

[1]All figures referenced in Part 4 are found in the Appendix at the end of Part 4.

arrow). It consists of four basal bodies, two functional ones which give rise to the flagella and two somewhat smaller accessory ones lying at approximately 60° to the functional basal bodies (Fig. 6). The spatial arrangement within the complex is very similar to that of Entosiphon sulcatum (Part 2), with the angle between the functional and accessory basal bodies being considerably greater in Eutreptia (i.e. 60° vs. 8°). Much electron-dense material surrounds the basal bodies themselves, particularly at the posterior ends (Figs. 7, 9). The striated fiber connecting the two functional basal bodies (Fig. 7) is morphologically similar to that of Entosiphon (Part 2). A smaller fiber connects the posterior functional basal body and its accessory basal body at their posterior ends (Fig. 6).

Microtubular Flagellar Roots

Three flagellar roots arise in the basal body region and extend anteriorly along the reservoir membrane. Their spatial arrangement in the basal body complex corresponds to the euglenoid root pattern described in Part 2: one root lies distal to each functional basal body and a third root lies between the two functional basal bodies, but nearer the posterior one (Fig. 9).

Dorsal microtubular root (DR). The dorsal root contains five microtubules at basal body level (Fig. 10). A well-defined electron-dense band lies proximal to the DR

here, and fibers connect the DR to bb_1 (Fig. 13). A striated fibrous root, extending from bb_1 toward bb_1', passes next to the DR, possibly providing a physical linkage between the root and the basal body complex (Fig. 13). Anteriorly, the individual microtubules of the DR are connected to one another by fine fibers, probably microtubule-associated proteins (MAPs), on the side near the reservoir membrane; similar fibrils extend from each side of the root (Fig. 14). In addition, a series of linear elements is attached, ladderlike, to the DR adjacent to the reservoir membrane near the F_1 basal body (Figs. 3-5, 7, 8). The DR is identifiable as a band of five closely spaced microtubules extending as far as the anterior end of the stigma (Figs. 13, 14), but is not noted in the canal region.

At the anterior end of the basal body complex, a band of singlet microtubules originates adjacent to the right side of the DR (as seen from the posterior end of the cell), the dorsal microtubular band (DMT, Figs. 2, 11, 12). The DMT then expands to cover the right and dorsal margins of the reservoir. A portion of the DMT lies between the stigma and the reservoir membrane, forming a large sheet of microtubules near the anterior end of the reservoir (Fig. 15). In the reservoir-canal transition zone, the DMT elements become the doublets which line the canal and are continuous with the pellicle microtubules (Figs. 16-18).

In the lower region of the reservoir, an electron-dense plate (P), is located between the DR and the DMT (Figs. 2, 12). This plate is larger at stigma level, and is located opposite the PFB of the anterior flagellum (Fig. 19). Whether this dense band contains microtubules could not be determined. The plate disappears anterior to the stigma and is not identified in the canal region.

No continuity between the transversely oriented canal microtubules and any of the flagellar roots could be identified.

Intermediate microtubular root (IR). As in Entosiphon, the intermediate root of Eutreptia lies between the two basal bodies and is closer to the posterior one (Fig. 9). The number of microtubules in the intermediate root differs from cell to cell in Eutreptia, varying between six and ten in the cells examined (eight cells had a sectioning angle which allowed this determination; cf. Figs. 2, 12, 13, 14). At basal body level, an electron-dense layer lies distal to the root (Figs. 9, 10). As the root extends anteriorly under the reservoir membrane, the dense layer disappears (Figs. 2, 11, 12-14); the IR microtubules are joined to one another by fine fibrils (Fig. 14), as are the DR microtubules.

At stigma level, the IR assumes a concave orientation about the axoneme of F_2; fibrils connect the individual

microtubules to one another (Fig. 15). Fibrillar material joins the F_2 membrane to the reservoir membrane in this reservoir-canal transition zone (Fig. 15-18). The IR continues anteriorly along the canal, maintaining a position opposite F_2.

Ventral microtubular root (VR). The largest of the three roots, composed of 10-20 microtubules in Eutreptia pertyi, the VR lies ventral to the basal body complex (Fig. 9, 10, 20). Figure 10 shows a fibrillar structure attached to one side of the VR in E. viridis. A similar attachment was noted in Entosiphon (not shown), and probably represents a linkage of the VR to the nonstriated root extending posteriorly in that organism.

Anteriorly, the VR microtubules separate to a greater extent than do the microtubules of the other reservoir bands (Fig. 2). Each microtubule manifests small extentions, the arms, and over the last one or two microtubules on the right side of the root, an electron-dense plate appears (Figs. 2, 12, 21). Endoplasmic reticulum subtends the distal side of the VR at stigma level (Fig. 15).

Near the reservoir-canal transition zone, the VR leaves the reservoir ventrally to follow a long anterior invagination (Figs. 22-29). This inpocketing corresponds, both morphologically and spatially, to the cytopharyngeal homologue (Cp) described by Willey and Wibel (1985b). This

structure seems to be composed of two opposing bands, one linear and microtubular and the other curved and electron-dense, surrounding a membrane-lined lumen. Whether the two bands are continuous (e.g., formed by curvature of the VR) or separate could not be determined.

Discussion

Comparison of Microtubular Flagellar Roots of Eutreptia and the Phagotrophic Entosiphon

The only other euglenoid flagellar roots which have been examined in detail are those of Entosiphon sulcatum (Parts 2, 3). In the basal body complex, the microtubular flagellar roots of Eutreptia and Entosiphon are quite similar: the DR is associated with bb_1, both the VR and IR are near bb_2, and all three roots extend anteriorly beneath the reservoir membrane. The orientation of the DR, in cross-section, is usually tangential to bb_1; the VR and IR are both more or less parallel to the axis connecting the two functional basal bodies. The number of microtubules in the individual roots varies between the two genera, but there is also some variability from cell to cell, even within the same species.

The DR in both organisms consists of several very closely spaced microtubules, appressed in many instances. Associated with the DR, beginning in the lower reservoir region, are an electron-dense plate (P) and a band of

singlet microtubules, the DMT, that is continuous with the pellicle microtubules.

The IR's of the two organisms also have many similarities, being borne on a modified portion of the reservoir margin (on a ridge in Entosiphon and in a concave region in Eutreptia). The microtubules of the IR are widely spaced and are interconnected by fine fibrils. In Eutreptia, however, linkages to the overlying reservoir membrane have not been identified. In addition, the IR and F_2 bear a constant spatial relationship to one another, presumably due to the fibrillar connections identified in both. In Entosiphon, there was evidence that the IR separated into two branches; this situation was not observed in Eutreptia, although neither is this possibility eliminated. In Eutreptia, the positions of all three roots around the reservoir were quite constant, in contrast to the variation noted in Entosiphon. This may be due to the activity of the contractile vacuole in Entosiphon, whereas this organelle is not present in Eutreptia, a marine organism.

The VR of Entosiphon extends anteriorly from the basal body complex on the ventral side of the reservoir, and then circles to the dorsal side by way of the right margin. Evidence suggests that the VR then leaves the reservoir margin and becomes incorporated into the siphon structure as an extension of the left pharyngeal rod, although this

is not yet confirmed. In Eutreptia, the path of the VR is quite straightforward, running anteriorly from the basal body complex, adjacent to the reservoir membrane, to the reservoir-canal transition zone, where it diverges from the reservoir and forms the major support of the cytopharynx.

Comparison of Microtubular Roots of Eutreptia with other Green Euglenoids

Eutreptiales. The only other member of the Eutreptiales for which flagellar root information is available is Eutreptiella eupharyngea (Moestrup 1978, 1982, Walne et al. 1986), which differs from Eutreptia only in flagellar length, a rather weak criterion (Pringsheim 1953, Throndsen 1973). The present work is the first extensive ultrastructural examination of Eutreptia and deals with flagellar roots exclusively.

Moestrup (1978) identified a complex structure, which he termed the multilayered structure (MLS), associated with one of the flagellar roots of Eutreptiella. According to him (Moestrup 1978, 1982), this euglenoid MLS may be similar to the MLS in the Charophyceae and the spermatozoids of bryophytes and higher plants. A structure similar in appearance and associated with the DR is also present in Eutreptia.

In Eutreptiella, Moestrup (1978, fig. 18) showed a four-membered root adjacent to the reservoir membrane and

separated laterally from the stigma microtubules by an electron-dense plate. In Figure 17 (Moestrup 1978) a four-membered root in the basal body complex has a tangential orientation to the basal body, and a small connective fiber extends from the basal body and runs toward the root. These features identify the root in both of these figures as the DR, which is thus very similar to that of Eutreptia. One major difference appears to be in the much wider spacing of the DR, plate, and DMT complex of Eutreptiella at reservoir level, as shown in Figure 18 (Moestrup 1978). This difference is probably accounted for by the much larger diameter of the reservoir in Eutreptiella eupharyngea, the roots having become separated from one another, perhaps by the membrane flow activity of the reservoir.

Walne et al. (1986, fig. 24) describe another microtubular root in Eutreptiella eupharyngea for which Eutreptia has no parallel. It consists of a double layer of microtubules, 10 in each layer, just beneath the ventral region of the reservoir. This difference in flagellar root morphology, if found consistently, would argue for the continued separation of the two genera.

Euglenales. The Euglenales are distinguished from the Eutreptiales principally by the presence of only one emergent flagellum instead of two: the anterior flagellum (F_1) is emergent while the posterior one (F_2) ends within

the reservoir (Leedale 1967). Except for the lack of a PAR in the much shorter F_2, the flagella appear to be identical to those of the Eutreptiales and Entosiphon (personal observation).

Willey and Wibel (1985b) have reported on the microtubular roots in the reservoir region of Colacium, a photosynthetic unicell which can settle, absorb its single emergent flagellum, produce a stalk, and form dendroid colonies. Information on other eulgenalean roots comes from published work by Piccinni and Mammi (Euglena gracilis var. Z, 1978) and West et al. (Trachelomonas hispida var. coronata, 1980), in addition to my unpublished observations on Euglena gracilis var. bacillaris and a fortuitous Euglena sp. contaminant in the Eutreptia pertyi culture.

An indication of the differences between the flagellar roots of Eutreptia and Euglena is the fact that the presence of the contaminant was detected by discrepancies between the flagellar roots of the two organisms. Specifically, the ventral roots of the several Euglena species examined consist of a distinctive 5 (or 6) + 4 (or 5) microtubular arrangement: 5 widely spaced microtubules with arms, plus 4 closely placed microtubules overlain by a thin electron-dense plate (Appendix, Fig. 4; Piccini and Mammi 1978, fig. 7). Interestingly, a similar arrangement exists in Euglena granulata (Walne 1971, fig. 4) but involving many more microtubules (27 + 12). All are

similar morphologically to the VR of Eutreptia: a long band of widely spaced microtubules, often with arms on the individual tubules, and with a plate over the terminal one or two microtubules on the side away from the IR. This arrangement was also described by Willey and Wibel (1985b) in Colacium, the total number of microtubules varying between 7 and 12.

In Colacium the PMT, a very linear arrangement of 5 microtubules joined by a fine filament on the side distal to the reservoir, lies adjacent to the DMT at the left side of the stigma (Willey and Wibel 1985b). A similar root exists in Euglena sp. (Appendix, Figs. 1, 4) and E. gracilis var. bacillaris (Appendix, Fig. 8). Based on morphology and positional relationship with respect to the VR, these roots correspond to the IR in Eutreptia and Entosiphon. A spatial relationship between the IR and F_2 has not been observed in the euglenalean species, nor is there a modification of the reservoir margin (i.e., ridge or concave region) associated with the IR.

The DR and its accompanying plate are more difficult to locate in published micrographs, possibly because they are smaller and may be easily concealed as part of the stigma microtubules. They are, however, evident in Euglena gracilis var. Z (Piccinni and Mammi 1978, fig. 9).

The Cytopharynx

The cytopharynx of Eutreptia is similar to that of Colacium, in that both arise in the reservoir-canal transition zone, and both are lined by an extension of the VR (MTR; Willey and Wibel 1985b). Since a cytopharynx has also been found in a number of other members of the Euglenales [Trachelomonas, Euglena acus, three strains of Euglena gracilis (Willey and Wibel 1985b; Part 4), Euglena mutabilis (Melkonian 1985), Euglena sp. (Part 4), and Phacus pleuronectes and Eutreptiella eupharyngea, unpubl. data], it is reasonable to assume that it may be a common feature of the green euglenoids. Such a structure is not present in Entosiphon, supporting the hypothesis that the siphon is homologous with the cytopharyngeal remnant in the green euglenoids. In Entosiphon there is some evidence to show that the VR becomes incorporated into the supporting structure of the siphon as part of the left pharyngeal rod. This, too, lends credence to the siphon-cytopharynx homology because the presumptive VR homologue, the MTR, forms part of the structural support of the bodonid cytopharynx.

Summary

The euglenoid flagellar root pattern established in Parts 2 and 3 is found also in Eutreptia, where the trajectories of the roots are more easily traced. The straightforward path of the roots in Eutreptia is

attributed to the organisms lack of both a complex ingestion apparatus and a contractile vacuole. The dorsal root and its accompanying electron-dense plate and band of singlet microtubules varies little in the two organisms. The intermediate root is associated with the posterior flagellum and with a modification of the reservoir margin. The ventral root is incorporated into the cytopharynx and is thus homologous with the MTR of the euglenoid Colacium and the bodonids.

This study extends our knowledge of euglenoid flagellar roots by providing detailed information on a presumably primitive green organism. It confirms the presence of a cytopharynx in this organism and identifies the cytopharynx-associated flagellar root as the euglenoid ventral root. The conservative nature of the euglenoid flagellar root pattern is also verified.

APPENDIX: PART 4

A complete list of abbreviations is provided on p. xv.

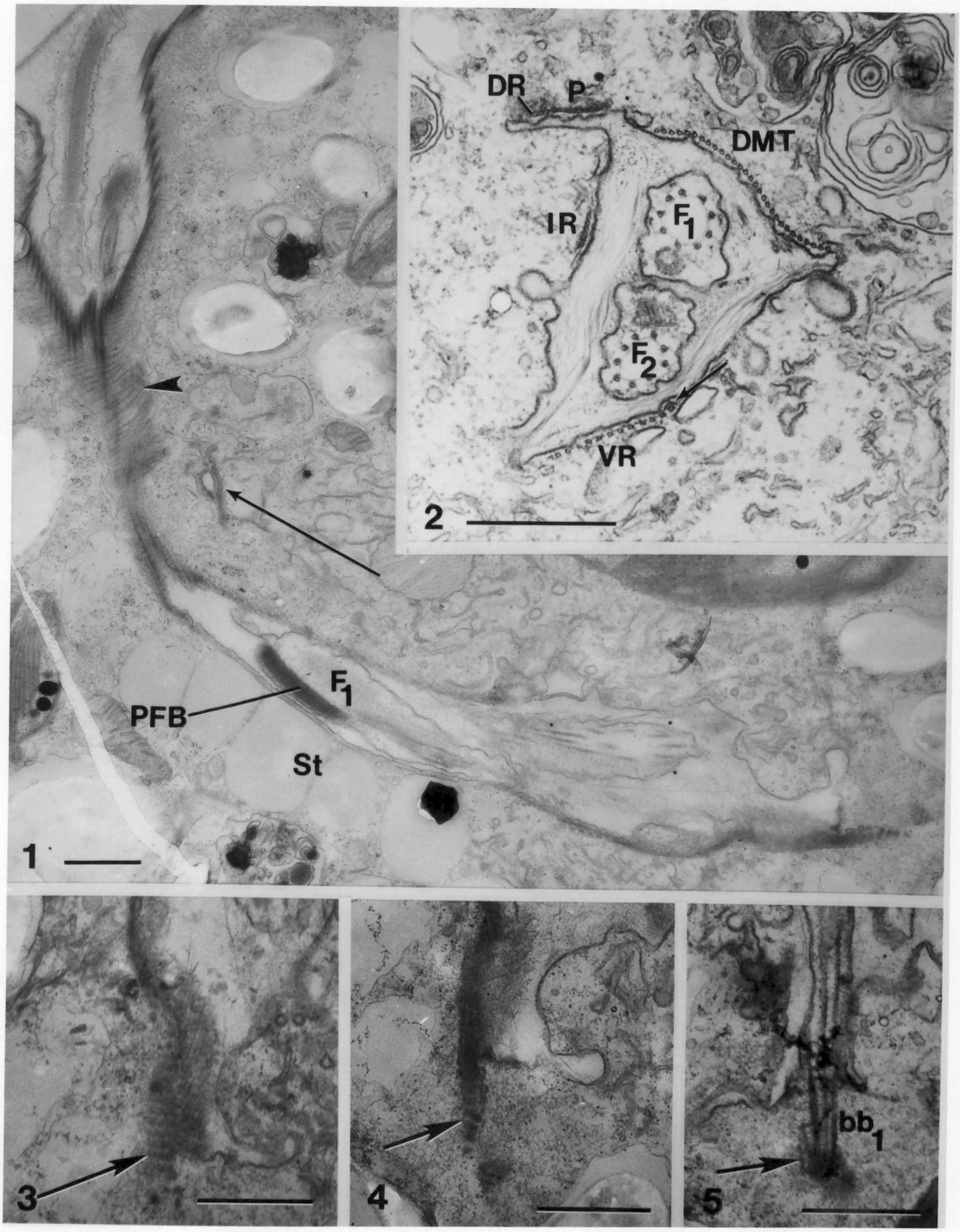
Figure 1. Longitudinal view of reservoir-canal complex of Eutreptia pertyi. Transversely oriented microtubules (arrowhead) encircle the canal from which emerge the two flagella. Paraflagellar body (PFB) of the anterior flagellum (F_1) is located near the stigma (St). Cytopharynx (arrow) is near reservoir-canal transition zone. Scale bar = 1.0 μm.

Figure 2. Transverse section of reservoir of E. pertyi. The three cytoplasmic microtubular flagellar roots are just beneath the reservoir membrane (DR = dorsal root, IR = intermediate root, VR = ventral root). Adjacent to the DR is an electron-dense plate (P) beside a long band of singlet microtubules (DMT). A small electron-dense plate is located over the last microtubule of the VR (arrow). Scale bar = 1.0 μm.

Figure 3. Longitudinal view of striated structure (arrow) near the base of F_1. First of three nonadjacent serial sections of Eutreptia pertyi. Scale bar = 1.0 um.

Figure 4. Longitudinal section near base of F_1. Electron-dense region is anterior to striated structure. Second of three nonadjacent serial sections. Scale bar = 1.0 μm.

Figure 5. Longitudinal section of the base of F_1. A part of the striated structure is present at the posterior end of the basal body (arrow). Third of three nonadjacent serial sections. Scale bar = 1.0 μm.


DR
P
DMT
IR
F1
F2
VR
2
PFB
F1
St
1
3
4
bb1
5

A complete list of abbreviations is provided on p. xv.

Figure 6. Longitudinal section through reservoir-canal system of Eutreptia pertyi. The anterior portion of the canal is to the left. Two basal bodies, connected by an electron-dense fiber (arrow), lie in the cytoplasm at the base of the narrow reservoir; two flagella extend through the system, and the stigma (St) lies on the dorsal side of the anterior region of reservoir. Scale bar = 1.0 μm.

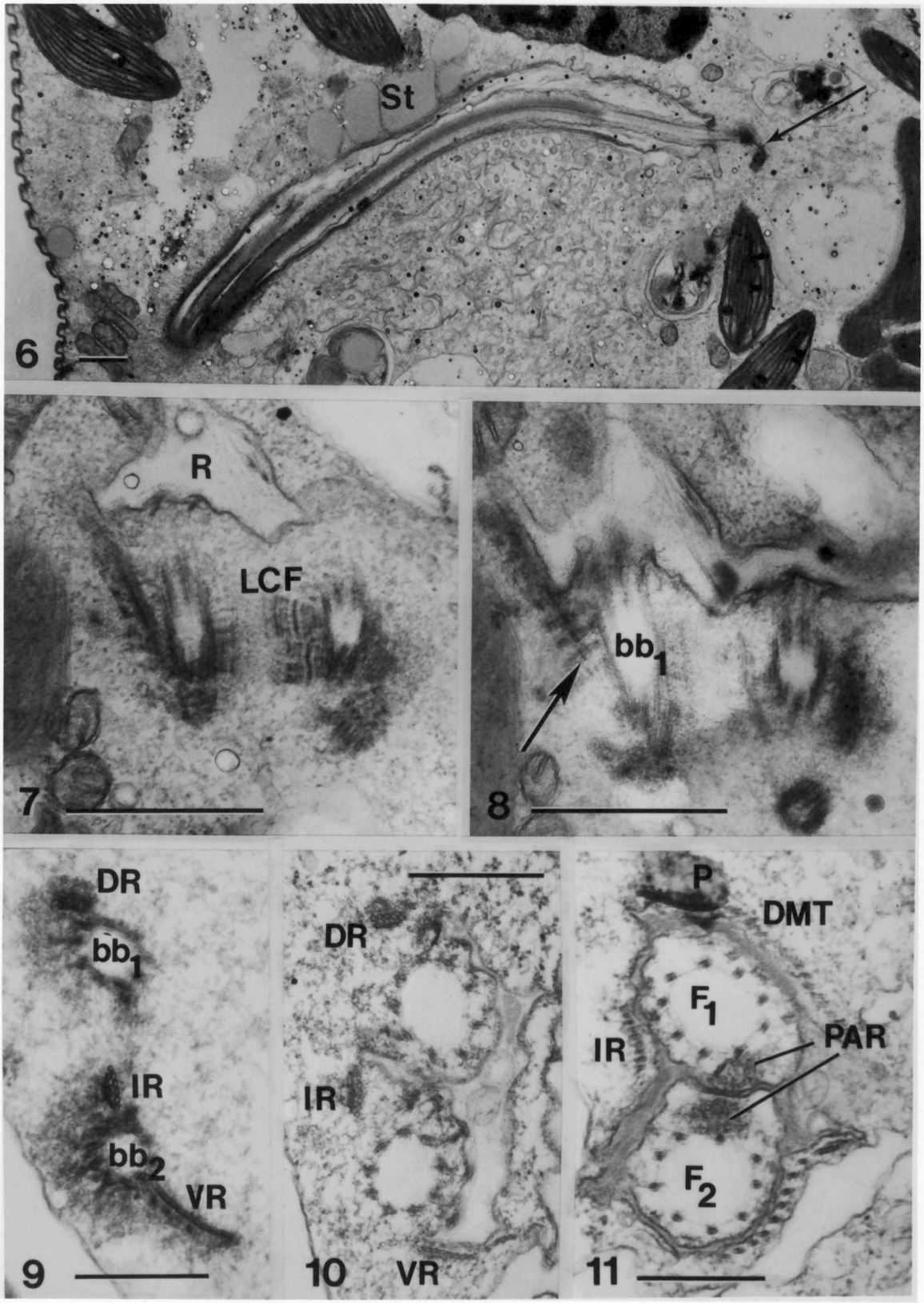
Figure 7. The two functional basal bodies in oblique section. The right portion of the large striated connective fiber (LCF) extends between them. R = reservoir. Eutreptia pertyi. Scale bar = 1.0 μm.

Figure 8. Oblique thick section (adjacent to Fig. 7) through the functional basal bodies. Striated structure (arrow) is associated with DR which extends anteriorly from bb_1. Scale bar = 1.0 μm.

Figure 9. The basal body complex of Eutreptia viridis has an arrangement similar to other euglenoids. There are three microtubular flagellar roots, one beside each of the two functional basal bodies, and one between them, nearer to bb_2. First of three nonadjacent serial sections. Scale bar = 0.5 μm.

Figure 10. Transverse section through flagellar transition zone of E. viridis. At the level where the flagella emerge into the reservoir, the VR consists of two segments, one with 8 microtubules, the IR has 6 microtubules, and the DR has 5 microtubules, all with associated electron-dense layers. Second of three nonadjacent serial sections. Scale bar = 0.5 μm.

Figure 11. Transverse section through base of the narrow reservoir. The IR is on a ridge projecting into the reservoir between the two flagella, which are identifiable by their paraxial rods (PAR). An electron-dense plate (P) and a band of singlet microtubules (DMT) are associated with the DR (not distinct in this micrograph). Third of three nonadjacent serial sections. E. viridis. Scale bar = 0.5 μm.


St
6
R
LCF
7
bb1
8
DR
bb1
IR
bb2
VR
9
DR
IR
10
VR
P
DMT
F1
IR
PAR
F2
11

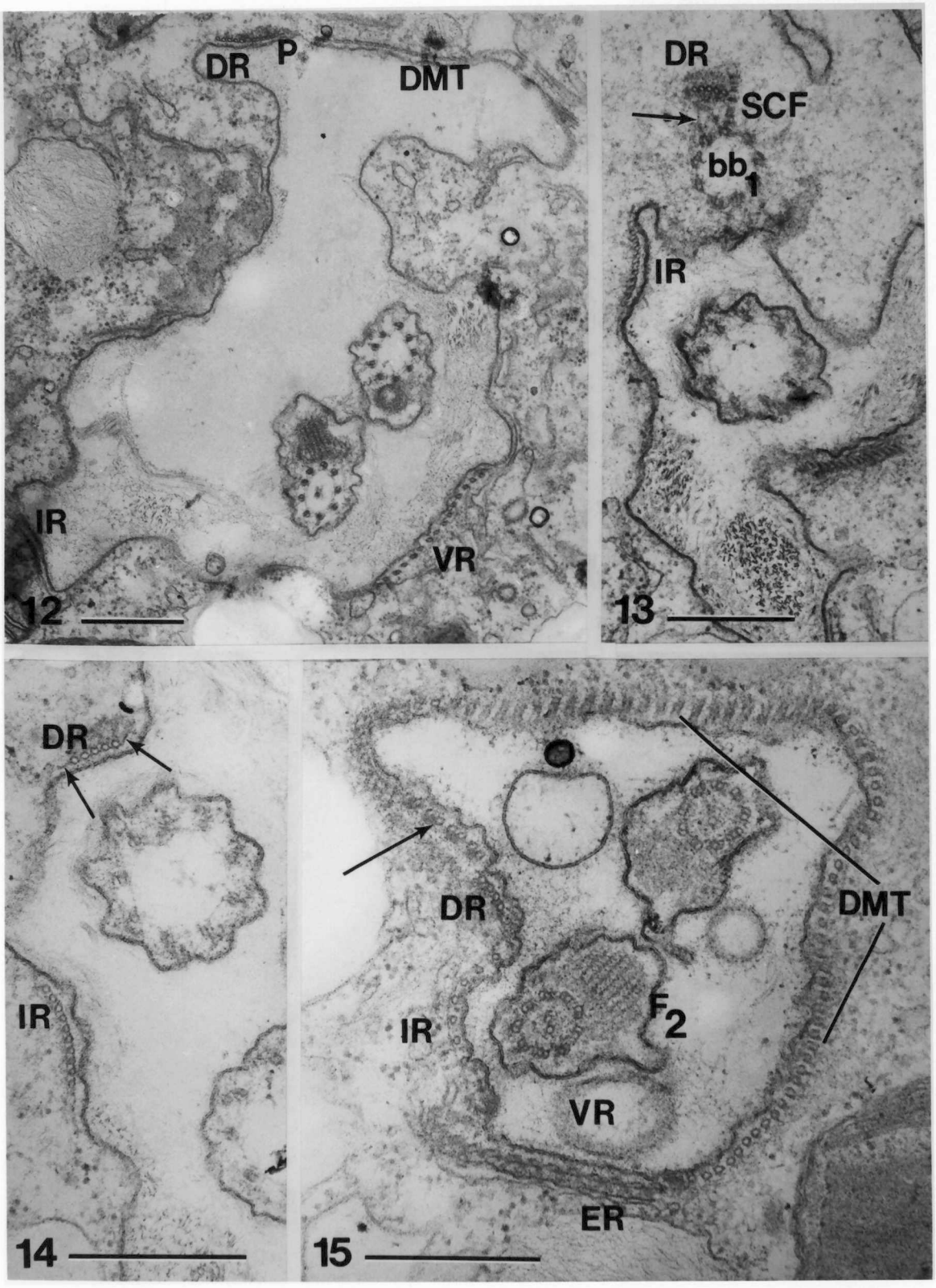
A complete list of abbreviations is provided on p. xv.

Figure 12. Transverse section of the middle region of the reservoir. The DR has 5 interconnected microtubules; adjacent to the DR is an electron-dense plate (P) and on the opposite side of the plate is a row of singleton microtubules (DMT). Eutreptia pertyi. Scale bar = 0.5 μm.

Figure 13. The DR is attached to the anterior basal body (bb_1) by fine filaments (arrow). A small striated connective fiber (SCF) extends from bb_1 past the DR, probably toward bb_1' (not shown). Eutreptia pertyi. Scale bar = 0.5 μm.

Figure 14. Fine filaments within the IR and the DR connect the individual microtubules to one another. There are filamentous extensions on either end of the DR (arrows). Eutreptia pertyi. Scale bar = 0.5 μm.

Figure 15. Transverse section through the reservoir at stigma level. The dorsal and right sides of the reservoir are lined by the stigma-related microtubules which are continuous with the DMT posteriorly. Adjacent to the stigma band, the microtubules are paired (arrow) and the DR is evident. The IR forms a concave arrangement around the axoneme of F_2, and fibrils interconnect the component microtubules. The VR is subtended by an element of endoplasmic reticulum (ER). Eutreptia pertyi. Scale bar = 0.5 μm.


DR
P
DMT
IR
VR
12
DR
SCF
bb1
IR
13
DR
IR
14
DR
DMT
F2
IR
VR
ER
15

A complete list of abbreviations is provided on p. xv.

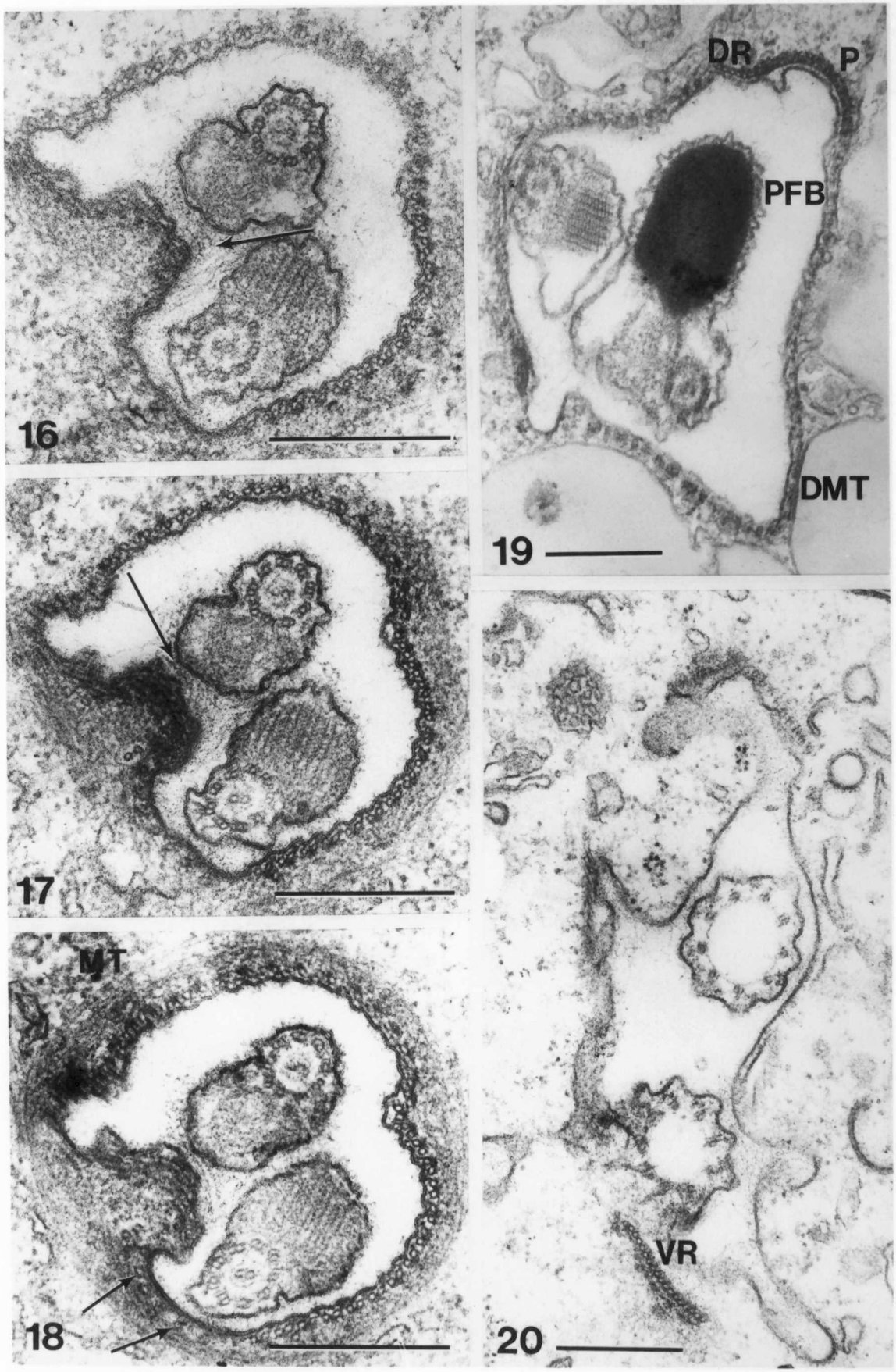
Figure 16. Transverse section through the reservoir-canal transition zone of Eutreptia pertyi. Fibrillar material (arrow) connects the two flagella to a ridge on the left side of the canal. First of three adjacent serial sections. Scale bar = 0.5 μm.

Figure 17. Transverse section anterior to Fig. 16. Fibrils (arrow) connect PAR region of flagella to canal ridge. Microtubular pairs, evident in cross-section, line the dorsal, right, and ventral margins of the canal. Second of three adjacent serial sections. Scale bar = 0.5 μm.

Figure 18. Transverse section of canal region, anterior to Fig. 17. Opposite the axoneme of F_2, singlet microtubules (arrows) line the canal membrane. The canal collar, composed of transversely oriented microtubules (MT) and fibers, completely encircles the canal (cf. Figs. 16, 17). Third of three adjacent serial sections. Scale bar = 0.5 μm.

Figure 19. Transverse section of E. pertyi at level of paraflagellar body (PFB). Electron-dense plate (P) between DR and DMT is especially well developed opposite the PFB. Scale bar = 0.5 μm.

Figure 20. Lower region of the reservoir has numerous membrane-lined invaginations. The VR is the longest of the microtubular roots, here including 18 microtubules, and is associated with electron-dense layers. E. pertyi. Scale bar = 0.5 μm.


16
17
MT
18
DR
P
PFB
DMT
19
VR
20

A complete list of abbreviations is provided on p. xv.

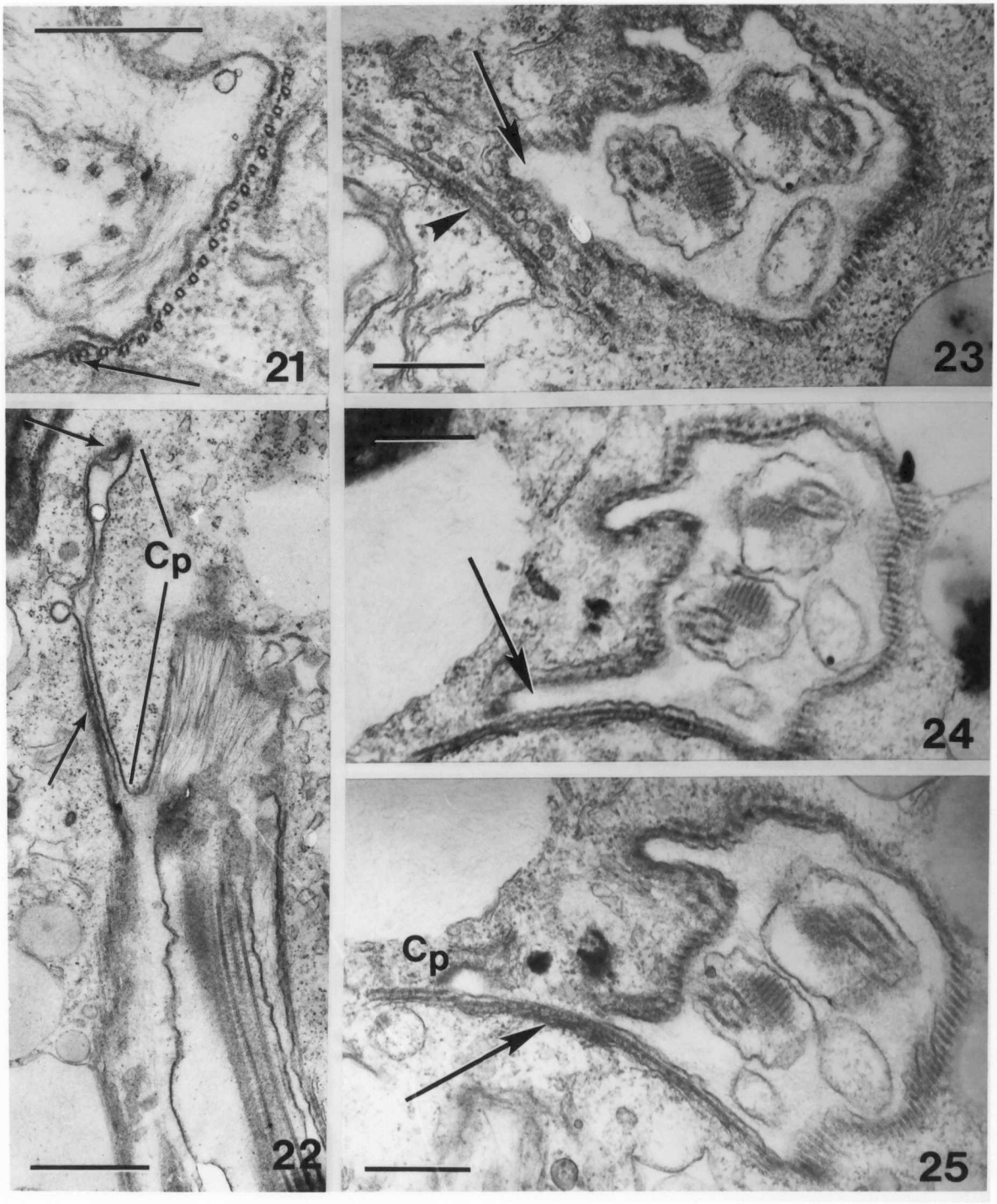
Figure 21. The microtubules of the VR are widely spaced and have small arms attached to them. The last two microtubules (arrow) have a small overlying plate. Eutreptia pertyi. Scale bar = 0.5 μm.

Figure 22. Longitudinal view of the cytopharynx (Cp) in E. pertyi. The Cp is composed of a membrane-lined lumen and supportive microtubules (arrows), and extends ventrally from the reservoir-canal transition zone. Scale bar = 1.0 μm.

Figure 23. Invagination of reservoir membrane forms the base of the cytopharynx (arrow). Band of cytoplasmic microtubules (arrowhead) may join VR to support the cytopharynx. Third of three nonadjacent serial sections. Scale bar = 0.5 μm.

Figure 24. Oblique section shows continuity of cytopharyngeal pocket (arrow) with reservoir-canal in the transition zone. Second of three nonadjacent serial sections. Scale bar = 0.5 μm.

Figure 25. Oblique thick section shows VR (arrow) connecting cytopharyngeal pocket (Cp) to canal of E. pertyi. Most anterior of three nonadjacent serial sections. Scale bar = 0.5 μm.


21
23
Cp
22
24
Cp
25

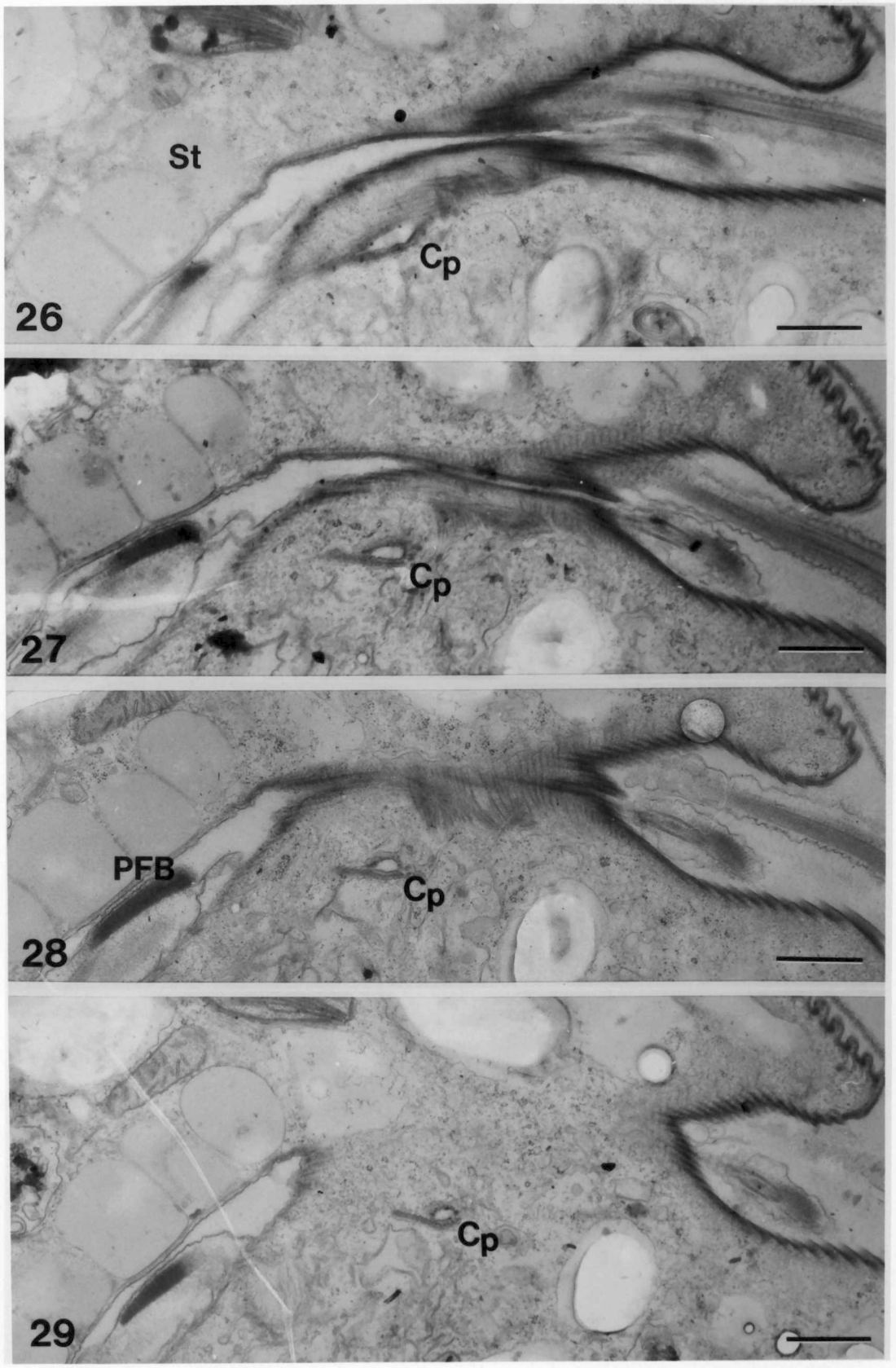
A complete list of abbreviations is provided on p. xv.

Figure 26. Longitudinal section through reservoir-canal transition zone of Eutreptia pertyi. Cytopharyngeal remnant (Cp) is continuous with reservoir by means of microtubular supporting bands. Stigma (St) is located on dorsal side of reservoir. First of four adjacent serial sections. Scale bar = 1.0 μm.

Figure 27. Longitudinal section adjacent to Fig. 26. Cp is on ventral side of canal. Second of four adjacent serial sections. Scale bar = 1.0 μm.

Figure 28. Longitudinal section shows canal collar of transversely oriented microtubules. Paraflagellar body (PFB) of F_1 lies opposite stigma. Third of four adjacent serial sections. Scale bar = 1.0 μm.

Figure 29. Longitudinal section adjacent to canal. The Cp is membrane-lined and bordered by two curved microtubular bands. Fourth of four adjacent serial sections. Scale bar = 1.0 μm.


St
Cp
26
Cp
27
PFB
Cp
28
Cp
29

PART 5. CONCLUSION

Several separate lines of evidence now suggest that the Euglenophyceae are, at most, only distantly related to other algal classes. Ragan and Chapman (1978) summarize a large volume of biochemical and physiological data (e.g. presence of specific enzymes, histones, biosynthetic pathways, etc.) and conclude that "Biochemically, the Euglenophyceae bear little resemblance to `other' algae, with the exception of characters pertaining to the chloroplast . . . ." In addition, comparison of nucleotide sequences of cytoplasmic phenylalanine transfer RNA (tRNA) indicates that the euglenoids would be more appropriately classified as animals rather than plants (Chang et al. 1981). Cytoplasmic tRNA from Euglena gracilis differs from that of a variety of animals (e.g. Drosophila, chicken, mouse, rabbit, human, salmon) by only four to six nucleotides out of a total of 76, while there is a difference of 16 nucleotides between Euglena and higher plant (i.e. bean, Phaseolus vulgaris) cytoplasmic tRNA. On the other hand, tRNA sequences from the chloroplasts of Euglena and bean are quite similar, differing by only five nucleotides (Hasegawa et al. 1981). This evidence supports the suggestion (Stewart and Mattox 1975, Gibbs 1978, Whatley 1981) that the photosynthetic euglenoids resulted when a green alga (or its chloroplast) developed an endosymbiotic relationship with a colorless protozoan host.

Other molecular sequence data, as well as pronounced

morphological similarities, identify the kinetoplastid flagellates as probable ancestors of the euglenoids. For example, Dayhoff and Schwartz (1981) and Baba et al. (1981) conclude that Euglena gracilis and two Crithidia species (trypanosomes) are closely related, based on amino acid sequences of cytochrome c from mitochondria. Nucleotide sequencing of 5S ribosomal RNA, available for more than 100 protists, reveals a remarkably similar picture (e.g. Delihas et al. 1981, Kumazaki et al. 1983, Walker 1985): Euglena and Crithidia consistently are nearest neighbors when clustering routines are applied to the data. Interestingly, Kumazaki et al. (1983) describe the multicellular animals as sharing a direct common ancestor with the Euglena/Crithidia line.

The biochemical data on the kinetoplastid flagellates, cited above, centers almost exclusively on the trypanosomes due to their ready availability in culture; the bodonids have been largely ignored. For this reason, no direct molecular comparisons between euglenoids and bodonids are available. However, considerably more morphological information exists on the bodonids. Thus, because the trypanosomes are highly modified for a parasitic existence, and because they undergo complex structural changes throughout their life cycle, morphological comparisons between the bodonids and euglenoids, rather than between

the trypanosomes and euglenoids, are emphasized in the present work.

Morphological and ultrastructural similarities between the euglenoids and kinetoplastids are summarized in some detail by Kivic and Walne (1984). In addition to having a similar overall external morphology, representative bodonids and euglenoids both exhibit the unusual creeping movement called metaboly, or euglenoid movement. The flagella, usually two in number, arise from an anterior depression, each flagellum manifesting a distinctive paraxial rod. The mitotic and cytokinetic patterns are similar in the two groups, and are considerably different from those of most other protists. Finally, the mitochondria have flat, rather than tubular, cristae and a similar type of contractile vacuole, when present. Kivic and Walne (1984) also describe several additional areas of probable homology between the microtubular cytoskeletons of the two groups; these are examined in detail in the present work.

Flagellar Root Systems

The euglenoid flagellar root systems investigated thus far consist of three microtubular roots originating in the basal body complex and extending anteriorly beneath the reservoir membrane (Fig. 1[1]). The dorsal root (DR), a

[1]Figures referenced in Part 5 are in Appendix: Part 5.

small band of several closely spaced microtubules, arises near the basal body of the anterior flagellum (bb_1). At reservoir level two more components are associated with it: an electron-dense plate (P) and a band of singlet microtubules (the DMT) which is continuous anteriorly with the pellicle microtubules. The DMT is associated with the stigma, if present, and the plate seems to have a predictable spatial relationship with the anterior flagellum (F_1) and with the paraflagellar swelling (PFB), if present. A second root, the intermediate (IR), originates between the two functional basal bodies, close to the posterior one (bb_2). It may give rise to a band of microtubules lining the ventral surface of the cell. The IR microtubules are interconnected by fine fibrils, and the root bears a predictable spatial relationship to the emergent posterior flagellum (F_2; i.e., root lies opposite axoneme or PAR). The ventral root (VR) arises on the right side of the posterior functional basal body and probably becomes incorporated anteriorly into the ingestion apparatus or its equivalent. A portion of the VR is slightly offset away from the reservoir membrane and is usually overlain by an electron-dense plate.

Comparison of Euglenoid and Kinetoplastid Root Systems

A comparison of the euglenoid root system with that of the bodonids is complicated by the fact that, although the paths of the bodonid roots are well defined with respect to

the flagellar pocket, cytopharynx and pellicle, their origins within the basal body complex have not been as fully described. This is unfortunate because, in the euglenoids, the pattern of microtubular roots in the basal body complex appears to be a very conserved aspect of the system. A complete description of spatial relationships within the bodonid basal body complex will greatly facilitate comparison of the two groups.

Because the trypanosomes are a highly derived group, and because their homology with the bodonids has been well established (Honigberg et al. 1964, Vickerman 1976), they will not be considered in this comparison.

Dorsal root. The euglenoid dorsal root (DR) corresponds to the dorsal connector of the bodonids. The two are morphologically very similar in the basal body complex, having a small number (approximately 3-5) of adjoining microtubules overlain by an attached electron-dense plate. They are both spatially related to a band of singlet microtubules which gives rise to the peripheral cytoskeleton (dorsal fiber in bodonids, pellicle microtubules in euglenoids). Brugerolle et al. (1979) suggested that the dorsal connector (probably the DR in euglenoids) may serve as a nucleating center for the dorsal fiber (DMT in euglenoids), based on the presence of amorphous electron-dense material at the location where one ends and the other begins.

A number of structural relationships suggest that the reservoir membrane and associated flagellar roots are far more than a channel through which the flagella pass on their way to the external medium. In two euglenoids (Entosiphon and Peranema) the plate overlies a fibrous structure (Part 3; Hilenski and Walne 1985). In Eutreptia the plate lies directly opposite from the PFB, presumably a part of the photosensory apparatus (Part 4). In Entosiphon, fibrillar connections join the posterior flagellum to the reservoir membrane adjacent to the DR (Part 2). The anterior flagellum may be similarly attached to the reservoir-canal membrane (Entosiphon, Eutreptia, Parts 3 and 4). Furthermore, there is some evidence to suggest that the striated structure near the basal body complex (Eutreptia, Entosiphon, Parts 2 and 4) is probably associated with the dorsal root; it may be analogous to the large striated fiber in Peranema which underlies the plate associated with the DR in that organism. The dorsal root and associated structures (plate and DMT) may be components of a complex system, perhaps sensory in function.

Intermediate root. The euglenoid intermediate root (IR) and the bodonid ventral fiber (FV) both arise adjacent to the recurrent flagellum and extend anteriorly along the left side of the reservoir. In the bodonids, the FV departs from the reservoir membrane and extends posteriorly just beneath the pellicle on the ventral surface of the

cell. If the bodonid recurrent flagellum adheres to the cell body, then it is attached to the region of the cell membrane overlying the FV.

The euglenoid IR has not been traced completely, due in part to displacement of roots by other cellular activities, e.g. endo- and exocytosis. There is evidence that, in Entosiphon, the IR splits into two segments, one following a path similar to the FV in the bodonids, i.e., running posteriorly along the ventral ridge. The other segment may enter the siphon, becoming associated with the cytopharynx. In the bodonids there are two or more bands of microtubules associated with the cytopharynx, one of which might be an extension of the FV. Further investigation of the siphon tip region of Entosiphon is needed to determine the exact routes of these microtubular bands, which may prove to be a difficult task.

Ventral root. In the bodonids, the reinforced microtubules (MTR) extend from the basal body complex along the reservoir membrane, curve backwards at the preoral crest, and extend posteriorly along the margin of the cytopharynx (Brugerolle et al. 1979, Kivic and Walne 1984). Assuming homology among the bodonid cytopharynx, the cytopharyngeal homologue of the green euglenoids (Willey and Wibel 1985a, b), and the siphon of Entosiphon, then the ventral root (VR) described in this study is homologous with the bodonid MTR by virtue of its similar position with

respect to the same organelles. The electron-dense arms noted on the microtubules of the VR in Eutreptia and the dark webbing surrounding the cytopharyngeal microtubules in Colacium (Willey and Wibel 1985) correspond to the more elaborate reinforcement on the MTR of the bodonids (Brugerolle et al. 1979) and of Isonema (Schuster et al. 1968, Porter 1973).

Taxon to taxon variation in the VR may prove useful in determining phylogenetic relationships within the Euglenophyceae. For example, the VR of Entosiphon consists of two loosely associated microtubular segments, whereas in Eutreptia the VR has a long row of microtubules with arms, and a small electron-dense curved plate is located over the terminal one or two microtubules of that root. In yet another variation, in Euglena spp. the VR regularly has an unusual 5 + 4 arrangement, with a well-defined flat plate over the four-membered segment. These variations could define a progression in the development of the small plate-bearing segment and in the integrity of the root as a whole.

Ingestion Apparatus

Willey and Wibel (1985a, b) have proposed that a small invagination in the reservoir-canal transition zone of Colacium represents an evolutionary remnant of a cytopharynx, such as that found today in both the bodonids

and trypanosomes. Similar structures have been identified in Trachelomonas, Euglena acus, two strains of Euglena gracilis (Willey and Wibel 1985b), and Euglena mutabilis (Melkonian 1985). During the present study, a cytopharynx has been found also in Eutreptia pertyi (Part 4), Euglena gracilis var. bacillaris, Euglena sp. (Appendix), and in Phacus pleuronectes and Eutreptiella eupharyngea (unpubl. data). In those micrographs in which a determination can be made, the cytopharynx is consistently situated in the reservoir-canal transition zone.

In both Colacium (Willey and Wibel 1985a, b) and Eutreptia the VR (called the MTR in Colacium, Table 4 in Part 1) forms a major structural support of the cytopharynx. In Entosiphon, there is good evidence that the VR also becomes part of the structural support of the siphon (Part 3). The tortuous pathway of the VR, connecting the posterior functional basal body to the ingestion apparatus, as well as the location of the root origin near bb_2, strongly indicates homology of the VR and MTR.

The structural evidence of all three flagellar roots presented here provides good support for the recently proposed euglenoid-kinetoplastid-Isonema superphylum (Corliss 1984, Kivic and Walne 1984).

Phylogenetic Speculation

Willey and Wibel (1985a) present an evolutionary scheme for the new superphylum based on location of the cytopharynx. They propose that the ventrally located cytostome (mouth of the cytopharynx) evolved toward a position inside the euglenoid reservoir-canal; acquisition of a chloroplast endosymbiont would, through pressures imposed by photosynthesis (e.g. osmotic changes), encourage enlargement of the reservoir. They further suggest that continued phagotrophy not only would have been unnecessary but also would pose a distinct functional problem, leading to the elimination of phagotrophy in green euglenods (Willey and Wibel 1985b).

I propose an extension to their hypothesis and suggest that the euglenoid canal collar, composed of transversely oriented microtubules and filaments, has proved a critical constraining factor in euglenoid evolution. Bodonids, the hypothetical progenitors of the euglenoids, ingest particulate food through the cytostome which opens directly to the environment; they have no canal (Brooker 1971, Vickerman and Preston 1976). Entosiphon also has no constraining transverse microtubules; the cytopharynx (siphon) is essentially in direct contact with the environment through the anterior depression, and is used for ingestion of solid particles (Mignot 1966; D. J. Patterson, pers. comm.). In Peranema, the cytostome is

located within a very short canal that is surrounded by a few transversely oriented microtubules and a dense canal thickening (Nisbet 1974). The microtubular collar that is typical of presumably advanced euglenoids is not present.

Green euglenoids, on the other hand, have a well-developed microtubular collar surrounding a narrow canal. Such a constraining collar may, in fact, explain the apparent absence of any green euglenoids which also ingest solid food. Pringsheim (1948) noted that this was unusual, for in other algal groups where colorless representatives of a photosynthetic class ingest particles, (e.g. Chrysophyceae, Cryptophyceae, Dinophyceae), the green forms are also able to ingest solid food. In fact, in the Chrysophyceae such particulate food has been found to amount to as much as 30% of the total body weight per day (Bird and Kalff 1986).

A hypothetical set of evolutionary events leading to the variation in extant euglenoid organisms is outlined in Figure 2. The earliest forms probably had two openings to the environment, a cytostome and the flagellar opening (e.g., bodonids), which then moved closer together, becoming located in a communal anterior depression (e.g., Entosiphon). The walls of this opening became strengthened by the presence of canal thickenings and a few transverse microtubules (e.g. Peranema), which may have provided support for the voracious cutting and sawing activity of

the rodorgan (Chen 1950). At this point, chloroplast acquisition by a phagotrophic ancestor would have eliminated the need for particulate food. The canal collar, which would severely limit particulate intake, could have developed, perhaps for the adaptive advantages outlined by Willey and Wibel (1985a). In this hypothetical green euglenoid, then, the cytostome has been displaced to the base of the canal microtubules, the cytopharynx no longer being functional (or only minimally so) in phagotrophy; it now lies in the reservoir-canal transition zone.

One possible source of confirmation for this hypothesis may lie in completely tracing the paths of the flagellar roots in the more advanced euglenoids. I have suggested that the IR may split into two segments, one associated with the cytopharynx and the other turning to run posteriorly along the ventral cell surface. In euglenoids with a well-developed canal, such a segmentation might result in a few IR microtubules accompanying the cytopharynx at the reservoir-canal transition zone. The remainder may proceed anteriorly along the canal and then curve posteriorly to line the ventral cell surface. In Eutreptia (Part 4) the IR does line the canal as described; a similar root exists in Menoidium (Leedale and Hibberd 1974, Fig. 16), although my identification of it as the IR

is based solely on morphological similarity to the PMT of Colacium (Willey and Wibel 1985b).

The sequence presented in Figure 2 implies that any euglenoid with a well-developed canal collar will have the cytopharynx, if present, located at the base of the collar in the reservoir-canal transition zone. If this is true, then the colorless euglenoids with canal collars (e.g. Rhabdomonas, Menoidium) should prove to have a cytopharynx located at the base of the canal microtubules. A cytopharynx in this position would identify them as much more recently evolved than the phagotrophic euglenoids, in contrast to the close relationship suggested by Leedale and Hibberd (1974). Hence, the Heteronematales are suggested to be a primitive group and the Rhabdomonadales a more advanced one, probably derived from intermediate green forms.

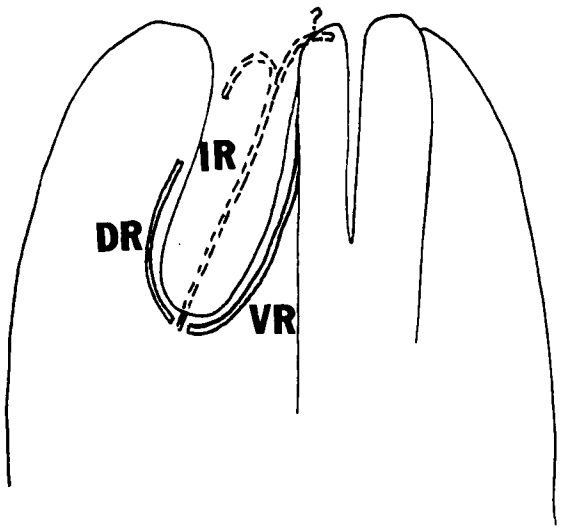
Summary

This study presents the first detailed description of a euglenoid flagellar root system. The roots of two different euglenoids, a colorless phagotroph (Entosiphon) and a presumably primitive phototroph (Eutreptia), are described and compared with available data on other euglenoids and on the bodonids. A general euglenoid flagellar root pattern is described in considerable detail, based on these comparisons. The relative position of the

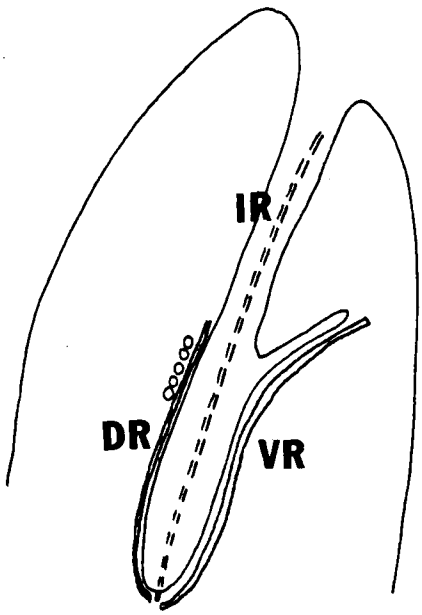
roots within the basal body complex is quite stable among the euglenoids, and might thus be useful for determining phylogenetic relationships at higher taxonomic levels. The morphology of the ventral root and the nature of the association of the roots with other cell organelles is more variable and will probably be most useful at lower taxonomic levels, e.g., within the Euglenophyceae. Such analysis, however, awaits the description of the roots of other euglenoid species. Finally, comparison of the euglenoid root system with that of the bodonids suggests considerable similarity and, together with available biochemical and morphological data, supports the recently proposed supergroup, the Euglenozoa.

APPENDIX: PART 5

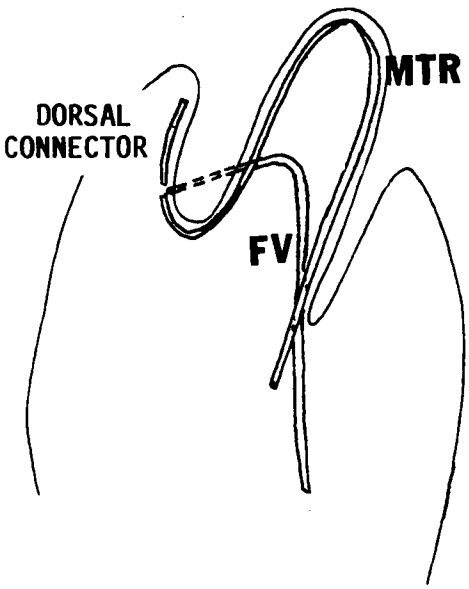
Figure 1. Diagrammatic comparison of the paths of the three flagellar roots among Entosiphon, Eutreptia, and some bodonids. DR = dorsal root, IR = intermediate root, VR = ventral root. Not to scale.



Entosiphon



Eutreptia



Bodonid

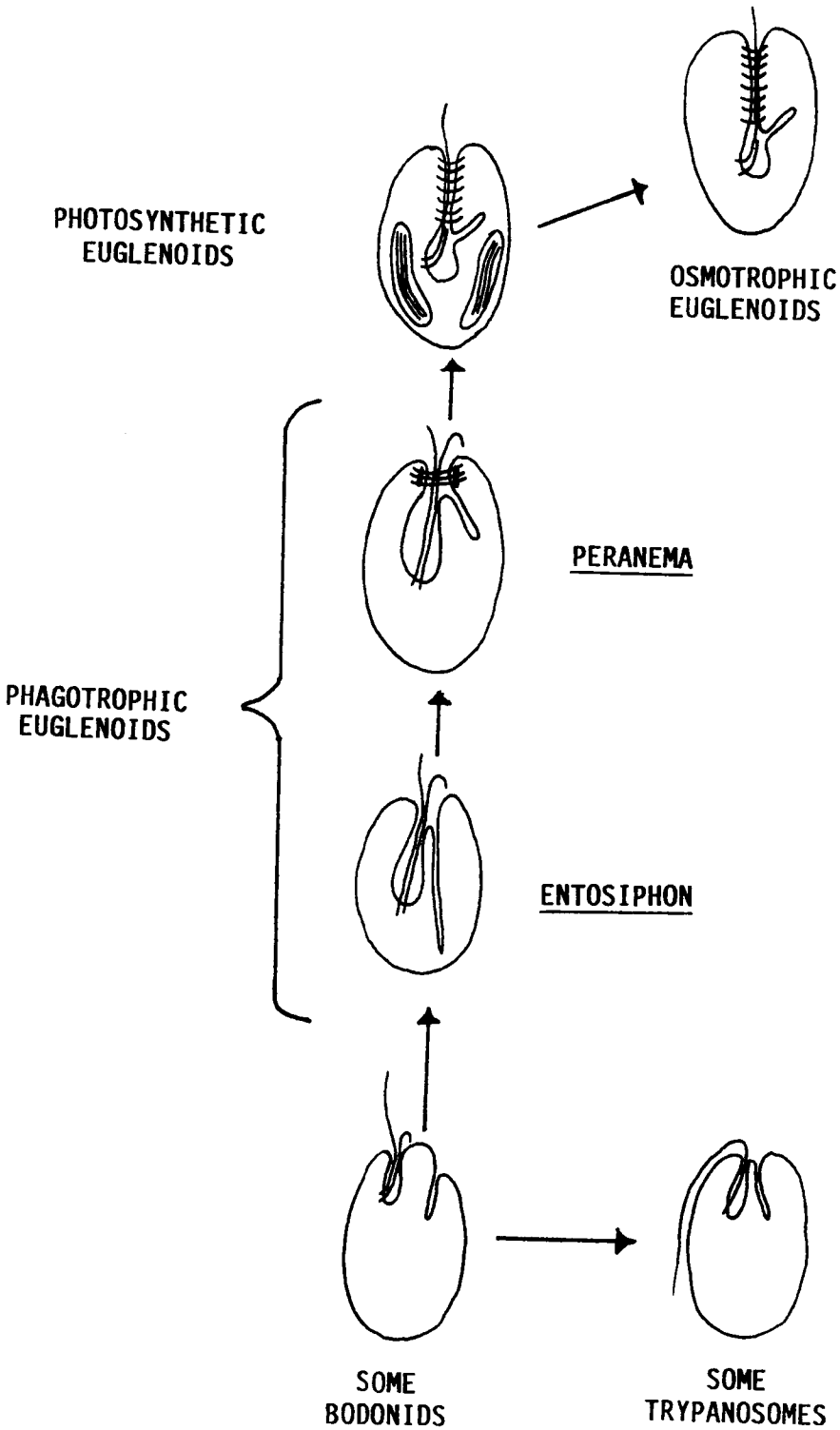


Figure 2. Hypothetical evolutionary sequence within the Euglenozoa, based primarily on relationships among the cytostome, flagellar pocket, and canal microtubules.

LIST OF REFERENCES

Andersen, R. A. 1985. The flagellar apparatus of the golden alga Synura uvella: Four absolute orientations. Protoplasma 128:94-106.

Anderson, W. A. & Ellis, R. A. 1965. Ultrastructure of Trypanosoma lewisi: Flagellum, microtubules, and the kinetoplast. J. Protozool. 12:483-99.

Arnott, J. R. & Walne, P. L. 1967. Observations on the fine structure of the pellicle pores of Euglena granulata. Protoplasma 64:330-4.

Baba, M. L., Darga, L. L., Goodman, M. & Czelusniak, J. 1981. Evolution of cytochrome c investigated by the maximum parsimony method. J. Mol. Evol. 17:197-213.

Bird, D. F. & Kalff, J. 1986. Bacterial grazing by planktonic lake algae. Science 231:493-5.

Bourrelly, P., Coute, A. & Rino, J. A. 1976. Ultrastructure de la cuticle de quelques eugleniens. I. Euglena oxyuris var. minor Defl. et Euglena spirogyra var. fusca (Klebs) Lemm. Protistologica 12:623-8.

Bovee, E. C. 1972. The Trypanosomatidae: Possibly descendant from euglenoids? J. Protozool. 18 (Suppl.):14.

Brugerolle, G., Lom, J., Nohynkova, E., & Joyon, L. 1979. Comparaison et evolution des structures cellulaires chez plusiers especes de bodonides et cryptobides appartenant aux genres Bodo, Cryptobia, et Trypanoplasma (Kinetoplastida, Mastigophora). Protistologica 15:197-221.

Buetow, D. E. [Ed]. 1968. The Biology of Euglena I. General Biology and Ultrastructure. Academic Press, New York.

Burzell, L. A. 1973. Observations on the proboscis-cytopharynx complex and flagella of Rynchomonas metabolita Pshenin 1964 (Zoomastigophorea, Bodonidae). J. Protozool. 20:385-93.

Burzell, L. A. 1975. Fine structure of Bodo curvifilus Griessmann (Kinetoplastida: Bodonidae). J. Protozool. 22:35-39.

Calkins, G. N. 1926. The Biology of the Protozoa. Lee and Febiger, Philadelphia.

Cavalier-Smith, T. 1978. The evolutionary origin and phylogeny of microtubules, mitotic spindles, and eukaryote flagella. BioSystems 10:93-114.

Chang, S. H., Hecker, L. I., Brum, C. K. , Schnabel, J. J., Heckman, J. E., Silberklang, M., RajBhandary, U. L., & Barnett, W. E. 1981. The nucleotide sequence of Euglena cytoplasmic phenylalanine transfer RNA. Evidence for possible classification of Euglena among the animal rather than the plant kingdom. Nucleic Acids Res. 9:3199-204.

Chen, Y. T. 1950. Investigations of the biology of Peranema trichophorum (Euglenineae). Quart. J. Microsc. Sci. 91:279-308.

Christen, H. R. 1963. Sur Taxonomie der Farblosen Euglenien. Nova Hedwigia 4:437-65.

Christensen, T. 1962. Alger. In Bocher, T. W., Lange, M., and Sorensen, T. [Eds.] Botanik 2:1-178. Munksgaard, Cohenhagen.

Chu, S. P. 1947. Contribution to our knowledge of the genus Euglena. Sinensia 17:75-136.

Corliss, J. O. 1984. The kingdom Protista and its 45 phyla. BioSystems 17:87-126.

Dayhoff, M. O. & Schwartz, R. M. 1981. Evidence on the origin of eukaryotic mitochondria from protein and nucleic acid sequences. Ann. N. Y. Acad. Sci. 361: 92-104.

Delihas, N., Andersen, J., Andresini, W., Kaufman, L., & Lyman, H. 1981. The 5S ribosomal RNA of Euglena gracilis cytoplasmic ribosomes is closely homologous to the RNA of the trypanosomatid protozoa. Nucleic Acids Res. 9:6627-33.

Dodge, J. D. 1973. The Fine Structure of Algal Cells. Academic Press, New York.

Dodge, J. D. 1980. Morphology and phylogeny of flagellated protists. In Schwemmler, W. & Schenk, H. E. A. [Eds.] Endocytobiology. Endosymbiology and Cell Biology. 1:33-50.

Donnelly, L. S. 1979. Comparative cellular ultrastructure and chemical characterization of envelopes of three species of Trachelomonas (Euglenophyta). Ph. D. Dissertation, University of Tennessee, Knoxville, Tennessee.

Dynesius, R. A. & Walne, P. L. 1975. Ultrastructure of the reservoir and flagella in Phacus pleuronectes (Euglenophyceae). J. Phycol. 11:125-30.

Eyden, B. P. 1977. Morphology and ultrastructure of Bodo designis Skuja 1948. Protistologica 13:169-179.

Farmer, M. A. & Triemer, R. E. 1985. Ultrastructural analysis of the flagellar apparatus of Distigma proteus (Euglenophyceae). Book of Abstracts, Second Internat. Phycol. Congr. Copenhagen, Denmark.

Fize, A. & Michel, R. 1972. Ultrastructure d'Astasia fennica Michajlow (Euglenida) parasite du tube digestif de copepodes cyclopidae. Protistologica 8:143-53.

Floyd, G. L., Hoops, H. J. & Swanson, J. A. 1980. Fine structure of the zoospore of Ulothrix belkae with emphasis on the flagellar apparatus. Protoplasma 104:17-31.

Gibbs, S. P. 1978. The chloroplasts of Euglena may have evolved from symbiotic green algae. Can. J. Bot. 56:2883-9.

Gillott, M. A. & Gibbs, S. P. 1983. Comparison of the flagellar rootlets and periplast in two marine cryptomonads. Can. J. Bot. 61:1964-78.

Gomez, M. P., Harris, J. B., & Walne, P. L. 1974. Studies of Euglena gracilis in aging cultures. II. Ultrastructure. Brit. Phycol. J. 9:175-93.

Goodenough, U. W. & Weiss, R. L. 1978. Interrelationships between microtubules, a striated fiber, and the gametic mating structure of Chlamydomonas reinhardi. J. Cell Biol. 76:430-8.

Graham, L. E. & McBride, G. E. 1975. The ultrastructure of multilayered structures associated with flagellar bases in motile cells of Trentepohlia aurea. J. Phycol. 11:86-96.

Guttman, H. N. 1971. Internal cellular details of Euglena gracilis visualized by scanning electron microscopy. Science 171:290-2.

Guttman, H. N. & Ziegler, H. 1974. Clarification of structures related to function in Euglena gracilis. Cytobiologie 9:10-22.

Hall, R. P. 1926. Kinetic elements and nucleus in the family Astasiidae of the euglenoid flagellates. (Author's Abstract) Anat. Rec. 34:155.

Hall, R. P. 1934. A note on the flagellar apparatus of Peranema trichophorum and the status of the family Peranemidae Stein. Trans. Amer. Microsc. Soc. 53: 237-44.

Hasegawa, M. Yano, T.-A., & Miyata, T. 1981. Phylogeny of transfer RNA and origins of organelles. Precambrian Res. 14:81-98.

Hilenski, L. L. 1980. Ultrastructural and experimental investigations of the euglenoid flagellate, Peranema trichophorum (Ehrenberg) Stein, with special reference to flagella, mucocysts and feeding apparatus. Ph. D. Dissertation, University of Tennessee, Knoxville, Tennessee.

Hilenski, L. L. & Walne, P. L. 1985. Ultrastructure of the flagella of the colorless phagotroph Peranema trichophorum (Euglenophyceae). II. Flagellar roots. J. Phycol. 21:125-34.

Hitchen, E. T. 1974. The fine structure of the colonial kinetoplastid flagellate Cephalothamnium cyclopum Stein. J. Protozool. 21:221-31.

Hoffman, C. and Bouck, G. B. 1976. Immunological and structural evidence for patterned intussusceptive surface growth in a unicellular organism. J. Cell Sci. 69:693-715.

Hoffman, L. R. & Manton, I. 1962. Observations on the fine structure of the zoospore of Oedogonium cardiacum with special reference to the flagellar apparatus. J. Exptl. Bot. 13:443-9.

Hoffman, L. R. & Manton, I. 1963. Observations on the fine structure of Oedogonium: II. The spermatozoid of O. cardiacum. Amer. J. Bot. 50:455-63.

Hollande, A. 1942. Etude cytologique et biologique de quelques flagellés libres. Arch. Zool. Exp. Gen. 83:1-268.

Honigberg, B. M., Balamuth, W., Bovee, E. C., Corliss, J. O., Gojdics, M., Hall, R. P., Kudo, R. P., Levine, N. D., Loeblich, A. R., Jr., Weiser, J., & Wenrich, D. H. 1964. A revised classification of the phylum Protozoa. J. Protozool. 11:7-20.

Hoops, H. J. & Floyd, G. L. 1982. Ultrastructure of the flagellar apparatus of Pyrobotrys (Chlorophyceae). J. Phycol. 18:455-462.

Hoops, H. J. & Floyd, G. L. 1983. Ultrastructure and development of the flagellar apparatus and flagellar motion in the colonial green alga Astrephomene gubernaculifera. J. Cell Sci. 63:21-41.

Huber-Pestalozzi, G. 1955. Das Phytoplankton des Susswassers. 4. Euglenophyceen. E. Schweizerbart'sche Verlagbuchhandlung, Stuttgart.

Irvine, D. E. G. & John, D. M. [Eds.] 1984. Systematics of the Green Algae. Systematics Assoc. Special Vol. 27, Academic Press, London.

Jahn, T. L. 1946. The euglenoid flagellates. Quart. Rev. Biol. 21:246-74.

Kivic, P. A. & Vesk, M. 1972. Structure and function in the euglenoid eyespot apparatus: The fine structure and response to environmental changes. Planta 105: 1-14.

Kivic, P. A. & Vesk, M. 1974. The structure of the eyespot apparatus in bleached strains of Euglena gracilis. Cytobiologie 10:88-101.

Kivic, P. A. & Walne, P. L. 1984. An evaluation of a possible phylogenetic relationship between the Euglenophyta and Kinetoplastida. Origins Life 13: 269-88.

Klebs, F. 1883. Uber die Organisation einiger Flagellaten-Gruppe und ihre Beziehungen zu Algen und Infusorien. Untersuchungen aus dem Botanisches. Institut zu Tubingen I:233-362.

Kumazaki, T., Hori, H., & Osawa, S. 1983. Phylogeny of protozoa deduced from 5S rRNA sequences. J. Mol. Evol. 19:411-9.

Lackey, J. B. 1929. The cytology of Entosiphon sulcatum (Duj.) Stein. Arch. fur Protistenk. 66:176-200.

Lackey, J. B. 1933. Studies in the life histories of Euglenida. III. The morphology of Peranema trichophorum Ehrenberg, with special reference to its kinetic elements and the classification of the Heteronemidae. Biol. Bull. 65:238-48.

Leedale, G. F. 1964. Pellicle structure in Euglena. Brit. Phycol. Bull. 2:291.

Leedale, G. F. 1967a. Euglenida/Euglenophyta. Ann. Rev. Microbiol. 21:31-48.

Leedale, G. F. 1967b. Euglenoid Flagellates. Prentice-Hall, Englewood Cliffs, N. J.

Leedale, G. F. 1970. Observations on the mitochondrial reticulum in living Euglena gracilis. Cytobiologie 1:195-202.

Leedale, G. F. 1978. Phylogenetic criteria in euglenoid flagellates. BioSystems 10:183-7.

Leedale, G. F. 1982. Ultrastructure. pp. 1-27, In Buetow, D. E. [Ed.] The Biology of Euglena Vol. III. Physiology. Academic Press, New York, 363 pp.

Leedale, G. F. & Hibberd, D. J. 1974. Observations on the cytology and fine structure of the euglenoid genera Menoidium Perty and Rhabdomonas Fresenius. Arch. Protistenkd. 116:319-45.

Leedale, G. F., Meeuse, B. J. D. & Pringsheim, E. G. 1965. Structure and physiology of Euglena spirogyra. I and II. Arch. Mikrobiol. 59:68-102.

Lembi, C. A. 1975. The fine structure of the flagellar apparatus of Carteria. J. Phycol. 11:1-9.

Lembi, C. A. & Walne, P. L. 1969. Interconnections between cytoplasmic microtubules and basal bodies of tetrasporalean pseudocilia. J. Phycol. 5:202-5.

Lom, J., Paulin, J. J., & Nohynkova, E. 1980. The fine structure of the fish trypanosome, Trypanosoma danilewskyi: I. Presence of a cytopharyngeal complex in bloodstream trypomastigotes. Protistologica 16:365-73.

Manton, I. 1965. Some phyletic implications of flagellar structures in plants. In Preston, R. D. [Ed.] Advances in Botanical Research 2. Academic Press, London. pp. 1-34.

Margulis, L. 1970. Origins of Eukaryotic Cells. Yale University Press, New Haven, Connecticut.

Mattox, K. R. & Stewart, K. D. 1984. Classification of the green algae: A concept based on comparative cytology. In Irvine, D. E. G. & John, D. M. Systematics Assoc. Special Vol. 27: Systematics of the Green Algae. pp. 29-72.

McQuade, A. B. 1983. Origins of the nucleate organisms II. BioSystems 16:39-55.

Melkonian, M. 1977. The flagellar root system of zoospores of the green alga Chlorosarcinopsis (Chlorosarcinales) as compared with Chlamydomonas (Volvocales). Plant Syst. Evol. 128:79-88.

Melkonian, M. 1980. Ultrastructural aspects of basal body associated fibrous structures in green algae: a critical review. BioSystems 12:85-104.

Melkonian, M. 1985. Structure and function of flagellar roots. Book of Abstracts, Second Intern. Phycol. Congr., Copenhagen, Denmark.

Mignot, J.-P. 1963. Quelques particularités de L'ultrastructure d'Entosiphon sulcatum (Duj.) Stein, flagellé euglénien. C. R. Acad. Sci. (Paris) 257:2530-2533.

Mignot, J.-P. 1964. Observations complémentaires sur la structure des flagelles d'Entosiphon sulcatum (Duj.) Stein, flagellé euglénien. C. R. Acad. Sci. Paris 258:3360-3363.

Mignot, J.-P. 1965. Ultrastructure des euglèniens. I. Etude de la cuticle chez differentes èspeces. Protistologica 1:5-15.

Mignot, J.-P. 1966. Structure et ultrastructure de quelques Euglenomonadines. Protistologica 2:51-117.

Mignot, J.-P. 1967. Affinités des euglenomonadines et des chloromonadines; remarques sur la systematique des Euglenida. Protistologica 3:25-60.

Mignot, J.-P. 1981. Sur la necessité d'une révision de la classification des Phytomastigophorea. Proc. Sixth Int. Cong. Protozool. Warsaw, Poland.

Miller, K. R. & Miller, G. J. 1978. Organization of the cell membrane in Euglena. Protoplasma 95:11-24.

Moestrup, Ø. 1972. Observations on the fine structure of spermatozoids and vegetative cells of the green alga Golenkinia. Brit. Phycol. J. 7:169-183.

Moestrup, Ø. 1974. Ultrastructure of the scale-covered zoospores of the green alga Chaetosphaeridium, a possible ancestor of the higher plants and bryophytes. Biol. J. Linn. Soc. 6:111-25.

Moestrup, Ø. 1978. On the phylogenetic validity of the flagellar apparatus in green algae and other chlorophyll A and B containing plants. BioSystems 10:117-44.

Moestrup, Ø. 1982. Flagellar structure in algae: A review, with new observations particularly on the Chrysophyceae, Phaeophyceae (Fucophyceae), Euglenophyceae, and Reckertia. Phycologia 21:427-528.

Nisbet, B. 1974. An ultrastructural study of the feeding apparatus of Peranema trichophorum. J. Protozool. 21:39-48.

Nohynkova, E. 1984. A new pathogenic Cryptobia from freshwater fishes: A light and electron microscopic study. Protistologica 20:188-95.

O'Kelly, C. J. & Floyd, G. L. 1984. Flagellar apparatus absolute orientations and the phylogeny of the green algae. BioSystems 16:227-51.

Osafune, T. & Schiff, J. A. 1980. Stigma and flagellar swelling in relation to light and carotenoids in Euglena gracilis var. bacillaris. J. Ultrastruct. Res. 73:336-49.

Palisano, J. R. & Walne, P. L. 1972. Acid phosphatase activity and ultrastructure of aged cells of Euglena granulata. J. Phycol. 8:81-8.

Piccinni, E. & Mammi, M. 1978. Motor apparatus of Euglena gracilis: Ultrastructure of the basal portion of the flagellum and the paraflagellar body. Boll. Zool. 45:405-14.

Pickett-Heaps, J. D. 1975. Structural and phylogenetic aspects of microtubular systems in gametes and zoospores of certain green algae. In Duckett, J. G. & Racey, P. A. [Eds.] The Biology of the Male Gamete. Biol. J. Linn. Soc. Vol. 7 (Suppl. 1):37-44.

Pickett-Heaps, J. D. & Marchant, H. 1972. The phylogeny of the green algae: A new proposal. Cytobios 6: 255-64.

Pitelka, D. R. 1969. Fibrillar systems in protozoa. In Chen, T.-T. [Ed.] Research in Protozoology. 3: 279-388.

Pitelka, D. R. 1974. Basal bodies and root structures. In Sleigh, M. A. [Ed.] Cilia and Flagella. Academic Press, New York. pp. 437-469.

Porter, D. 1973. Isonema papillatum, sp. nov., a new colorless marine flagellate: A light and electron microscopic study. J. Protozool. 28:78-83.

Pringsheim, E. G. 1948. Taxonomic problems in the Euglenineae. Biol. Revs. (Cambridge Philos. Soc.) 23:46-61.

Pringsheim, E. G. 1953. Observations on some species of Trachelomonas grown in culture. New Phytol. 52: 93-113, 238-266.

Pringsheim, E. G. 1956. Contributions toward a monograph of the genus Euglena. Nova Acta Leopoldina 18:1-168.

Pringsheim, E. G. 1963. Farblosen Algen. Gustav Fischer Verlag, Stuttgart.

Ragan, M. A. & Chapman, D. J. 1978. A Biochemical Phylogeny of the Protists. Academic Press, New York.

Ringo, D. L. 1963. Electron microscopy of Astasia longa. J. Protozool. 10:167-73.

Ringo, D. L. 1967. Flagellar motion and fine structure of the flagellar apparatus in Chlamydomonas. J. Cell Biol. 33:543-71.

Roberts, K. R., Stewart, K. D. & Mattox, K. R. 1981. The flagellar apparatus of Chilomonas paramecium (Cryptophyceae) and its comparison with certain zooflagellates. J. Phycol. 17:159-67.

Roberts, K. R. 1985. The flagellar apparatus of Oxyrrhis marina (Pyrrophyta). J. Phycol. 21:641-55.

Roberts, K. R., Stewart, K. D. & Mattox, K. R. 1984. Structure and absolute configuration of the flagellar apparatus in the isogametes of Batophora (Dasycladales, Chlorophyta). J. Phycol. 20:183-91.

Rosowski, J. R. & Lee, K. W. 1978. Cryptoglena pigra: A euglenoid with one chloroplast. J. Phycol. 14:160-6.

Rosowski, J. R. & Willey, R. L. 1977. Development of mucilagenous surfaces in euglenoids. I. Stalk morphology of Colacium mucronatum. J. Phycol. 13: 16-21.

Roth, L. E. 1958. A filamentous component of protozoan fibrillar systems. J. Ultrastruc. Res. 1:223-34.

Roth, L. E. 1959. An electron-microscope study of the cytology of the protozoan Peranema trichophorum. J. Protozool. 6:107-16.

Round, F. E. 1980. The evolution of pigmented and unpigmented unicells - a reconsideration of the protista. BioSystems 12:61-70.

Sato, T. 1968. A modified method for lead staining of thin sections. J. Electron Microsc. (Tokyo) 17:158-9.

Schuster, F. L., Goldstein, S., & Hershenov, B. 1968. Ultrastructure of a flagellate, Isonema nigricans nov. gen. nov. sp., from a polluted marine habitat. Protistologica 4:141-55.

Schuster, F. L. & Hershenov, B. 1974. Khawkinea quartana, a colorless euglenoid flagellate. I. Ultrastructure. J. Protozool. 21:33-9.

Sleigh, M. A. 1973. The Biology of Protozoa. Edward Arnold, London.

Smith, G. M. 1950. The Fresh-water Algae of the United States. McGraw-Hill Book Co., New York.

Solomon, J. A., Walne, P. L., & Kivic, P. A. 1984. Ultrastructure of the flagellar root system of Entosiphon sulcatum. J. Phycol. 20(suppl.):17.

Sommer, J. R. & Blum, J. J. 1964. Pellicular changes during division in Astasia longa. Explt. Cell Res. 35:423-425.

Sommer, J. R. & Blum, J. J. 1965. Cell division in Astasia longa. Exp. Cell Res. 39:504-27.

Spurr, A. R. 1969. A low-viscosity epoxy resin embedding medium for electron microscopy. J. Ultrastr. Res. 26:31-43.

Stewart, K. D. & Mattox, K. R. 1975. Comparative cytology, evolution and classification of the green algae with some consideration of the origin of other organisms with chlorophylls a and b. Bot. Rev. 41:104-35.

Stewart, K. D. & Mattox, K. R. 1980. Phylogeny of phytoflagellates. In Cox, E. R. [Ed.] Developments in Marine Biology II. Phytoflagellates. Elsevier/North Holland, New York. pp. 433-62.

Swale, E. M. F. 1973. A study of the colourless flagellate Rhynchomonas nasuta (Stokes) Klebs. Biol. J. Linn. Soc. 5:255-64.

Taylor, F. J. R. 1976. Flagellate phylogeny: A study in conflicts. J. Protozool. 23:28-40.

Taylor, F. J. R. 1978. Problems in the development of an explicit hypothetical phylogeny of the lower eukaryotes. BioSystems 10:67-89.

Taylor, M. G., Floyd, G. L. & Hoops, H. J. 1985. Development of the flagellar apparatus and flagellar position in the colonial green alga Platydorina caudata (Chlorophyceae). J. Phycol. 21:533-46.

Throndsen, J. 1973. Fine structure of Eutreptiella gymnastica (Euglenophyceae). Norw. J. Bot. 20:271-88.

Vickerman, K. 1976. The diversity of the kinetoplastid flagellates. In Lumsden, H. R. & Evans, D. A. [Eds.] Biology of the Kinetoplastida, Vol. I. Academic Press, London. pp. 1-34.

Vickerman, K. & Preston, T. M. 1976. Comparative cell biology of the kinetoplastid flagellates. In Lumsden, H. R. & Evans, D. A. [Eds.] Biology of the Kinetoplastida, Vol. I. Academic Press, London. pp. 34-130.

Walker, W. F. 1985. 5S and 5.8S ribosomal RNA sequences and protist phylogenetics. BioSystems 18:269-78.

Walne, P. L. 1971. Comparative ultrastructure of eyespots in selected euglenoid flagellates. In Parker, B. C. & Brown, R. M., Jr. [Eds.] Contributions in Phycology. Allen Press, Lawrence, Kansas. pp. 107-20.

Walne, P. L. & Arnott, H. J. 1967. The comparative ultrastructure and possible function of eyespots: Euglena granulata and Chlamydomonas eugametos. Planta 77:325-53.

Walne, P. L., Moestrup, Ø., Norris, R. E., Ettl, H., & Pearson, B. 1986. Light- and electron-microscopical studies of Eutreptiella eupharyngea sp. nov. (Euglenophyceae) from Danish and American waters. Phycologia (in press).

Weinman, D., White, E. A., & Antipa, G. A. 1984. Trypanosoma lucknowi, a new species of trypanosome from Macaca mulatta with observations of its fine structure. J. Protozool. 31:429-33.

West, L. K., Walne, P. L., & Rosowski, J. R. 1980. Trachelomonas hispida var. coronata (Euglenophyceae). I. Ultrastructure of cytoskeletal and flagellar systems. J. Phycol. 16:489-97.

Whatley, J. M. 1981. Chloroplast evolution - ancient and modern. Ann. N. Y. Acad. Sci. 361:154-65.

Willey, R. L., Durban, E. M. & Bowen, W. R. 1973. Ultrastructural observations of a Colacium palmella: The reservoir, eyespot and flagellum. J. Phycol. 9:211-5.

Willey, R. L. & Wibel, R. G. 1985a. A cytostome/ cytopharynx in green euglenoid flagellates (Euglenales) and its phylogenetic implications. BioSystems 18:369-76.

Willey, R. L. & Wibel, R. G. 1985b. The reservoir cytoskeleton and a possible cytostomal homologue in Colacium (Euglenophyceae). J. Phycol. 21:570-7.

APPENDIX

Euglena sp.

Among the cells of Eutreptia pertyi examined (Part 4) were a few cells of another euglenoid organism. They were thought for a long time to be Eutreptia cells because they were of the same size, were highly metabolic, and the cellular organization was obviously euglenoid (Figs. 1-5). The apparent discontinuity of the flagellar roots through the reservoir region, however, finally led to the realization that there were two different organisms. The procedures used for fixation, embedding and sectioning were identical to those used for Eutreptia pertyi (Part 4).

The contaminant was identified as belonging to the genus Euglena by its chloroplasts, the presence of one emergent and one nonemergent flagellum (cf. Figs. 1, 2), and the pronounced metaboly.

The organism, Euglena sp., has four basal bodies (not shown) at one side of the reservoir. The three microtubular flagellar roots are arranged in the typical euglenoid pattern (Fig. 5; Parts 2, 4). At reservoir level (Fig. 1) a wide DMT is associated with the stigma, and on the left side of the reservoir, the microtubular roots are evident. The VR contains nine microtubules in a 5 + 4 arrangement, with a plate over the terminal four (Fig. 4). Between the DMT and the VR are two, or possibly three, microtubular bands: the lowest band (Fig. 1, lowest arrow) is sectioned obliquely, so the detail is obscured; the

middle band (middle arrow) is composed of five microtubules in a linear array, similar to the PMT of Colacium (Willey and Wibel 1985b); the uppermost band (upper arrow) is the least distinct, but is mentioned because this configuration occurs regularly. Were it not for this third band, the roots of Euglena sp. would be easily identified as the IR (lower arrow) and DR (middle arrow).

In the canal region (Fig. 2), the DMT microtubules are paired, and a band of singlet microtubules, probably the IR, is present on the ventral side. Near the reservoir-canal transition zone, a vesicle with microtubules on at least one side is identified as the cytopharyngeal remnant (Fig. 3).

The flagellar roots of this organism, Euglena sp., are similar to those of Colacium (Willey and Wibel 1985b). They differ from those of Eutreptia and Entosiphon principally in the morphology of the VR and the IR. Whether the PMT corresponds to the IR or DR of other euglenoids, or represents an additional reservoir microtubular band, is undetermined.

Euglena gracilis var. bacillaris

Early in this work, before the organisms were selected for intensive study, some preliminary investigations were carried out on Euglena gracilis var. bacillaris (UTEX L 884). A few of the results are presented here (Figs. 6-8)

because they provide further comparative information on roots of the presumably advanced euglenoids. Cells were prepared for electron microscopy as described for Eutreptia viridis, except that all procedures were performed at room temperature.

As shown in Figure 6, there are two separate microtubular bands (arrows) associated with the presumptive cytopharynx (Cp). The Cp shown in this micrograph is considerably larger than those presented elsewhere (e.g. Part 4, Figs. 26-29), which may explain why the two bands are so widely separated. The size of the Cp probably fluctuates, perhaps as a result of membrane flow activity (Willey and Wibel 1985).

At the upper level of the reservoir (Fig. 7), the VR is clearly identifiable by its distinctive 5 + 4 morphology. To its left, the presumptive IR is located on a ridge projecting into the reservoir. While this feature is not present in Eutreptia (Part 4), it is characteristic of Entosiphon (Part 2).

In the overview of the reservoir of E. gracilis var. bacillaris shown in Figure 8, the flagella arise on the side of the reservoir, similar to the arrangement in the bodonids (see Part 3, Fig. 34). In the bodonids, the MTR circles around the right side of the reservoir and extends anteriorly, eventually joining the cytopharynx. Figure 8 presents evidence that the VR, suggested homologue of the

bodonid MTR (Parts 3, 4), follows a similar pathway around the reservoir. The portion of the VR shown at the bottom of the micrograph is in the basal body complex; the portion of the VR at the top of the micrograph, identifiable by its morphology, is probably continuous with the former but is here located on the opposite side of the reservoir. A trajectory which could account for the view shown in Figure 8 is that of the bodonid MTR where the root describes a semicircle around the reservoir. In Entosiphon and Eutreptia, where the basal bodies are situated posterior to the reservoir, the root trajectories described in Parts 2-4 would not produce the transverse view shown in Figure 8.

Adjacent to the VR shown at the top of Figure 8 is a linear array of microtubules at an angle to the reservoir membrane (arrow), closely resembling the PMT of Colacium (Willey and Wibel 1985b).

This very limited evidence from Euglena gracilis indicates that the flagellar root systems of E. gracilis and those of other photosynthetic euglenoids are very similar to one another. In particular, the morphologies of the VR and the PMT are almost identical. Moreover, similar basal body placement in Euglena and the bodonids, together with the evidence shown in Figure 8, suggests that the paths of the VR and MTR in those organisms may be nearly the same. If this proves to be so, it would mean that the roots of the presumably advanced Euglena follow a path

similar to their presumed early ancestor, while the proposed intermediate forms, the more primitive Entosiphon and Eutreptia, have a somewhat dissimilar pathway. Resolution of this apparent contradiction requires a thorough study of the flagellar roots of the supposedly advanced euglenoids.

A complete list of abbreviations is provided on p. xv.

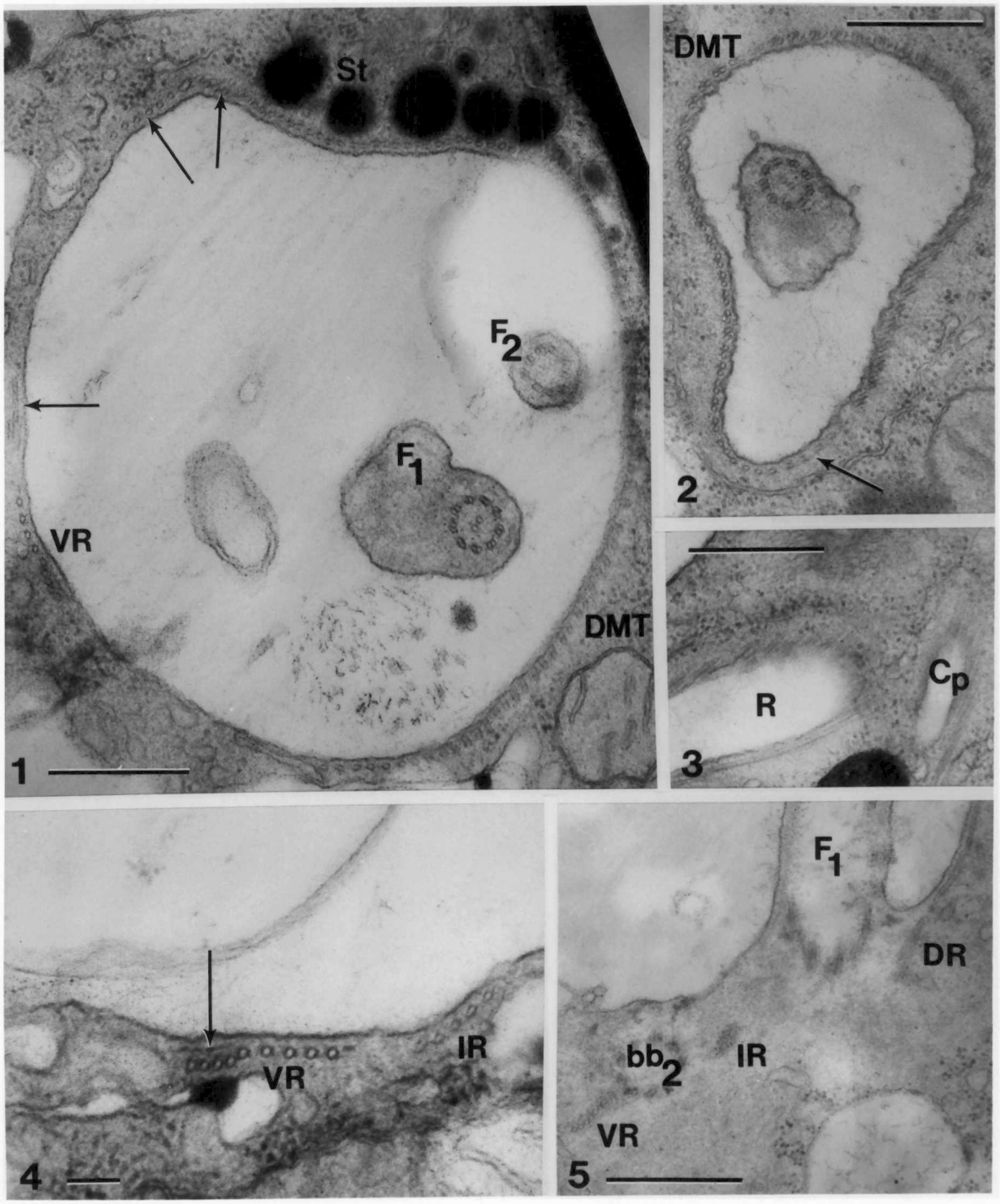
Figure 1. Transverse section through the reservoir of the contaminant, Euglena sp. The stigma (St) lies near the dorsal margin and the two flagella (F_1 and F_2) are within the reservoir. As many as five microtubular bands surround it: the dorsal microtubules (DMT), ventral root (VR), and possibly three others (arrows). Scale bar = 0.5 μm.

Figure 2. At canal level, the microtubules of the DMT are paired. The presumptive intermediate root (arrow) is on the ventral margin. Euglena sp. Scale bar = 0.5 μm.

Figure 3. Reservoir-canal (R) region of Euglena sp. The putative cytopharynx (Cp), with its border of microtubules, is evident. Scale bar = 0.5 μm.

Figure 4. The ventral root of Euglena sp. is composed of two segments. One is set back slightly from the reservoir membrane and overlain with an electron-dense plate (arrow). The IR lies to the right of the VR (right to left orientation is reversed in this micrograph). Scale bar = 0.1 μm.

Figure 5. The basal flagellar region of Euglena sp. The euglenoid flagellar root pattern, with the DR near F_1 and the IR and VR near bb_2, is evident. Scale bar = 0.5 μm.

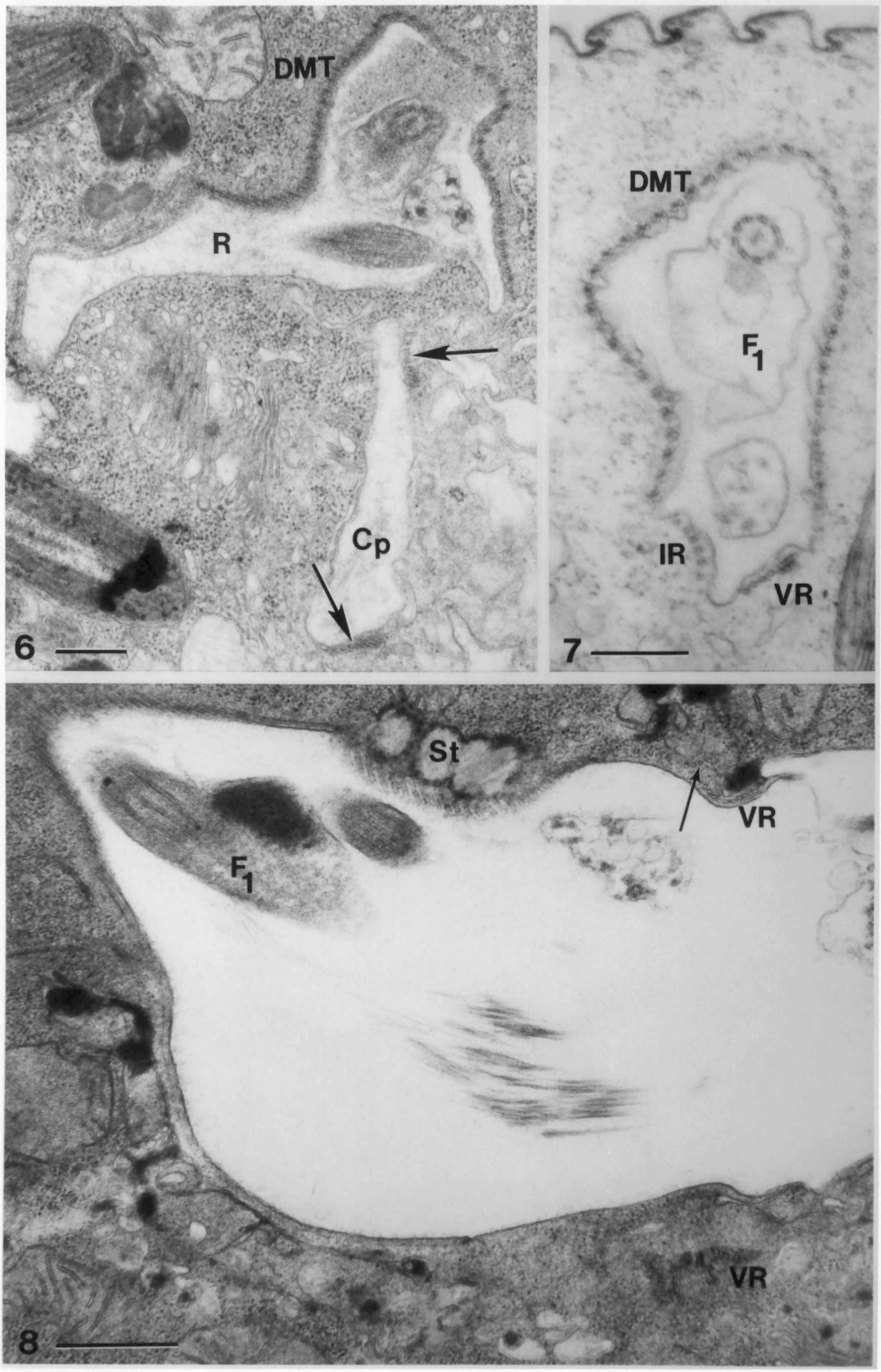

St
F2
F1
VR
DMT
1
DMT
2
R
Cp
3
IR
VR
4
F1
DR
bb2
IR
VR
5

A complete list of abbreviations is provided on p. xv.

Figure 6. The dorsal margins of the reservoir of Euglena gracilis var. bacillaris are lined by the dorsal microtubules (DMT). The cytopharynx (Cp), ventral to the reservoir, has two microtubular bands associated with it (arrows). Scale bar = 0.5 μm.

Figure 7. A transverse section of the anterior region of the reservoir of E. gracilis. The intermediate root (IR) is identifiable by the number of microtubules and by its position on a ridge. The VR has two distinct segments, one overlain by a plate. The DMT is composed of paired microtubules and the DR is not evident. Scale bar = 0.5 μm.

Figure 8. An oblique section of the reservoir through the basal body complex and stigma. In E. gracilis, shown here, the flagella arise on the side of the reservoir instead of at the base. The VR is evident both adjacent to the posterior basal body and on the opposite side of the reservoir, near another microtubular band (arrow), probably the IR. Scale bar = 0.5 μm.


DMT
R
Cp
6
DMT
F1
IR
VR
7
St
VR
F1
VR
8

VITA

Jean Marie Adamson Solomon, daughter of Mr. and Mrs. Robert A. Adamson, was born on September 27, 1942, in Baltimore, Maryland. She was educated in the Baltimore City Schools and graduated from Eastern High School in 1960. She earned a B. S. degree, Cum Laude with Honors in Biology, from Allegheny College, Meadville, Pennsylvania, in 1964 and an M. S. degree in Statistics from the University of Tennessee, Knoxville, in 1979. She became interested in algae while a summer student at the Chesapeake Biological Laboratory, Solomons, Maryland (1963), and has done graduate work at the Marine Biological Laboratory, Woods Hole Oceanographic Institution; the University of Miami Institute of Marine Sciences; Friday Harbor Laboratories of the University of Washington, Seattle; University of Maryland at College Park; Rutgers University of New Jersey; and the University of Arizona, Tucson. From 1968 to 1970, she taught biology and chemistry at East Brunswick High School, East Brunswick, New Jersey. She has worked in the Environmental Sciences Division, Oak Ridge National Laboratory since 1977 and began her doctoral program at the University of Tennessee in 1981. She is a member of the Association for Women in Science, the American Association for the Advancement of Science, the Phycological Society of America, the International Phycological Society, the American Society

for Limnology and Oceanography, and the Society for Evolutionary Protistology.

She is married to Allen Morris Solomon, originally of Roseville, Michigan, and has two children, Robert and Charles, who were born in 1971.